DESIGN, SYNTHESIS, AND EVALUATION OF LUBRICIN MIMETIC POLYMERS AND THEIR LUBRICATION OF CARTILAGE AND BONE

A Dissertation

Presented to the Faculty of the Graduate School

of Cornell University

In Partial Fulfillment of the Requirements for the Degree of

Doctor of Philosophy

by

Zhexun Sun

August 2018

DESIGN, SYNTHESIS, AND EVALUATION OF LUBRICIN MIMETIC POLYMERS AND THEIR LUBRICATION OF CARTILAGE AND BONE

Zhexun Sun, Ph. D.

Cornell University 2018

The body naturally creates biomacromolecules to lubricant joints and provide incredibly low friction under tremendous load for decades. One of the biolubricants, lubricin, demonstrates boundary mode lubrication and chondroprotective abilities that arise from its composition and structure. As a promising therapeutic approach for the treatment of joint diseases such as osteoarthrosis (OA), the challenge to produce lubricin recombinantly restricts its clinical application, which inspires the design of synthetic molecules that mimic lubricin's structure.

In this dissertation, a class of lubricin mimetic diblock copolymers, consisting of a cationic cartilage binding block and a brush lubrication block, are synthesized and their tribological properties are evaluated in comparison to lubricin (Chapter 2). Like lubricin, the tribological properties of these polymers are dependent on the molecular architecture. The roles of structure are explored to characterize how changing the molecular architecture affects the lubrication on cartilage surfaces and the results are summarized as a set of design principles of synthetic lubricants (Chapter 3). Additionally, this class of polymers demonstrates their ability to bind to and lubricate bone surfaces, which is absent in natural lubricin, thus extending its potential application as a therapeutic approach for OA treatment (Chapter 4).

BIOGRAPHICAL SKETCH

Zhexun Sun was born in a small town of Hubei Province, China. Being the first member of his family pursuing a career in science, he was trained as a synthetic chemist in Wuhan University and Rutgers University, by Prof. Aiwen Lei and Prof. Spencer Knapp. Following graduation from Rutgers University in 2012, he started a job as a chemist in Nitto Denko Automotive, working on energy absorbing materials design for automobiles. After realizing his interests in the biomedical field, Zhexun joined the Biomedical Engineering department at Cornell University as a MEng student in 2013 and was accepted to the PhD program a year later. During his time at Cornell, Zhexun conducted research on designing synthetic joint lubricants for osteoarthritis treatment under the supervision of Dr. David Putnam.

To my loving parents and all of my friends.

ACKNOWLEDGMENTS

My gratitude to my advisor, Dr. David Putnam, is beyond words. Since my first day in graduate school, Dr. Putnam believed in me like nobody else and has given me endless support. His patience, guidance, and most importantly, his trust in my independence, have allowed me to grow as a scientist. Dr. Putnam has set an example of excellence as a researcher, mentor, instructor, and role model. I also owe many thanks my major collaborator and committee member, Dr. Lawrence Bonassar, whose advice has shape my thinking as an independent researcher and who has helped to keep my research on the right track all the time. My gratitude extends to my committee member, Dr. Christopher Ober, for his insight and support in completing this body of work.

The completion of this dissertation would have been impossible without the company of Team Putnam. In the past five years, I had the fortune to work with the most amazing group of researchers. To all the Putnam crew who have always supported me: Lindsey, Nicole, Bailey, Mingchee, Jose, Hannah, Jaclyn, Can, Yehou, Hania, and of course Sarah, thanks for making the work in lab full of joy and weirdness.

Outside of Putnam lab, the student members of Lubrication group have consistently brought new ideas and perspectives to my research. I would like to thank Liz, Jill, Becka, and Sierra for their continued help and support that instilled in me knowledge and confidence to solve problems.

My gratitude also extends to the fantastic friends I've made along the way. Without them, life in Ithaca wouldn't be as radiant as it is. I would like to give special thanks to my close friends, Aaron, Terence, and Dan, for their encouragement, love, support, and being a significant part of my life.

Most importantly, I need to thank my wonderful family. My parents, Xiaoqin and Zhiyong, have always been unconditionally supportive every step of the way, and I will be forever indebted to them.

TABLE OF CONTENTS

LIST OF ABBREVIATIONS

OA:	osteoarthritis
CDC:	Center for Disease Control and Prevention
NSAID:	non-steroidal anti-inflammatory drugs
IA:	intraarticular
HA:	hyaluronic acid
COF:	coefficient of friction
CACP:	camptodactyly-arthropathy-coxa vera-pericarditis
GAG:	glycosaminoglycan
PEG:	poly (ethylene glycol)
METAC:	methacryloxyethyltrimethylammonium
PEO_{45}MEMA:	PEG-methylether methacrylate
MMA:	methyl methacrylate
PAA:	polyacrylic acid
DMEM	Dulbecco's Modified Eagles's medium
DP:	degree of polymerization
GPC:	gel permeation chromatography
RAFT:	reversible addition-fragmentation chain-transfer
ACPA:	4,4'-azobis 4-cyanopentanoic acid
CPADB:	4-cyanopentanoic acid dithiobenzoate
DMAEA:	2-(dimethylamino) ethyl acrylate
PEGMA:	poly(ethylene glycol) methyl ether acrylate
PDMAEA:	poly(dimethylamino ethyl acrylate)
PDMAEA-PEGMA:	diblock copolymer with tertiary amine based binding block
qPDMAEA:	binding block decorated with quaternary amine
qPDMAEA-PEGMA:	diblock copolymer with quaternary amine based binding block

CTA:	chain transfer agent
MWCO:	molecular weight cut off
DI:	deionized
PBS:	phosphate buffered saline
NaCl:	sodium chloride
EtBr:	ethyl bromide
SFA:	surface force apparatus
AFM:	atomic force microscopy
UV:	ultraviolet
FECO:	fringes of equal chromatic order
ANOVA:	analysis of variance

CHAPTER 1

INTRODUCTION

1.1 Osteoarthritis and Therapeutic Interventions

Osteoarthritis (OA) is the most common form of arthritis and the leading cause of disability worldwide. According to the US Center for Disease Control and Prevention (CDC), an estimated 52.5 million adults (22.7%) annually had been diagnosed with some form of arthritis from 2010-2012, and this number is expected to increase to 78 million US adults (26%) by 2040[1], especially in people aged 55 and above[2]. Estimated by a logistic regression model by Jordan *et al*[3], 1 in 2 people are expected to develop knee OA by age 85 and 2 in 3 obese people. In 2005, the annual health care burden of OA exceeded $185 billion[4] and the costs are expected to rise as median age and life expectancy increase. The challenge for the treatment of OA comes from its complex pathogenesis[5]. Many factors including congenital genes, obesity, injury or overuse of joints, inflammation disorders, and abnormal hormone expression could contribute to the development of OA. Traditionally conceptualized as a disease featured with hyaline articular cartilage loss, OA is now widely accepted as an organ level disease of the joint, characterized with focal degradation of articular cartilage, remodeling of subchondral bone, as well as inflammation of surrounding synovial tissue[6].

Current strategies for OA treatment mainly aim to relieve symptoms such as joint pain, fatigue, and swelling through pharmacological and non-pharmacological interventions[7]. Oral non-steroidal anti-inflammatory drugs (NSAIDs) were reported to be effective in reducing knee pain for short term treatment in random placebo controlled trials[8]. Intraarticular (IA) injection of

corticosteroids is another approach that has been highly recommended by multiple clinical guidelines for short term pain management[9]. IA administration of viscosupplements such as hyaluronic acid (HA) demonstrated efficacy to relieve pain under the hypothesis that HA can help protect the cartilage against repeated friction and wear[10]. Several physical therapy modalities, especially land-based exercises, have been reported in the clinical guidelines to combine with pharmacological treatment for optimal management[9]. However, none of the abovementioned palliative treatments can prevent the progression of the disease into late stage OA, when joint arthroplasty becomes the only option left to improve the quality of patient life.

1.2 Intraarticular Therapy

Among all the interventions described above, intraarticular (IA) therapy for OA has become standard because of its symptomatic treatment and minimum systemic side-effects[11,12]. Several types of pharmacological agents have been used intraarticularly in double blind randomized clinical trials. For instance, corticosteroids are very potent anti-inflammatory agents for pain and symptom relief. A survey of rheumatologists in the United States suggested that more than 95% use them at least sometimes and 53% frequently to treat OA[13]. Corticosteroids exert their anti-inflammatory action by interrupting the inflammatory and immune cascade at several levels[12]. The beneficial effect of corticosteroids on OA treatment include quick pain relief, decreased incidence and size of osteophytes, and reduced cartilage lesion severity as shown in animal models[14] and clinical trials[15]. The perceived efficacy and lack of major toxicity have made IA corticosteroid injections one of the mainstays of the management of OA, in particular, OA of the knee.

Another commonly used drug in IA therapy is HA, which is a polysaccharide existing naturally in cartilage and synovial fluid that plays essential roles in maintaining viscoelastic

properties of the synovial fluid[16]. Also known as viscosupplementation, IA injection of HA is a novel, safe, and possibly effective treatment of OA. The concept of viscosupplementation is based on the hypothesis that HA could help restore the viscoelasticity of the synovial fluid and promote the endogenous synthesis of hyaluronan to improve joint mobility and articular function. In comparison to corticosteroids that usually have an onset within 24-48 hours but less than 1 month of efficacy, HA injections show similar benefits to steroids at one month but with superiority after a few months[11].

Despite the efficacy of IA therapy in certain cases, contradictory data and results are also obtained because of a powerful response to placebo[11]. According to a review of eight clinical trials assessing IA steroids versus placebo, both placebo and treated groups showed significant decrease in pain from week 1 to the final assessment at week 8[11]. Confounding results also occur in clinical trials studying the efficacy of HA. For instance, no significant benefit of IA administration of 750 kD HA over placebo during a five-week treatment period was observed in a double-blind placebo controlled study[17]. The lack of strong, convincing, and reproducible evidence to any of IA therapies demonstrate a strong clinical need for insightful investigation of OA mechanism and novel treatments.

1.3 Joint Lubrication

Because of the adverse mechanical and biological consequences that can arise from inferior joint lubrication, research has focused on restoring healthy lubricating function to diseased and injured joints[18–20]. Over the last several decades, tribosupplementation has emerged as a therapeutic strategy in the field of OA treatment to reduce pain and protect the joint. Briefly, tribosupplementation is the concept of utilizing IA injection of lubricants to minimize the friction and protect the contacting cartilage layer within the joints. Articular cartilage is the smooth tissue

that coats the articulating ends of bones in joints. The primary physiological function of cartilage is to provide a low friction interface that distributes loads across the joint over millions of cycles per year and a lifetime of use. Consisting of primarily water, type II collagen and proteoglycans, the articular cartilage possesses tribology properties that are fundamentally different from that of traditional fluid-lubricated surfaces defined by the classic Stribeck curve[21].

In the classic Stribeck curve, which describes the mode of lubrication on impermeable and hard materials, two extremes of lubrication regimes known as hydrodynamic mode lubrication and boundary mode lubrication are generally revealed as shown in Fig. 1.1[21]. In hydrodynamic mode, the average separation distance between two articulating surfaces is greater than that of the surface roughness, which leads to the formation of a fluid film in between that supports most of the friction load. The frictional properties therefore largely depend on the material properties of the bulk fluid, specifically the fluid viscosity[22]. In boundary mode, friction properties are primarily governed by direct solid-solid interactions[23] as the mean separation distance of the two opposing surfaces in this mode is less than that of the surface roughness. The friction properties in boundary mode lubrication are therefore largely dependent on the chemicophysical properties of the surface. Between the two extremes of lubrication is mixed lubrication, where surface asperities and the bulk fluid together share the frictional load support. Mixed lubrication occurs when separation distances of articulating materials are approximately equal to the mean surface roughness.

The frictional properties of the joint are primarily governed by the interplay of synovial fluid and articular cartilage. Compression of the tissue results in the pressurization of the interstitial fluid which supports a substantial amount of load[23], allowing articular cartilage to have relatively low coefficient of friction (COF). Due to the compliance of soft material-like properties,

localized interstitial fluid may form but not able to fully separate the surfaces as it may flow into and out of the contact. A phenomenon called “elastoviscous transition” instead of hydrodynamic mode may occur, which is governed by pore size or permeability[21]. After the interstitial fluid equilibrates, the pressure dissipates on the extracellular matrix component of articular cartilage, shifting the lubrication mechanism to the boundary mode. Existing in both cartilage tissue and synovial fluid, HA effectively lubricates cartilage by exhibiting viscoelastic behavior in the hydrodynamic mode lubrication[24]. This viscoelastic behavior is compromised in the case of OA where the concentration and molecular weight of HA are reduced[25]. Reintroducing HA into joints is expected to restore the joint tribology properties by effectively altering lubrication mode toward elastoviscous lubrication[21,26]. However, high friction and wear of OA cartilage happens in the boundary mode conditions, which inspires the investigation on the key molecule for the boundary mode lubrication mechanism of articular cartilage.

1.4 Lubricin

First isolated from bovine synovial fluid in 1981 by Swann *et al*[27], lubricin is a highly glycosylated mucinous protein with a molecular weight of ~227 kDa and contour length of ~200 nm[28]. Also known as superficial zone protein or proteoglycan 4, lubricin localizes in synovial fluid and on the superficial layer of articular cartilage, where it is secreted by synovial fibroblasts[29] and superficial zone chondrocytes[30]. Lubricin reduces the friction coefficient of articular cartilage in boundary lubrication by as much as 70 percent[31]. This potent lubrication ability arises from the structure of lubricin (Fig 1.2). The central mucin-like domain of lubricin consists of a core protein extensively glycosylated by oligosaccharides that attract and retain water near the molecule[32]. The C-terminus of lubricin binds the protein to the cartilage surface, whereas the cysteine rich N-terminus controls aggregation[32]. This heterogeneous structure

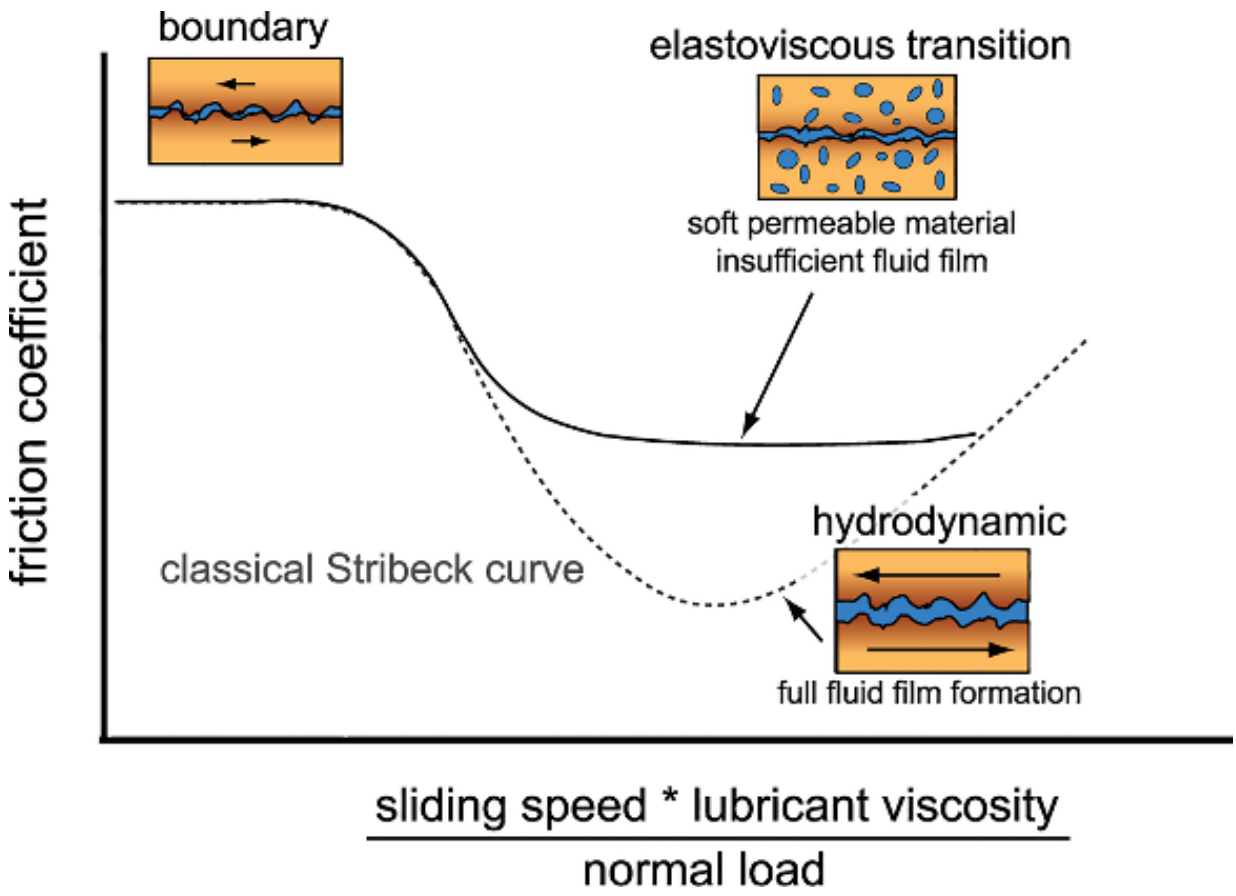

Figure 1.1. A classical Stribeck curve (dotted line) maps the transition of lubrication from boundary mode to hydrodynamic mode with the changes of lubrication parameters including sliding speed, viscosity, and pressure. Fluid film plays a larger role in hydrodynamic friction. Due to cartilage's permeable structure, lubrication does not reach full hydrodynamic mode (solid line). An elastoviscous transition from the boundary mode happens due to the insufficient fluid film formation between the soft and permeable surfaces. Figure copied from Bonnevie *et al* with permission[21].

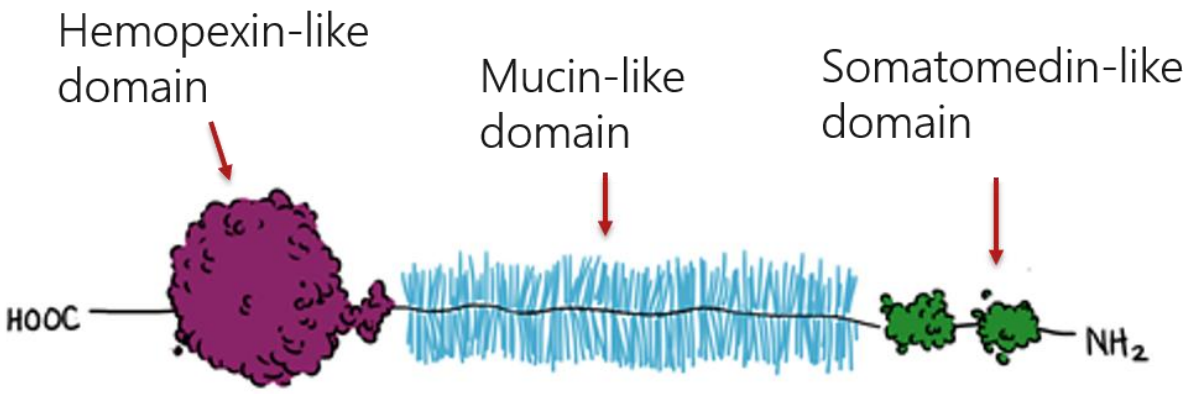

Figure 1.2. Schematic representation of the structure of lubricin. The lubrication ability of lubricin stems from its central mucin-like domain that attracts and retains water and the C-terminus hemopexin-like domain that binds the molecule on the cartilage surface. The N-terminus is a polyfunctional somatomedin-like domain that is responsible for self-assembling and interaction with other proteins.

enables lubricin to lubricate both hydrophobic and hydrophilic surfaces in the boundary mode[33]. Biologically, lubricin has demonstrated the ability to mediate cell adhesion and to bind and signal through CD 44[34] and toll-like receptors[35,36] on chondrocytes and synoviocytes.

Loss-of-function mutations in the lubricin encoding gene *PRG4* cause the autosomal recessive disorder camptodactyly-arthropathy-coxa vera-pericarditis syndrome (CACP)[30]. Lubricin mutant mice were characterized by non-inflammatory arthropathy, synovial hyperplasia as well as superficial zone chondrocyte apoptosis[37–39]. The expression of lubricin is reduced in animal models of OA and clinical trials, including rat[40], guinea pig[41], sheep[42], and human patients[43,44]. Lubricin concentrations in the synovial fluid of patients with ACL injury decreased significantly to less than 100 μg/ml right after injury and then gradually restored to a normal level of about 250 μg/ml after 12 months[43]. The decrease in synovial fluid lubricin concentrations following knee injury is linked to the potential cause of secondary OA as a consequence of lack of boundary lubrication. In the rat model of OA, IA supplementation of native lubricin as well as recombinant lubricin both show inhibition of disease progression characterized with increased glycosaminoglycan (GAG) content, reduced surface roughness, and decreased joint friction coefficient[45,46]. These studies suggest that OA in the peri-injury period following meniscus or anterior cruciate ligament trauma can be mitigated by the introduction of exogenous lubricin.

However, the widespread use of lubricin as a therapy for osteoarthritis is hindered by the production at a clinically needed level owing to the difficulty to synthesize multiple amino acid repeats in the protein core, as well as the high degree of glycoprotein[47]. Bacterial and insect cell lines cannot easily produce lubricin's highly glycosylated structure, and mammalian cell lines have also failed to reliably produce full-length lubricin. Production of lubricin from Chinese

hamster ovary cell lines generates molecules with truncated mucin domains which was shown to lubricate articular cartilage in boundary mode but was less effective than full-length lubricin[45]. Currently there is no commercial product of lubricin and the cost for lubricin is expected to exceed $10,000/mg of material.

1.5 Synthetic Lubricants

A plethora of work in the scientific literature concerning bottlebrush-like structure polymers for the purposes of lubrication has been published (Table 1.1). These studies not only create synthetic lubricants but also elucidate the lubrication mechanism in the boundary mode. Spencer *et al* have done much work synthesizing a series of bottlebrush-like polymer analogues with a structure of polylysine backbones grafted with poly (ethylene glycol) (PEG)[48,49]. This type of polymer adsorbed onto oxide surface via a charge-charge interaction between the positively charged polylysine backbone and the negatively charged substrate surface. The polymer thus would adsorb flatly onto the surface while the side chains would solvate and extend outwards in aqueous solution. Using atomic force microscopy (AFM) to probe friction forces at the interfaces of polymer coated metal oxide substrate under physiological pH solutions, friction was observed to systematically vary with the PEG side chain conformation, which was determined by the ratio of the distance between PEG chains on the surface (L) and side chain length (R_g). It was observed that the minimum COF was encountered at $L/2R_g \approx 0.5$, the point where PEG side chains adopted a fully stretched conformation[50].

Similarly, Claesson *et al* designed a series of random di-block copolymers with bottlebrush-like architecture consisted of methacryloxyethyltrimethylammonium chloride (METAC) and PEG-methylether methacrylate ($PEO_{45}MEMA$)[51]. Increased monomer ratio of positively charged METAC to $PEO_{45}MEMA$ in the copolymer structure altered the binding geometry of polymer on

the surface from partially adherence to the surface at lower METAC ratio to adsorbed flatly via its backbone at higher ratio. Using a similar AFM setup in Spencer's work to measure the friction force, the unexpected results showed that comb-like structure of an ideal brush layer is not necessary for achieving a low COF in the asymmetric mica-silica system. This type of polymer actually functions better at 20-30% molar ratio of METAC when the backbone is partially adhered[51].

Israelachvili *et al* recently developed a bio-inspired lubricin mimetic polymer following an ABA tri-block copolymer structure[52]. The A group is able to interact with negatively charged surfaces such as mica via its densely grafted quaternary amines. The B block is a bottlebrush-like core consisting of poly(methyl methacrylate) (PMMA) and conjugated with poly(2-methacryloyloyxethyl phosphorylcholine). Assessed by surface force apparatus (SFA), this lubricant adopted a loop conformation when coated on the mica surfaces, giving rise to a weak and long-range repulsive interaction force between the two approaching surfaces. Stronger repulsive force appeared under high compression (1.5 MPa), likely due to the repulsion between the side chains of the polymer. When submitted to shear at sliding speed varied from 0.01-100 μm/s, the systems show excellent lubrication properties with a friction coefficient as low as ~ 0.001[52].

However, while these materials lubricated mica or metal oxide surfaces, the physiological relevance of the results are unknown. Grinstaff *et al.* reported a more physiologically relevant polyanion biolubricant that performs similarly to synovial fluid in an *ex vivo* human cartilage mode[53]. A rotational tribometer adapting a rod-on-rod configuration was built by pairing extracted human osteochondral plugs. Each pair of cartilage sample was compressed to 18% strain, and then allowed to relax for 60 min before the friction measurement at an effective

velocity of 0.3 mm/s. By mimicking the structure of hyaluronic acid, this polymer reduced the friction at the interface of cartilage and demonstrated its potential in joint lubrication as a new type of viscosupplement.

Benetti *et al*. evaluated the lubrication ability of a tissue-reactive graft copolymer featuring a poly(glutamic acid) backbone and cyclic poly(2-methyl-2-oxazoline) side chains[54]. The polymer chemically absorbed on the cartilage surface via Schiff bases and exposed the cyclic sidechains at the interface to resist compression. Using a ball-on-disc microtribometer, two opposing cartilage surfaces were incubated with the cyclic polymer first, then articulated in a solution of polymer in bovine synovial fluid at linear reciprocating speed of 5 mm/s, applying maximum contact pressures of 0.5-0.9 MPa. By adopting a cyclic side chain conformation, this class of polymer demonstrated enhanced surface passivation and improved lubrication properties compared to similar species presenting a linear side chain.

The Putnam lab has recently reported a library of bottle brush copolymers consisting of PEG grafted onto a polyacrylic acid (PAA) core that mimicked the mucin-like domain of lubricin, and a thiol terminus that anchored the polymers to cartilage surfaces like lubricin's C-terminus[55]. Evaluated by a custom-built tribometer[56], the boundary mode friction was measured at the interface between the polymer treated cartilage plugs and the bare glass surface at oscillating sliding speed of 3 mm/s, applying 30% strain. Six out of eight polymers reduced the boundary mode friction relative to lubricin-removed cartilage plugs and the lubrication in this case is highly correlated to the binding of the lubricant on the surface. However, the cartilage binding mechanism(s) that led to these results were unclear and the low binding limited their further application.

In conclusion, many bioinspired synthetic polymers have been designed for the application of lubrication. Despite their success in achieving lubrication in varied models, few have demonstrated similar or approaching efficacy in biologically relevant system in comparison to natural lubricants. Inspired by the principles established in those studies, we aim to develop a superior synthetic lubricant to rival the remarkable tribological phenomenon in the body – the lubrication of joints.

Table 1.1. Structure and composition of synthetic lubricants and their tribology evaluation setup

Authors	Structure	Composition	Tribology Measurement
Spencer+[48,49,50]	Bottlebrush-like 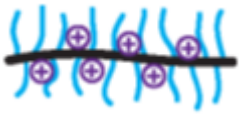	Backbone: polylysine Side chain: PEG	AFM measurement of sodium borosilicate microspheres against polymer coated metal oxide surface in HEPES solution
Claesson+[51]	Bottlebrush-like 	Backbone: polymethyl acrylate Side chain: PEG and positively charged amine	AFM measurement of silica colloidal probe against polymer coated mica surface in 0.1 mM $NaNO_3$
Israelachvili+[52]	Bottlebrush-like ABA triblock polymer 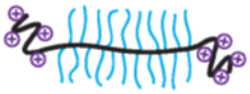	Backbone: polymethyl acrylate Side chain in A block: positively charged amine Side chain in B block: polyzwitterion	SFA measurement of friction between polymer coated mica surfaces in PBS solution or pure water
Grinstaff+[53]	Linear polyanion 	Poly(7-oxanorbornene-2 carboxylate)	Rotational rod-on-rod tribometer with cartilage against cartilage interface in PBS solution containing polymer
Benetti+[54]	Graft polymer with cyclic sidechains 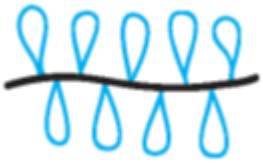	Backbone: poly(glutamic acid) Sidechain: cyclic poly(2-methyl-2-oxazoline)	Ball-on-disc microtribometer with polymer coated cartilage against cartilage interface in bovine synovial fluid containing polymer
Putnam and Bonassar+[55]	Bottlebrush-like 	Backbone: poly(acrylic acid) Sidechain: PEG	Pin-on-plate tribometer with polymer coated cartilage against bare glass surface in PBS

1.6 References

(1) Barbour KE, Helmick CG, Theis KA, Murphy LB, Hootman JM, Brady TJ, et al. Prevalence of Doctor-Diagnosed Arthritis and Arthritis-Attributable Activity Limitation — United States, 2010–2012. *MMWR. Morb. Mortal. Wkly. Rep.* **2013**, *62* (44), 869–873.

(2) Lawrence, R. C.; Felson, D. T.; Helmick, C. G.; Arnold, L. M.; Choi, H. Estimates of the Prevalence of Arthritis and Other Rheumatic Conditions in the United States, Part II. *Arthritis Rheum* **2008**, *58* (1), 26–35.

(3) Murphy, L.; Schwartz, T. A.; Helmick, C. G.; Renner, J. B.; Tudor, G.; Koch, G.; Dragomir, A.; Kalsbeek, W. D.; Luta, G.; Jordan, J. M. Lifetime Risk of Symptomatic Knee Osteoarthritis. *Arthritis Care Res.* **2008**, *59* (9), 1207–1213.

(4) Kotlarz, H.; Gunnarsson, C. L.; Fang, H.; Rizzo, J. A. Insurer and Out-of-Pocket Costs of Osteoarthritis in the US: Evidence from National Survey Data. *Arthritis Rheum.* **2009**, *60* (12), 3546–3553.

(5) Man, G. S.; Mologhianu, G. Osteoarthritis Pathogenesis - a Complex Process That Involves the Entire Joint. *J. Med. Life* **2014**, *7* (1), 37–41.

(6) Lane, N. E.; Brandt, K.; Hawker, G.; Peeva, E.; Schreyer, E.; Tsuji, W.; Hochberg, M. C. OARSI-FDA Initiative: Defining the Disease State of Osteoarthritis. *Osteoarthr. Cartil.* **2011**, *19* (5), 478–482.

(7) Lohmander, L. S.; Roos, E. M. Clinical Update: Treating Osteoarthritis. *Lancet* **2007**, *370* (9605), 2082–2084.

(8) Bjordal, J. M.; Ljunggren, A. E.; Klovning, A.; Slørdal, L. Non-Steroidal Anti-Inflammatory Drugs, Including Cyclo-Oxygenase-2 Inhibitors, in Osteoarthritic Knee Pain: Meta-Analysis of Randomised Placebo Controlled Trials. *BMJ* **2004**, *329* (7478),

1317.

(9) Alshami, A. M. Knee Osteoarthritis Related Pain: A Narrative Review of Diagnosis and Treatment. *Int. J. Health Sci. (Qassim).* **2014**, *8* (1), 85–104.

(10) O'Hanlon, C. E.; Newberry, S. J.; Booth, M.; Grant, S.; Motala, A.; Maglione, M. A.; FitzGerald, J. D.; Shekelle, P. G. Hyaluronic Acid Injection Therapy for Osteoarthritis of the Knee: Concordant Efficacy and Conflicting Serious Adverse Events in Two Systematic Reviews. *Syst. Rev.* **2016**, *5* (1), 186.

(11) Gossec, L.; Dougados, M. Intra-Articular Treatments in Osteoarthritis: From the Symptomatic to the Structure Modifying. *Ann. Rheum. Dis.* **2004**, *63* (5), 478–482.

(12) Uthman, I.; Raynauld, J.-P.; Haraoui, B. Intra - Articular Therapy in Osteoarthritis. *Postgr. Med J* **2003**, *79* (934), 449–453.

(13) Hochberg, M. C.; Perlmutter, D. L.; Hudson, J. I.; Altman, R. D. Preferences in the Management of Osteoarthritis of the Hip and Knee: Results of a Survey of Community-Based Rheumatologists in the United States. *Arthritis Care Res.* **1996**, *9* (3), 170–176.

(14) Pelletier, J.-P. and; Martel-Pelletier, J. Protective Effects of Corticosteroids on Cartilage Lesions and Osteophyte Formation in the Pond-Nuki Dog Model of Osteoarthritis. *Arthritis Rheum.* **1989**, *32* (2), 181–193.

(15) Raynauld, J.-P.; Buckland-Wright, C.; Ward, R.; Choquette, D.; Haraoui, B.; Martel-Pelletier, J.; Uthman, I.; Khy, V.; Tremblay, J.-L.; Bertrand, C.; et al. Safety and Efficacy of Long-Term Intraarticular Steroid Injections in Osteoarthritis of the Knee A Randomized, Double-Blind, Placebo-Controlled Trial. *Arthritis Rheum.* **2003**, *48* (2), 370–377.

(16) Karlsson, J.; Sjögren, L. S.; Lohmander, L. S. Comparison of Two Hyaluronan Drugs and

Placebo in Patients with Knee Osteoarthritis. A Controlled, Randomized, Double-Blind, Parallel-Design Multicentre Study. *Rheumatology (Oxford).* **2002**, *41* (11), 1240–1248.

(17) Henderson, E. B.; Smith, E. C.; Pegley, F.; Blake, D. R. Intra-Articular Injections of 750 KD Hyaluronan in the Treatment of Osteoarthritis: A Randomised Single Centre Double-Blind Placebo-Controlled Trial of 91 Patients Demonstrating Lack of Efficacy. *Ann. Rheum. Dis.* **1994**, *53* (8), 529–534.

(18) Jay, G. D. Characterization of a Bovine Synovial Fluid Lubricating Factor. I. Chemical, Surface Activity and Lubricating Properties. *Connect. Tissue Res.* **1992**, *28* (1–2), 71–88.

(19) McCutchen, C. W. The Frictional Properties of Animal Joints. *Wear* **1962**, *5* (1), 1–17.

(20) Schmidt, T. A.; Gastelum, N. S.; Nguyen, Q. T.; Schumacher, B. L.; Sah, R. L. Boundary Lubrication of Articular Cartilage: Role of Synovial Fluid Constituents. *Arthritis Rheum.* **2007**, *56* (3), 882–891.

(21) Bonnevie, E. D.; Galesso, D.; Secchieri, C.; Cohen, I.; Bonassar, L. J. Elastoviscous Transitions of Articular Cartilage Reveal a Mechanism of Synergy between Lubricin and Hyaluronic Acid. *PLoS One* **2015**, *10* (11), 1–15.

(22) Gropper, D.; Wang, L.; Harvey, T. J. Hydrodynamic Lubrication of Textured Surfaces: A Review of Modeling Techniques and Key Findings. *Tribol. Int.* **2016**, *94*, 509–529.

(23) Daniel, M. Boundary Cartilage Lubrication: Review of Current Concepts. *Wiener Medizinische Wochenschrift* **2014**, *164* (5–6), 88–94.

(24) Swann, D. A.; Radin, E. L.; Nazimiec, M.; Weisser, P. A.; Curran, N.; Lewinnekt, G. Role of Hyaluronic Acid in Joint Lubrication. *Ann. Rheum. Dis.* **1974**, No. 33, 318–326.

(25) Dahl, L.; Dahl, I. M. S.; Engstrom-Laurent, A. Concentration and Molecular Weight of Sodium Hyaluronate in Synovial Fluid from Patients with Rheumatoid Arthritis and Other

Arthropathies. *Ann.Rheum.Dis.* **1985**, *44*, 817–822.

(26) Jay, G. D.; Haberstroh, K.; Cha, C. J. Comparison of the Boundary-Lubricating Ability of Bovine Synovial Fluid, Lubricin, and Healon. *J. Biomed. Mater. Res.* **1998**, *40* (3), 414–418.

(27) Swann, D. A.; Slayter, H. S.; Silver, F. H. The Molecular Structure of Lubricating Glycoprotein-1, the Boundary Lubricant of Articular Cartilage. *J. Biol. Chem.* **1981**, *256* (11), 5921–5925.

(28) Swann, D. A.; Silver, F. H.; Slayter, H. S.; Stafford, W.; Shore, E. The Molecular Structure and Lubricating Activity of Lubricin Isolated from Bovine and Human Synovial Fluids. *Biochem. J.* **1985**, *225* (1), 195–201.

(29) Elsaid, K. A. A.; Fleming, B. C. C.; Oksendahl, H. L. L.; Machan, J. T. T.; Fadale, P. D. D.; Hulstyn, M. J. J.; Shalvoy, R. M.; Jay, G. D. D. Decreased Lubricin Concentrations and Markers of Joint Inflammation in the Synovial Fluid of Patients with Anterior Cruciate Ligament Injury. *Arthritis Rheum.* **2008**, *58* (6), 1707–1715.

(30) Rhee, D. K.; Marcelino, J.; Baker, M.; Gong, Y.; Smits, P.; Lefebvre, V.; Jay, G. D.; Stewart, M.; Wang, H.; Warman, M. L.; et al. The Secreted Glycoprotein Lubricin Protects Cartilage Surfaces and Inhibits Synovial Cell Overgrowth. *J. Clin. Invest.* **2005**, *115* (3), 622–631.

(31) Gleghorn, J. P.; Jones, A. R. C.; Flannery, C. R.; Bonassar, L. J. Boundary Mode Lubrication of Articular Cartilage by Recombinant Human Lubricin. *J. Orthop. Res.* **2009**, *27* (6), 771–777.

(32) Zappone, B.; Greene, G. W.; Oroudjev, E.; Jay, G. D.; Israelachvili, J. N. Molecular Aspects of Boundary Lubrication by Human Lubricin: Effect of Disulfide Bonds and

Enzymatic Digestion. *Langmuir* **2008**, *24* (4), 1495–1508.

(33) Chang, D. P.; Abu-Lail, N. I.; Coles, J. M.; Guilak, F.; Jay, G. D.; Zauscher, S.; Barbucci, R.; Lamponi, S.; Borzacchiello, A.; Ambrosio, L.; et al. Friction Force Microscopy of Lubricin and Hyaluronic Acid between Hydrophobic and Hydrophilic Surfaces. *Soft Matter* **2009**, *5* (18), 3438.

(34) Al-Sharif, A.; Jamal, M.; Zhang, L. X.; Larson, K.; Schmidt, T. A.; Jay, G. D.; Elsaid, K. A. Lubricin/Proteoglycan 4 Binding to CD44 Receptor: A Mechanism of the Suppression of Proinflammatory Cytokine-Induced Synoviocyte Proliferation by Lubricin. *Arthritis Rheumatol.* **2015**, *67* (6), 1503–1513.

(35) Iqbal, S. M.; Leonard, C.; C Regmi, S.; De Rantere, D.; Tailor, P.; Ren, G.; Ishida, H.; Hsu, C.; Abubacker, S.; Pang, D. S.; et al. Lubricin/Proteoglycan 4 Binds to and Regulates the Activity of Toll-Like Receptors In Vitro. *Sci. Rep.* **2016**, *6*, 18910.

(36) Alquraini, A.; Garguilo, S.; D'Souza, G.; Zhang, L. X.; Schmidt, T. A.; Jay, G. D.; Elsaid, K. A. The Interaction of Lubricin/Proteoglycan 4 (PRG4) with Toll-like Receptors 2 and 4: An Anti-Inflammatory Role of PRG4 in Synovial Fluid. *Arthritis Res. Ther.* **2015**, *17*, 353.

(37) Bao, J. P.; Chen, W. P.; Wu, L. D. Lubricin: A Novel Potential Biotherapeutic Approaches for the Treatment of Osteoarthritis. *Mol. Biol. Rep.* **2011**, *38* (5), 2879–2885.

(38) Cui, Z.; Xu, C.; Li, X.; Song, J.; Yu, B. Treatment with Recombinant Lubricin Attenuates Osteoarthritis by Positive Feedback Loop between Articular Cartilage and Subchondral Bone in Ovariectomized Rats. *Bone* **2015**, *74*, 37–47.

(39) Coles, J. M.; Zhang, L.; Blum, J. J.; Warman, M. L.; Jay, G. D.; Guilak, F.; Zauscher, S. Loss of Cartilage Structure, Stiffness, and Frictional Properties in Mice Lacking PRG4.

Arthritis Rheum. **2010**, *62* (6), 1666–1674.

(40) Elsaid, K. A.; Jay, G. D.; Chichester, C. O. Reduced Expression and Proteolytic Susceptibility of Lubricin/Superficial Zone Protein May Explain Early Elevation in the Coefficient of Friction in the Joints of Rats with Antigen-Induced Arthritis. *Arthritis Rheum.* **2007**, *56* (1), 108–116.

(41) Teeple, E.; Elsaid, K.; Fleming, B.; Jay, G. Coefficients of Friction, Lubricin, and Cartilage Damage in the Anterior Cruciate Ligament-Deficient Guinea Pig Knee. *J. Orthop. Res.* **2008**, *26* (2), 231–237.

(42) Young, A. A.; McLennan, S.; Smith, M. M.; Smith, S. M.; Cake, M. A.; Read, R. A.; Melrose, J.; Sonnabend, D. H.; Flannery, C. R.; Little, C. B. Proteoglycan 4 Downregulation in a Sheep Meniscectomy Model of Early Osteoarthritis. *Arthritis Res. Ther.* **2006**, *8* (2), R41.

(43) Elsaid, K. A.; Fleming, B. C.; Oksendahl, H. L.; Machan, J. T.; Fadale, P. D.; Hulstyn, M. J.; Shalvoy, R. M.; Jay, G. D. Decreased Lubricin Concentrations and Markers of Joint Inflammation in Synovial Fluids from Patients with Anterior Cruciate Ligament Injury. *Arthritis Rheum* **2008**, *58* (6), 1707–1715.

(44) Kosinska, M. K.; Ludwig, T. E.; Liebisch, G.; Zhang, R.; Siebert, H. C.; Wilhelm, J.; Kaesser, U.; Dettmeyer, R. B.; Klein, H.; Ishaque, B.; et al. Articular Joint Lubricants during Osteoarthritis and Rheumatoid Arthritis Display Altered Levels and Molecular Species. *PLoS One* **2015**, *10* (5), 1–18.

(45) Flannery, C. R.; Zollner, R.; Corcoran, C.; Jones, A. R.; Root, A.; Rivera-Bermúdez, M. A.; Blanchet, T.; Gleghorn, J. P.; Bonassar, L. J.; Bendele, A. M.; et al. Prevention of Cartilage Degeneration in a Rat Model of Osteoarthritis by Intraarticular Treatment with

Recombinant Lubricin. *Arthritis Rheum.* **2009**, *60* (3), 840–847.

(46) Jay, G. D.; Fleming, B. C.; Watkins, B. A.; McHugh, K. A.; Anderson, S. C.; Zhang, L. X.; Teeple, E.; Waller, K. A.; Elsaid, K. A. Prevention of Cartilage Degeneration and Restoration of Chondroprotection by Lubricin Tribosupplementation in the Rat Following Anterior Cruciate Ligament Transection. *Arthritis Rheum.* **2010**, *62* (8), 2382–2391.

(47) Jay, G. D.; Harris, D. A.; Cha, C. J. Boundary Lubrication by Lubricin Is Mediated by O-Linked β(1-3)Gal-GalNAc Oligosaccharides. *Glycoconj. J.* **2001**, *18* (10), 807–815.

(48) Huang, N.; Michel, R.; Voros, J.; Textor, M.; Hofer, R.; Rossi, A.; Elbert, D. L.; Hubbell, J. A; Spencer, N. D. Poly (l-Lysine) -g-Poly (Ethylene Glycol) Layers on Metal Oxide Surfaces : Surface-Analytical Characterization and Resistance to Serum and Fibrinogen Adsorption Poly (L-Lysine)-g-Poly(Ethylene Glycol) Layers on Metal Oxide Surfaces : Surface-An. *Langmuir* **2001**, *17* (2), 489–498.

(49) Pasche, S.; De Paul, S. M.; Vörös, J.; Spencer, N. D.; Textor, M. Poly(l-Lysine)-Graft-Poly(Ethylene Glycol) Assembled Monolayers on Niobium Oxide Surfaces: A Quantitative Study of the Influence of Polymer Interfacial Architecture on Resistance to Protein Adsorption by ToF-SIMS and in Situ OWLS. *Langmuir* **2003**, *19* (22), 9216–9225.

(50) Perry, S. S.; Yan, X.; Limpoco, F. T.; Lee, S.; Müller, M.; Spencer, N. D. Tribological Properties of Poly(L-Lysine)-Graft-Poly(Ethylene Glycol) Films: Influence of Polymer Architecture and Adsorbed Conformation. *ACS Appl. Mater. Interfaces* **2009**, *1* (6), 1224–1230.

(51) Pettersson, T.; Naderi, A.; Makuška, R.; Claesson, P. M. Lubrication Properties of Bottle-Brush Polyelectrolytes: An AFM Study on the Effect of Side Chain and Charge Density.

Langmuir **2008**, *24* (7), 3336–3347.

(52) Banquy, X.; Burdynska, J.; Lee, D. W.; Matyjaszewski, K.; Israelachvili, J. Bioinspired Bottle-Brush Polymer Exhibits Low Friction and Amontons-like Behavior. *J. Am. Chem. Soc.* **2014**, *136* (17), 6199–6202.

(53) Wathier, M.; Lakin, B. A.; Bansal, P. N.; Stoddart, S. S.; Snyder, B. D.; Grinstaff, M. W. A Large-Molecular-Weight Polyanion, Synthesized via Ring-Opening Metathesis Polymerization, as a Lubricant for Human Articular Cartilage. *J. Am. Chem. Soc.* **2013**, *135* (13), 4930–4933.

(54) Morgese, G.; Cavalli, E.; Rosenboom, J. G.; Zenobi-Wong, M.; Benetti, E. M. Cyclic Polymer Grafts That Lubricate and Protect Damaged Cartilage. *Angew. Chemie - Int. Ed.* **2018**, *57* (6), 1621–1626.

(55) Samaroo, K. J.; Mingchee Tan; Putnam, D.; Bonassar, L. J. Binding and Lubrication of Biomimetic Boundary Lubricants on Articular Cartilage. *J. Orthop. Res.* **2017**, *35*, 548–557.

(56) Gleghorn, J. P.; Jones, A. R. C.; Flannery, C. R.; Bonassar, L. J. Boundary Mode Frictional Properties of Engineered Cartilaginous Tissues. *Eur. Cells Mater.* **2007**, *14*, 20–28.

CHAPTER 2

BOUNDARY MODE LUBRICATION OF ARTICULAR CARTILAGE BY A LUBRICIN MIMETIC DIBLOCK COPOLYMER IS ARCHITECTURE DEPENDENT

2.1 Introduction

As the primary bearing surface, articular interfaces exhibit remarkable tribological function over decades of use[1]. The impressive lubricity and durability inspired the design of synthetic macromolecules that mimic the architecture of lubricating biomolecules[2–9]. However, very few synthetic polymers achieve lubrication comparable to endogenous articular surfaces, strongly supporting the need for new synthetic materials that rival the efficacy of natural materials. Here, we report the design and synthesis of a diblock copolymer with substantial lubrication capacity, whose architecture is inspired by the structure of lubricin, a natural glycoprotein that lubricates joints under boundary mode conditions (i.e., high normal load, slow speed).

Lubricin is a glycosylated protein found in synovial fluid[10], which plays a pivotal role in joint boundary mode lubrication[11,12] and the prevention of osteoarthritis[11,13,14]. Lubricin reduces the coefficient of friction (COF) of articular cartilage in the boundary mode by as much as 70 percent[12]. The potent lubrication arises from its structure: a central mucin-like domain to attract and retain water, and a cartilage-binding domain at the C-terminus to affix the molecule to the cartilage surface[15]. This architecture of lubricin is crucial to boundary mode lubrication of articular cartilage, as denaturation in either domain of lubricin causes partial or complete loss of lubrication capability[15,16]. Inspired by lubricin's architecture, we designed a diblock copolymer consisting of a large lubrication block (Mn ~ 200 kDa) to mimic the mucin-like domain of

lubricin and a small cartilage-binding block (Mn ~3 kDa) to mimic the C-terminus domain (Fig. 2.1). The lubrication domain of the diblock copolymer is made of a polyacrylic acid (PAA) backbone with polyethylene glycol (PEG) brushes, which enables the polymer to retain water and to resist compression. The binding domain is made of a PAA backbone decorated with quaternary amine groups to non-specifically interact with negatively-charged cartilage surface components such as aggrecan. Applying this polymer to lubricin-deficient bovine articular cartilage in PBS resulted in a significant reduction in COF under boundary mode conditions.

2.2 Materials and Methods

2.2.1 Materials and Equipment

All chemicals were purchased from Aldrich, or Fisher at the highest purity grade. All monomers were purified by a column filled with aluminum oxide (base or neutral) prior to use. Mica was purchased from S&J Trading Inc. as optical grade. Phosphate buffer saline (PBS) was purchased from Sigma-Aldrich. Dulbecco's Modified Eagles's medium (DMEM) was purchased from Corning cellgro. Collagenase was purchased from Worthington Biochemical Corp. Live/dead assay reagents were purchased from Life Technologies. The ^{1}H NMR spectra were performed on an Inova 400 MHz spectrometer with deuterated chloroform or deuterium oxide as the solvent. Broad or overlapping peaks, noted in spectra of polymers, are denoted "br". Degree of polymerization (DP) was determined by initial monomer to chain transfer agent (CTA) ratio and monomer conversion. Gel permeation chromatography (GPC) was performed with phosphate buffer saline (pH 7.4) at a flow rate of 0.8 ml/min. Using a Waters gel permeation chromatography system equipped with three Waters UltrahydrogelTM columns in series (2000 Å, 500 Å, and, 250 Å) at 30 °C, the molecular weights were measured against poly (methacrylic acid), sodium salt standards (1,670 to 110,000 g/mol). The hydrodynamic size was measured by

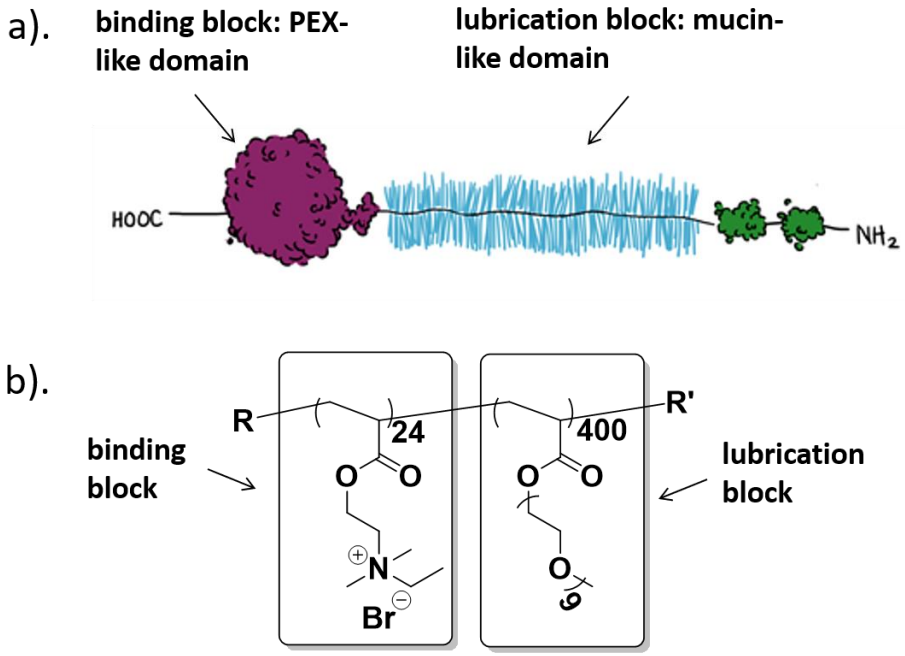

Figure 2.1. (a) Schematic representation of lubricin, the native boundary mode lubricant in synovial fluid showing the PEX-like cartilage binding domain and the mucin-like lubricating domain; (b) the synthetic diblock copolymer mimetic of lubricin showing the molecular compositions that mimic the functional domains of lubricin.

dynamic light scattering method using Malvern Zetasizer Nano ZS at concentration of 3 mg/ml in PBS at 25 °C.

2.2.2 Polymer Synthesis

The diblock copolymer was synthesized in three steps, as shown in Scheme 1. Starting with RAFT polymerization of 2-(dimethylamino) ethyl acrylate, a precursor "pre-binding" domain was produced[17]. Subsequent reversible addition-fragmentation chain-transfer (RAFT) polymerization of poly(ethylene glycol) methyl ether acrylate (Mn 480), using the "pre-binding" domain as the macro-initiator, added the lubrication domain to the copolymer. Finally, the tertiary amines in the "pre-binding" cartilage binding domain precursor were converted to quaternary ammonia by treatment with an excess of ethyl bromide to give the final product (Mn~200 kDa, PDI=1.6). The lubrication block only and the binding block only polymers were synthesized by one-step RAFT polymerization of the corresponding monomers. The random copolymer was synthesized by the RAFT polymerization of the mixture of two monomers followed by conversion of tertiary amine into quaternary amine.

A typical reaction scheme to produce a diblcok copolymer (qPDMAEA$_{24}$-PEGMA$_{400}$) is as follows: A mixed solution of DMAEA (4.30 g, 30 mmol), ACPA (14.0 mg, 0.05 mmol), and CPADB (139.5 mg, 0.5 mmol) in 5 mL of anisole was deoxygenated by 5 freeze-vacuum-thaw cycles before it was heated to 70 °C. The reaction was sealed and stirred for 48 h before it was quenched in a liquid nitrogen bath. The residue polymer was diluted with/dissolved in dichloromethane (DCM) first and then purified by precipitation in hexane (repeated 5 times). In the following step, PEGMEA (3.46 g, 7.2 mmol) was added to a solution containing PDMAEA24 **(**30.9 mg, 0.009 mmol), and ACPA (0.5 mg, 0.0018 mmol) in 6 ml of anisole. The mixture was deoxygenated by 5 freeze-vacuum-thaw cycles before it was heated to 65 °C. The

reaction was sealed and stirred for 8 h before it was quenched in a liquid nitrogen bath. The residual polymer was diluted with/dissolved in DCM first and then purified by precipitation in hexane (repeated 5 times). The obtained product from the second step was then converted into the final product by dropwise addition of ethyl bromide (0.3 ml, 4,0 mmol) into a solution containing $PDMAEA_{24}$-$PEGMEA_{400}$ (865.9 mg) in 3 ml of acetone at 0 °C. The mixture was stirred for 48 h at room temp and was then concentrated by evaporating the solvent with a dry nitrogen flow. The residue was dissolved in 3 ml of methanol and purified by hexane precipitation (repeated 5 times). The product was then dissolved in DI water and further purified by dialysis using Spectra/Por regenerated cellulose dialysis tubing (2 kDa MWCO) against DI water for additional 48 hours before lyophilization. All the intermediates and final products were characterized by ^{1}H NMR and GPC. Characterization results are listed in the Appendix.

2.2.3 Tribological Testing

Friction coefficients were measured on our custom-built tribometer[18]. Cartilage samples were obtained from the patellofemoral groove of neonatal (1-3 day old) bovine stifles. Shaped into a cartilage disc (6 mm in diameter by 2 mm high) by biopsy punch, samples were incubated in 1.5 M NaCl solution for 30 min, in PBS for additional 60 min, and then in polymer (3 mg/ml in PBS for diblock copolymer, equivalent molar for binding block only and lubrication block only) solution for 0-120 min[19]. The cartilage samples were loaded onto the tribometer against a polished glass flat counterface in a PBS bath with a tilt pad configuration. Before each friction test, samples were compressed to 30% strain and depressurized to average normal load of 3.4 N within 60 min. After the fluid pressure reached equilibrium, the glass counterface was reciprocated at a linear oscillation speed of 0.3 mm/s. Both the normal load and friction force were measured by a biaxial load cell. Coefficients were calculated as ratios of average friction

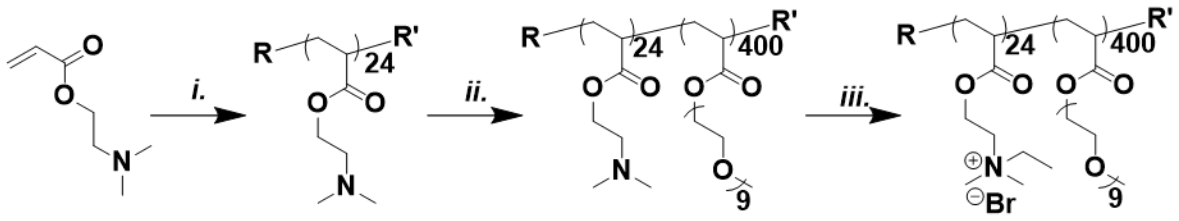

Scheme 2.1. Synthesis of lubricin-mimetic diblock copolymer. aKey: i. ACPA, CPADB, anisole, 70°C. ii. ACPA, DMAEA, anisole, 65°C. iii. EtBr, acetone, r.t.

force to equilibrium normal load during the sliding and averaged for both the forward and reverse sliding directions.

2.2.4 Surface Force Apparatus Experiment

Thin, homogeneous pieces of freshly cleaved, silvered mica were glued silver-side down onto semi-cylindrical fused silica discs (R=1cm and R=2cm) with UV curing glue (Norland 61). The surfaces were mounted opposing each other in a cross-cylindrical configuration in the SFA. After mounting, 50 µl of 3 mg/ml polymer solution in PBS was injected between the surfaces and incubated for one hour. The surfaces were then rinsed in PBS, and a droplet of PBS was injected, leaving only a surface-bound layer of polymer for friction and film thickness measurements.

Once samples were prepared in the surface force apparatus (SFA), both normal and friction force measurements were performed[20]. For normal force measurements, the lower surface was mounted on a double-cantilever spring (k=1650N/m and k=185N/m) for normal force detection. For friction force measurements, the lower spring was mounted on a double cantilever spring (k=1650N/m) attached to a piezoelectric bimorph slider. The bimorph slider was sheared across the upper surface which was mounted on a semiconductor strain gauge at 30µm/s to detect friction. Friction measurements were measured under incrementally increasing loads and friction coefficients were calculated using the slope of the friction vs. load data, $\Delta F_{friction} / \Delta F_{Load}$.

Once samples were prepared in the SFA, the surfaces were brought together using a stepper motor at speeds <10 nm/s. The interference pattern, known as fringes of equal chromatic order (FECO) were recorded and analyzed to determine both the uncompressed film thickness (the film thickness where surface interaction is initially detected) and the compressed film thickness[20].

2.2.5 Cytotoxicity Test

Primary articular chondrocytes were isolated from the femoral condyle of neonatal (1-3 day) bovine stifles. The cartilage was digested in a solution of DMEM with 1% antibiotics and 0.25% collagenase for 16-18 h. The solution was then filtered through a 100 μm cell strainer and the cells were centrifuged at 1500 rpm for 7 min. The supernatant was aspirated, and the cells were washed twice with 1X PBS and centrifugation at 1500 rpm for 5 min.

Cell viability was determined by using a live/dead assay with ethidium homodimer and calcein AM solutions. Primary articular chondrocyte (25,000 cells/well) or fibroblast (7500 cells/well) were pre-seeded in 96 well plates for 48 hours, followed by treatment with a varied concentration of polymer (0-12 mg/ml) contained DMEM solution for additional 24 hour before the assay. Images of the stained cells were obtained using fluorescence microscopy.

2.2.6 Statistics

One-way analysis of variance (ANOVA) and Student's t test were used to determine the statistical difference of the tribological results of polymer solution and controls on both articular cartilage and mica surfaces. Coefficients of friction generated in the competitive inhibition study and dosing study were fit in a sigmoidal dose-responsive curve: $COF = \frac{(COF_{max} - COF_{min})}{1+10^{(IC_{50}\ or\ EC_{50} - C)*Hillslop}} + COF_{min}$, respectively, where COF_{max} and COF_{min} are the maximum and minimum coefficient of friction, IC_{50} and EC_{50} are the concentration of inhibitor or drug that gives half-maximal response, C is the concentration of inhibitor or polymer, and $Hillslop$ describes the steepness of curves. Binding kinetic results were fit in a first order decay curve: $COF = (COF_o - COF_{min}) \times \exp(-t/tau) + COF_{min}$, respectively, where COF_o is the coefficient of friction in the absent of polymer binding, COF_{min} is the

minimal coefficient of friction at maximal polymer binding, and tau is the binding time constant. Data are presented as mean ± standard deviation (SD). All analyses were carried out using Prism GraphPad 7 with calculated p values being considered significant for $p < 0.05$.

2.3 Results

2.3.1 Cartilage Lubrication by Diblock Copolymer

To evaluate the polymer as a synthetic boundary mode lubricant, we assessed its tribological characteristics using a custom-built tribometer. Incubating the stripped cartilage with the diblock copolymer solution resulted in a decrease in COF from 0.391 ± 0.020 to 0.088 ± 0.039 (n = 4-11, $p < 0.0001$), which is equivalent to lubricin-treated groups (COF = 0.093 ± 0.011[12] shown as the dashed line in Fig. 2.2). To establish the importance of the diblock architecture on lubrication, the individual cartilage-binding and cartilage lubricating domains were also evaluated under the same conditions. Neither individual domain decreased COF, supporting the premise that both the binding and lubricating blocks of the copolymer are necessary to lubricate cartilage under boundary mode conditions.

2.3.2 Competitive Inhibition by Binding Block

The importance of the binding block to lubrication and its interaction with the cartilage surface was further demonstrated by a competitive binding analysis. The COFs of cartilage samples were measured after exposure to solutions composed of combinations of the binding block and the diblock copolymer in molar ratios ranging from 100:1 to 1:1 ([binding block : diblock copolymer]). The COFs of samples incubated with different molar ratios of [binding block : diblock copolymer] exhibited a dose-response behavior (Fig. 2.3), wherein higher concentrations of the binding domain inhibited lubrication by the diblock copolymer, suggesting

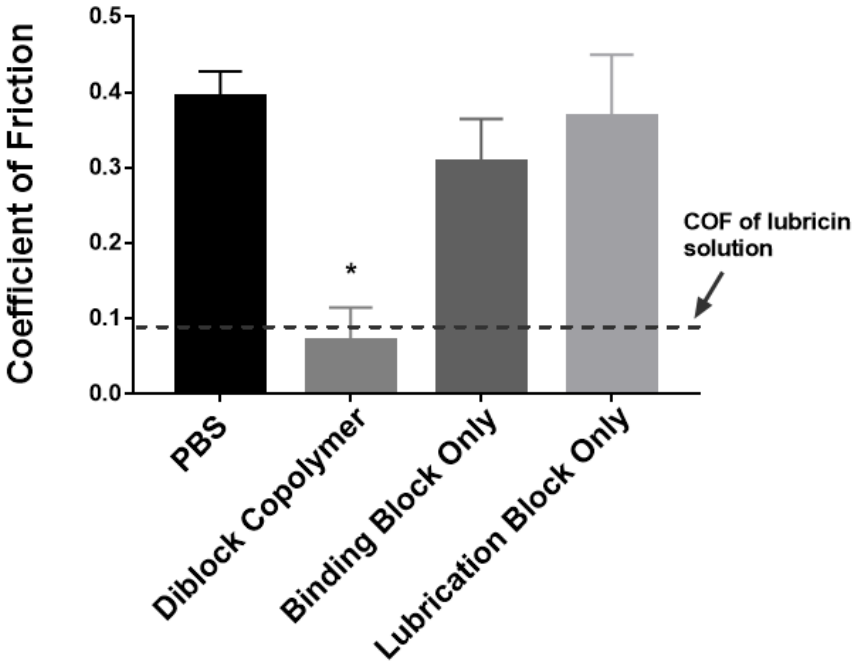

Figure 2.2. The lubricin-mimetic diblock copolymer significantly decreases COF of articular cartilage compared to samples treated with PBS, binding block only, or lubrication block only ($p<0.0001$). Dashed line represents COF of samples tested in recombinant human lubricin solution at 50 μg/ml.

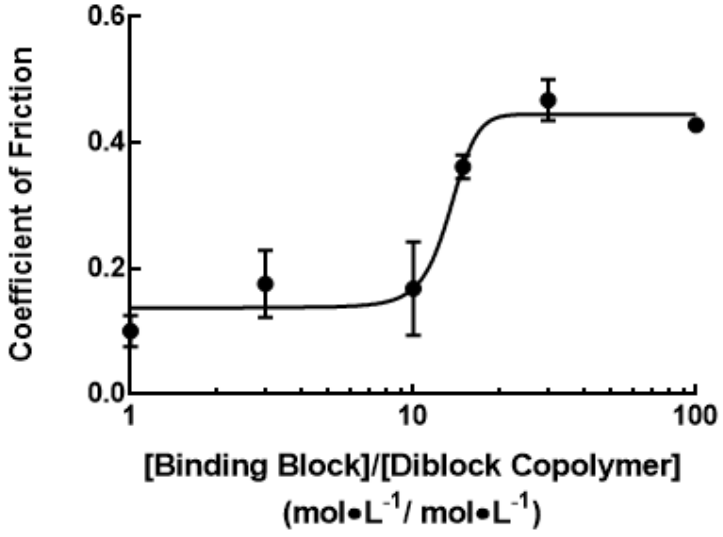

Figure 2.3. Competitive inhibition analysis showing the binding block acts as an inhibitor of lubrication when mixed with the diblock copolymer at varying molar ratios. Line is a model fit of a sigmoidal dose-response relationship (R^2=0.87, IC_{50}=13.45, n = 3-9, error bars represent ± 1 standard deviation).

that intimate interaction of the polymers with the cartilage surface is crucial for effective cartilage lubrication.

2.3.3 The Importance of Architecture

To further establish the importance of the diblock copolymer architecture on lubrication, a random copolymer with the same monomer composition as the diblock copolymer was synthesized. The failure of this polymer to lubricate articular cartilage under the same tribological conditions (Fig. 2.4a) further emphasized the importance of the diblock copolymer architecture. An accompanying study on the effect of molecular architecture on binding and lubrication was completed using negatively charged mica surfaces in a SFA to show that the lubricity characteristics were consistent between different surface types. Mica surfaces that were pre-incubated with the polymers in solution at 3 mg/ml for 120 min were sheared in PBS under boundary conditions (6 MPa compression load and linear oscillation speed of 30 μm/s). Similar to the results obtained for cartilage tribology, the measured COFs were 0.493 ± 0.082 for the random copolymer and 0.122 ± 0.035 for the diblock copolymer (Fig. 4a. n = 3-4, *$p < 0.0001$). Polymer film thickness on the mica surface was also characterized by measuring normal force as a function of distance between surfaces. At the onset of interaction, the diblock copolymer shows an uncompressed film thickness (61.2 ± 2.6 nm) that is twice as thick as its hydrodynamic size (24.8 ± 0.3 nm), suggesting a double molecular layer coating between the two mica surfaces; whereas the random copolymer exhibited a binary film thickness distribution (36.0 ± 13.5 nm) that matches with either 1 or 2 molecular layer thickness (hydrodynamic size: 21.4 ± 1.2 nm), indicating an insufficient coating on both mica surfaces. Under compression, the random copolymer also showed a much smaller thickness (3.6 ± 0.7 nm vs. 10.4 ± 0.6 nm) in comparison to the diblock copolymer, which approaches the distance measured between bare mica surfaces

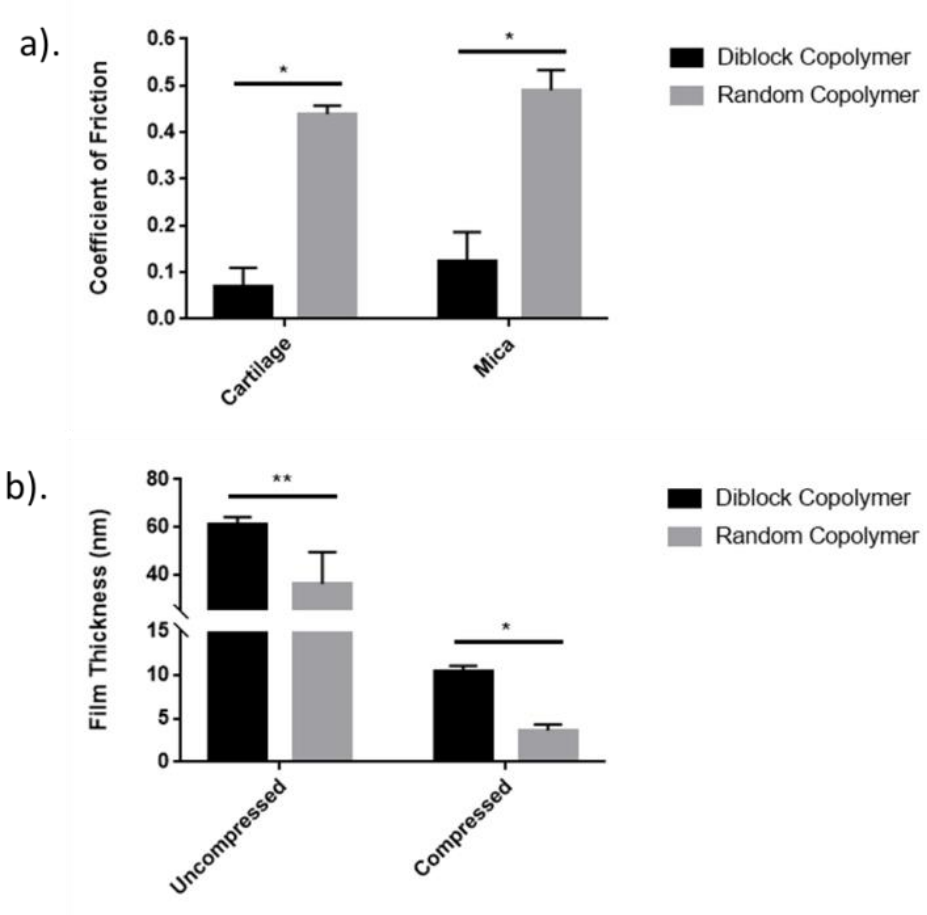

Figure 2.4. a) Random copolymer with the same composition but different architecture failed to lubricate cartilage and mica in comparison to the diblock copolymer architecture (n = 4-6, *: $p<0.0001$). b) Mica samples treated with random copolymer had smaller film thickness under both uncompressed and compressed conditions in comparison to diblock copolymer using SFA measurement (n = 3-5, *: $p<0.0001$, **: $p<0.01$), indicating a less efficient binding of random copolymer to the mica surface.

in PBS (data not shown). These data suggest that while both polymers formed a layer on the mica surface at the beginning of the experiment, the weak electrostatic interaction between the random copolymer and the mica surface failed to maintain the polymer film or to support the normal force throughout the analysis, thereby allowing the polymers to be forced out of the contact zone during compression. The boundary lubrication mode is defined as when the frictional properties are primarily governed by solid-solid interactions[21], and therefore largely dependent on the topology and chemical properties of the opposing surfaces. It is critical for a boundary mode lubricant to form a molecular layer that effectively coats the cartilage surface and that supports the normal load. The individual positively-charged quaternary ammonia groups that are randomly distributed in the polymer backbone were not able to efficiently bind to either cartilage or mica surfaces, which again, demonstrates the importance of the diblock architecture for lubrication.

2.3.4 Cartilage Lubrication Effectiveness

To better understand the effectiveness of the diblock copolymer on cartilage lubrication, some key lubrication characteristics were measured and compared to those of natural lubricin. Specifically, a dosing study was performed using cartilage samples that were treated with polymer solutions ranging from 0.01 to 10 mg/ml. The COFs (Fig. 2.5a) exhibited a dose-response behavior ($R^2 = 0.89$), which at the higher concentrations ($EC_{50} = 0.404$ mg/ml) were effectively reduced to a level comparable to that of naturally lubricated cartilage. Also, the binding kinetics of the diblock copolymer to the cartilage surface was measured in which cartilage samples were incubated at a saturation concentration (1 mg/ml) of polymer over time. When fit to a one-phase decay model ($R^2 = 0.95$), the binding kinetics curve (Fig. 2.5b) revealed

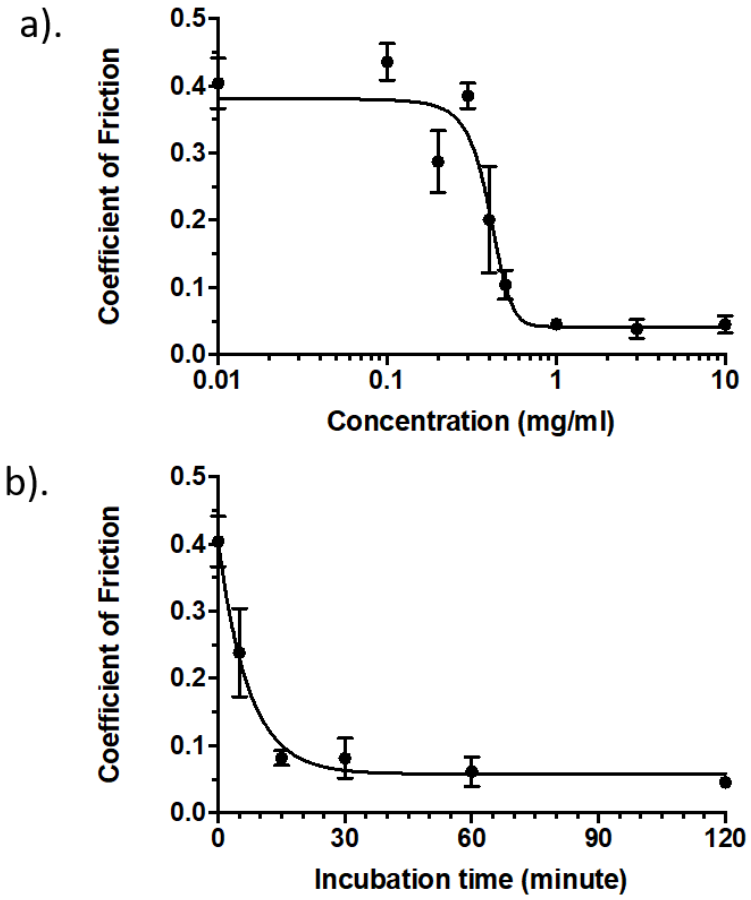

Figure 2.5. Dose-response curve (a) and binding kinetics curve (b) of diblock copolymer (n = 4-6). Dose-response curve is a model fit of a sigmoidal dose-response relationship (R^2=0.893, EC_{50}=0.404 mg/ml, n = 4-6, error bars represent ± 1 standard deviation). Binding kinetic curve is a model fit of a first-order decay relationship (R^2=0.948, tau = 7.19 min, n = 4-6, error bars represent ± 1 standard deviation).

a binding time constant (τ) of 7.19 min, which is comparable to that of natural lubricin (~9 min[12]).

2.3.5 Cytotoxicity Evaluation

The cytotoxicity of the diblock copolymer was assessed using the NIH 3T3 fibroblast cell line and primary chondrocytes isolated from bovine cartilage. In a live/dead assay, lives cells were labelled green with Calcein AM and dead cells were labelled red with ethidium homodimer-1. Minimal cell death was observed in both types of cells when incubated with polymer containing media at a varied concentration for 24 hours (Fig. 2.6).

2.4 Discussion

Synthetic polymers with structures that mimic natural biolubricants have been extensively studied over the past few decades. Inspired by natural bottle-brush polyelectrolytes, Spencer et al. explored a range of mucin analogues featured with a polylysine backbone and grafted PEG[2,3,22], or dextran[23] side chains to reduce the COFs on mica surfaces. Israelachvili and coworkers also reported a bioinspired bottle brush polymer that exhibited extremely low friction and Amontons-like behavior characterized by SFA. Both investigations report effective synthetic lubricants using pristine mica surfaces. However, while these materials lubricated the mica surface, the physiological relevance of the results is unknown. Grinstaff *et al* reported a more physiologically relevant polyanionic biolubricant that performs similar to synovial fluid in an *ex vivo* human cartilage mode[7]. By mimicking the structure of hyaluronic acid, this polymer reduced the friction at the interface of cartilage and demonstrated its potential in joint lubrication as a new type of viscosupplement. In our previous work, an analogue of bottle-brush polymers with a mucin-like structure successfully lubricated articular cartilage under boundary mode condition with COF

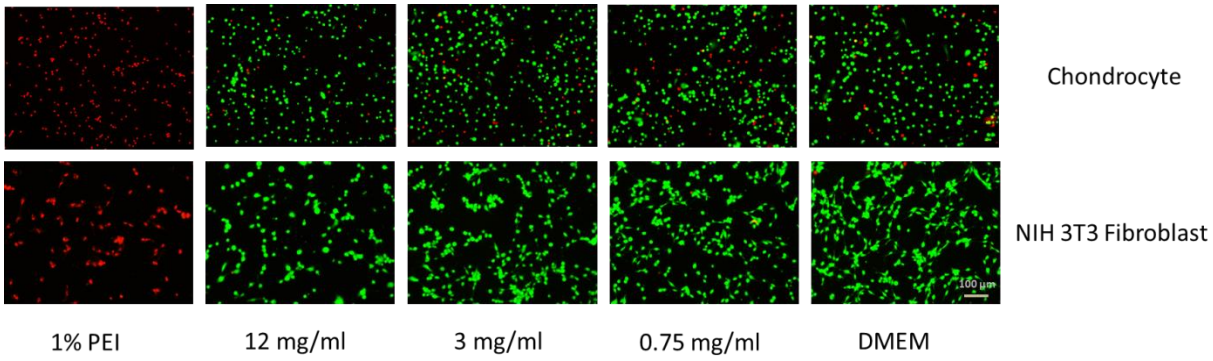

Figure 2.6. Live/dead assay of chondrocyte (top) and fibroblast (bottom) incubated with diblock copolymer. Live cells stained with Calcein-AM (green) and dead cells with EthD-1 (red).

ranging from 0.140 ± 0.024 to 0.248 ± 0.030, and binding time constants ranging from 20 to 39 min[24]. However, the cartilage binding mechanism(s) that led to these results were unclear and the low binding limited their further application. In this work, where both key lubrication characteristics were engineered into the lubricant by adopting a diblock architecture that facilitates binding and localization of the polymer to the cartilage surface, we show the importance of polymer architecture to lubrication. This approach could serve as a molecular design guide for future synthetic lubricants with even greater efficacy.

In summary, a diblock copolymer with a bio-inspired lubricin-mimetic structure successfully lubricates articular cartilage surfaces in the boundary mode as effectively and efficiently as natural lubricin. This work demonstrates the importance of the polymer architecture to its tribological properties and the necessity for the co-existence of binding and lubrication blocks for effective lubrication under these conditions. Results of this study highlight the potential of a lubricin-mimetic polymer as a therapeutic to prevent osteoarthritis by significantly reducing friction in the joint.

2.5 References

(1) Ateshian, G. A. The Role of Interstitial Fluid Pressurization in Articular Cartilage Lubrication. *J. Biomech.* **2009**, *42* (9), 1163–1176.

(2) Perry, S. S.; Yan, X.; Limpoco, F. T.; Lee, S.; Müller, M.; Spencer, N. D. Tribological Properties of Poly(L-Lysine)-Graft-Poly(Ethylene Glycol) Films: Influence of Polymer Architecture and Adsorbed Conformation. *ACS Appl. Mater. Interfaces* **2009**, *1* (6), 1224–1230.

(3) Mu, M.; Lee, S.; Spikes, H. A.; Spencer, N. D. The Influence of Molecular Architecture on the Macroscopic Lubrication Properties of the Brush-like Co-Polyelectrolyte Poly (L-Lysine)-g-Poly (Ethylene Glycol) (PLL-g-PEG) Adsorbed on Oxide Surfaces. *Tribol. Lett.* **2003**, *15* (4), 395–405.

(4) Pettersson, T.; Naderi, A.; Makuška, R.; Claesson, P. M. Lubrication Properties of Bottle-Brush Polyelectrolytes: An AFM Study on the Effect of Side Chain and Charge Density. *Langmuir* **2008**, *24* (7), 3336–3347.

(5) Banquy, X.; Burdynska, J.; Lee, D. W.; Matyjaszewski, K.; Israelachvili, J. Bioinspired Bottle-Brush Polymer Exhibits Low Friction and Amontons-like Behavior. *J. Am. Chem. Soc.* **2014**, *136* (17), 6199–6202.

(6) Raviv, U.; Giasson, S.; Kampf, N.; Gohy, J.-F.; Jérôme, R.; Klein, J. Lubrication by Charged Polymers. *Nature* **2003**, *425* (6954), 163–165.

(7) Wathier, M.; Lakin, B. A.; Bansal, P. N.; Stoddart, S. S.; Snyder, B. D.; Grinstaff, M. W. A Large-Molecular-Weight Polyanion, Synthesized via Ring-Opening Metathesis Polymerization, as a Lubricant for Human Articular Cartilage. *J. Am. Chem. Soc.* **2013**, *135* (13), 4930–4933.

(8) Zhulina, E. B.; Rubinstein, M. Lubrication by Polyelectrolyte Brushes. *Macromolecules* **2014**, *47* (16), 5825–5838.

(9) Lawrence, A.; Xu, X.; Bible, M. D.; Calve, S.; Neu, C. P.; Panitch, A. Synthesis and Characterization of a Lubricin Mimic (MLub) to Reduce Friction and Adhesion on the Articular Cartilage Surface. *Biomaterials* **2015**, *73*, 42–50.

(10) Swann, D. A.; Slayter, H. S.; Silver, F. H. The Molecular Structure of Lubricating Glycoprotein-1, the Boundary Lubricant of Articular Cartilage. *J. Biol. Chem.* **1981**, *256* (11), 5921–5925.

(11) Jay, G. D.; Waller, K. A. The Biology of Lubricin: Near Frictionless Joint Motion. *Matrix Biol.* **2014**, *39*, 17–24.

(12) Gleghorn, J. P.; Jones, A. R. C.; Flannery, C. R.; Bonassar, L. J. Boundary Mode Lubrication of Articular Cartilage by Recombinant Human Lubricin. *J. Orthop. Res.* **2009**, *27* (6), 771–777.

(13) Jay, G. D.; Fleming, B. C.; Watkins, B. A.; McHugh, K. A.; Anderson, S. C.; Zhang, L. X.; Teeple, E.; Waller, K. A.; Elsaid, K. A. Prevention of Cartilage Degeneration and Restoration of Chondroprotection by Lubricin Tribosupplementation in the Rat Following Anterior Cruciate Ligament Transection. *Arthritis Rheum.* **2010**, *62* (8), 2382–2391.

(14) Young, A. A.; McLennan, S.; Smith, M. M.; Smith, S. M.; Cake, M. A.; Read, R. A.; Melrose, J.; Sonnabend, D. H.; Flannery, C. R.; Little, C. B. Proteoglycan 4 Downregulation in a Sheep Meniscectomy Model of Early Osteoarthritis. *Arthritis Res. Ther.* **2006**, *8* (2), R41.

(15) Zappone, B.; Greene, G. W.; Oroudjev, E.; Jay, G. D.; Israelachvili, J. N. Molecular Aspects of Boundary Lubrication by Human Lubricin: Effect of Disulfide Bonds and

Enzymatic Digestion. *Langmuir* **2008**, *24* (4), 1495–1508.

(16) Jay, G. D.; Harris, D. A.; Cha, C. J. Boundary Lubrication by Lubricin Is Mediated by O-Linked β(1-3)Gal-GalNAc Oligosaccharides. *Glycoconj. J.* **2001**, *18* (10), 807–815.

(17) Pelet, J. M.; Putnam, D. An In-Depth Analysis of Polymer-Analogous Conjugation Using DMTMM. *Bioconjug. Chem.* **2011**, *22* (3), 329–337.

(18) Gleghorn, J. P.; Bonassar, L. J. Lubrication Mode Analysis of Articular Cartilage Using Stribeck Surfaces. *J. Biomech.* **2008**, *41* (9), 1910–1918.

(19) Gleghorn, J. P.; Jones, A. R. C.; Flannery, C. R.; Bonassar, L. J. Boundary Mode Frictional Properties of Engineered Cartilaginous Tissues. *Eur. Cells Mater.* **2007**, *14*, 20–28.

(20) Andresen Eguiluz, R. C.; Cook, S. G.; Tan, M.; Brown, C. N.; Pacifici, N. J.; Samak, M. S.; Bonassar, L. J.; Putnam, D.; Gourdon, D. Synergistic Interactions of a Synthetic Lubricin-Mimetic with Fibronectin for Enhanced Wear Protection. *Front. Bioeng. Biotechnol.* **2017**, *5*, 36.

(21) Daniel, M. Boundary Cartilage Lubrication: Review of Current Concepts. *Wiener Medizinische Wochenschrift* **2014**, *164* (5–6), 88–94.

(22) Ramakrishna, S. N.; Espinosa-Marzal, R. M.; Naik, V. V; Nalam, P. C.; Spencer, N. D. Adhesion and Friction Properties of Polymer Brushes on Rough Surfaces: A Gradient Approach. *Langmuir* **2013**, *29* (49), 15251–15259.

(23) Perrino, C.; Lee, S.; Choi, S. W.; Maruyama, A.; Spencer, N. D. A Biomimetic Alternative to Poly(Ethylene Glycol) as an Antifouling Coating: Resistance to Nonspecific Protein Adsorption of Poly(L-lysine)-*graft*-dextran. *Langmuir* **2008**, *24* (16), 8850–8856.

(24) Samaroo, K. J.; Mingchee Tan; Putnam, D.; Bonassar, L. J. Binding and Lubrication of

Biomimetic Boundary Lubricants on Articular Cartilage. *J. Orthop. Res.* **2016**.

CHAPTER 3

BINDING BLOCK LENGTH DETERMINES THE LUBRICATION BEHAVIORS OF LUBRICIN MIMETICS

3.1 Introduction

Friction between sliding surfaces in healthy joints is often at levels that engineers can only envy. The remarkable tribological properties of articular cartilage outperform most synthetic surfaces[1]. Much effort on illustrating the lubrication mechanism of the healthy joint has revealed several mechanical factors, most notably, lubrication by macromolecules in the synovial fluid[2–5]. The main macromolecules attributed to synovial fluid lubrication are lubricin[6] (also known as proteoglycan-4 and superficial zone protein) and hyaluronic acid[7] (HA). Previous studies using HA have revealed its role in maintaining the viscosity of synovial fluid[8], but did not support its lubricating properties in the boundary mode when studied *in vitro*[9,10]. Lubricin is a glycosylated protein considered to be the principal boundary mode lubricant in synovial fluid[4,11,12]. Even at relatively low concentrations, the molecule efficiently reduces the coefficient of friction (COF) of articular cartilage in the boundary mode by as much as 70 percent[3]. This effect encouraged its application for the treatment of osteoarthritis (OA) which is characterized by damaged articular cartilage and increased joint stiffness[13,14]. Lubricin levels in diseased or injured joints are reduced for up to 12 months in animal models of OA and clinical trials, including rat[15], guinea pig[16], sheep[17], and human patients[18]. The reintroduction of lubricin into OA joints has demonstrated its therapeutic effect in delaying the progression of disease by maintaining low

joint friction[4,19], slowing down the degradation of cartilage[16,20], and preventing remodeling of subchondral bone[21].

Despite its therapeutic potential, the clinical application of lubricin is hindered by high production cost resulting from multiple amino acid repeats in the protein core, as well as the high degree of glycosylation[22]. Considerable work[23–25] has been done to further the development of recombinant lubricin, but no product has yet to be commercialized.

The remarkable lubricating capacity of lubricin and its lack of availability have inspired the design of synthetic lubricants to mimic its function[26,27]. The potent lubricating ability of lubricin arises from its structure: a central mucin-like domain to attract and retain water[28], and a cartilage-binding domain at the C-terminus to affix the molecule to the cartilage surface[29]. Previous work by our group designed a diblock copolymer with lubricin inspired architecture and demonstrated its comparable lubricating ability to natural lubricin. The diblock copolymer consists of a large lubrication block (Mn ~ 200 kDa) to mimic the mucin-like domain of lubricin and a small cartilage-binding block (Mn ~3 kDa) to mimic the C-terminus domain (Fig. 2.1). The lubrication domain of the diblock copolymer is made of a polyacrylic acid (PAA) backbone with polyethylene glycol (PEG) brushes, enabling the polymer to retain water and resist compression. The binding domain is made of a PAA backbone decorated with quaternary amine groups to non-specifically interact with negatively-charged cartilage surface components such as aggrecan. Applying this polymer to lubricin-deficient bovine articular cartilage resulted in a significant reduction in COF under boundary mode conditions that was comparable to lubricin in the same system.

The inspiring results, that a synthetic lubricant rivaled the power of the most highly regarded natural lubricant, motivated further investigation into its molecular architecture. Earlier studies in

the literature using bottlebrush-like polymers revealed that friction forces measured under boundary mode conditions were affected by the length and the grafting density of the PEG side chain[30,31]. While the influence of the bottlebrush-like architecture is well understood, less is known regarding how the binding of brush polymers influences tribological properties, such as binding time constant and friction force. In this report, we first compared the lubricating ability of the diblock copolymers decorated with two types of binding functional groups in the binding block (i.e. tertiary amine v.s. quaternary amine). Polymers decorated with both types of amine successfully lubricated the articular cartilage surface using freshly prepared polymer solution. However, whereas polymer functionalized with quaternary amine maintained a low friction over time, the tertiary amine-based polymers gradually lost lubrication. This phenomenon suggested instability of the tertiary amine-based polymer in aqueous solution, which prevented its further application as a synthetic lubricant. This hypothesis was supported by an NMR study that identified the hydrolysis product and revealed a good correlation between the rate of hydrolysis and reduction of lubrication. In the second part of this chapter, we report a systematic exploration of the key molecular architecture parameters of this class of synthetic lubricant by presenting the dependence of tribological properties on the size of the binding and lubrication blocks. Results for two series of polymer samples, distinguished by the lubrication block size (degree of polymerization (DP) = 200 or 400), are reported; within each series, the polymers differed only in the binding block size (DP = 12, 24, 54, or 90). By varying only the length of each block of the copolymers, it was observed that the lubricating ability is solely dependent on the binding block in a manner intimately tied to the number of cartilage binding groups.

3.2 Materials and Methods

3.2.1 Materials and Equipment

All chemicals were purchased from Sigma-Aldrich, or Fisher at the highest purity grade. Monomers were purified by a column filled with aluminum oxide (basic or neutral) obtained from Sigma-Aldrich prior to use. Phosphate buffered saline (PBS) was obtained from Sigma-Aldrich. The ^{1}H NMR spectra were performed on an Inova 400 MHz spectrometer with deuterated chloroform or deuterium oxide as the solvent. Broad or overlapping peaks, noted in the spectra of polymers, are denoted "br". Degree of polymerization (DP) was determined by initial monomer to chain transfer agent (CTA) ratio and monomer conversion ratio. Gel permeation chromatography (GPC) was performed with PBS (pH 7.4) at a flow rate of 0.8 ml/min. Using a Waters gel permeation chromatography system equipped with three Waters Ultrahydrogel^{TM} columns in series (2000 Å, 500 Å, and, 250 Å) at 30 °C. The molecular weights were measured against poly (methacrylic acid), sodium salt standards (1,670 to 110,000 g/mol). The hydrodynamic sizes of the polymers were measured by dynamic light scattering using a Malvern Zetasizer Nano ZS at concentration of 3 mg/ml in PBS solution at 25 °C.

3.2.2 Polymer Synthesis

The diblock copolymer was synthesized in three steps (Scheme 2.1). Starting with reversible addition-fragmentation chain-transfer (RAFT) polymerization of 2-(dimethylamino) ethyl acrylate (DMAEA) by using 4,4'-azobis 4-cyanopentanoic acid (ACPA) as initiator and 4-cyanopentanoic acid dithiobenzoate (CPADB) as chain transfer reagent, a macroinitiator as precursor binding block was produced. Subsequent RAFT polymerization of poly(ethylene glycol) methyl ether acrylate (PEGMA, M_n 480), using the macroinitiator, added the lubrication domain to the copolymer. Finally, the tertiary amines in the cartilage binding block precursor were converted to quaternary amine by treatment with an excess of ethyl bromide to give the final product.

A typical reaction scheme to produce a diblock copolymer (e.g. qPDMAEA$_{24}$-PEGMEA$_{400}$) is as follows: A mixed solution of DMAEA (4.30 g, 30 mmol), ACPA (14.0 mg, 0.05 mmol), and CPADB (139.5 mg, 0.5 mmol) in 5 mL of anisole was deoxygenated by 5 freeze-vacuum-thaw cycles before it was heated to 70 °C. The reaction was sealed and stirred for 48 h before it was quenched in a liquid nitrogen bath. The product poly(dimethylamino) ethyl acrylate (PDMAEA$_{24}$) was diluted with/dissolved in dichloromethane (DCM) first and then purified by precipitation in hexane (repeated 5 times). In the following step, PEGMEA (3.46 g, 7.2 mmol) was added to a solution containing PDMAEA$_{24}$ **(**30.9 mg, 0.009 mmol), and ACPA (0.5 mg, 0.0018 mmol) in 6 ml of anisole. The mixture was deoxygenated by 5 freeze-vacuum-thaw cycles before it was heated to 65 °C. The reaction was sealed and stirred for 8 h before it was quenched in a liquid nitrogen bath. The residual polymer was diluted with/dissolved in DCM first and then purified by precipitation in hexane (repeated 5 times). The obtained product was then converted into the final product by dropwise addition of ethyl bromide (0.3 ml, 4,0 mmol) into a solution containing PDMAEA$_{24}$-PEGMEA$_{400}$ (865.9 mg) in 3 ml of acetone at 0 °C. The mixture was stirred for 48 h at room temperature and was then concentrated by evaporating the solvent with a dry nitrogen flow. The residue was dissolved in 3 ml of methanol and purified by precipitation in hexane (repeated 5 times). The final product was then dissolved in DI water and further purified by dialysis using Spectra/Por regenerated cellulose dialysis tubing (MWCO 2 kDa) against DI water for additional 48 hours before lyophilization. All the eight final products of diblock copolymer were characterized by ^{1}H NMR and GPC (as listed in the Appendix).

3.2.3 Tribological Testing

Coefficients of friction were measured on a custom-built tribometer[32]. Cartilage samples were obtained from the patellofemoral groove of neonatal (1-3 day old) bovine stifles. Shaped

into a cartilage disc (6 mm in diameter by 2 mm high) by biopsy punch, samples were incubated in 1.5 M NaCl solution for 30 min and then in PBS for an additional 60 min to remove the surface binding proteins before they were treated with polymer solution. In the stability study, the polymer aliquots (0.35 ml, 3 mg/ml, n=3) were taken at 6 h, 24 h, 48 h, and 72 h time point after they were fully dissolved in PBS solution for cartilage sample incubation. Each cartilage sample was incubated in the polymer aliquot for 120 min, and then loaded onto the tribometer against a polished glass flat counterface in a PBS bath with a tilt pad configuration. Before friction testing, samples were compressed to 30% strain and depressurized to an average normal load of 3.4 N (~350 g) within 60 min. After the fluid pressure reached equilibrium, the glass counterface was reciprocated at a linear oscillation speeds of 0.3 mm/s. Both the normal load and friction force were measured by a biaxial load cell. COFs were calculated as ratios of average friction force to equilibrium normal load during the sliding and averaged for both the forward and reverse sliding directions.

3.2.4 Tertiary Amine Hydrolysis Study

A solution of tertiary amine based binding block ($PDMAEA_{24}$) in deuterated PBS (528 μg/ml, 0.154 μmol) was incubated at 150 RPM at room temperature. Aliquots (0.6 ml) were taken at time point of 6, 24, 48, 72 h (n = 3) for ^{1}H NMR analysis using an Inova 600 MHz spectrometer. The percentages of remaining tertiary amine groups on the binding block at each time point were derived from the integration ratios of the O-methylene group on the starting material ((C=O)O-$\mathbf{CH_2}$-CH_2-, δ 4.13, br, 2 H) to the hydrolysis product (HO-$\mathbf{CH_2}$-CH_2-, δ 3.76, t, 2 H).

3.2.5 Analysis and Statistics

The binding kinetic data were plotted as functions of incubation time and fit into a first order decay curve: $COF = (COF_o - COF_{min}) \times \exp(-t/tau) + COF_{min}$ where COF_o is the coefficient of friction in the absent of polymer binding, COF_{min} is the minimal coefficient of friction at maximal polymer binding, and tau is the binding time constant. Data are presented either as mean ± standard deviation (SD) or mean ± 95% confidence interval (CI). All analyses were carried out using Prism GraphPad 7 with calculated p values being considered significant for $p < 0.05$.

3.3 Results

3.3.1 Tertiary Amine Stability Test

Using the custom-built tribometer, the friction properties of diblock copolymers decorated with tertiary amine and quaternary amine binding groups were evaluated as a function of time in solution at 6, 24, 48, and 72 h. The data in Fig. 3.1a portrays the distinct tribological behaviors of two polymers in PBS solution at pH 7.4. Showing similar lubricating ability at the beginning (6 h), the polymer functionalized with quaternary amine groups maintained a low COF over 72 h whereas the tertiary amine-based polymer gradually lost its lubricating ability within the same period of time.

This reduction of lubrication ability over time indicated the instability of the tertiary amine groups on the polymer. The tertiary amino groups in the binding block are linked to the PAA backbone through an ester bond, which can hydrolyze by an intramolecular base catalyzed hydrolysis mechanism[33] due to the neighboring amino group. This hypothesis was supported by a hydrolysis study using NMR to identify the generation of the hydrolysis product (2-dimethylamino ethanol) and quantify the hydrolysis rate (Fig. 3.1b). The percentage of remaining tertiary amine in the binding block correlates well to the lubricating behavior of the

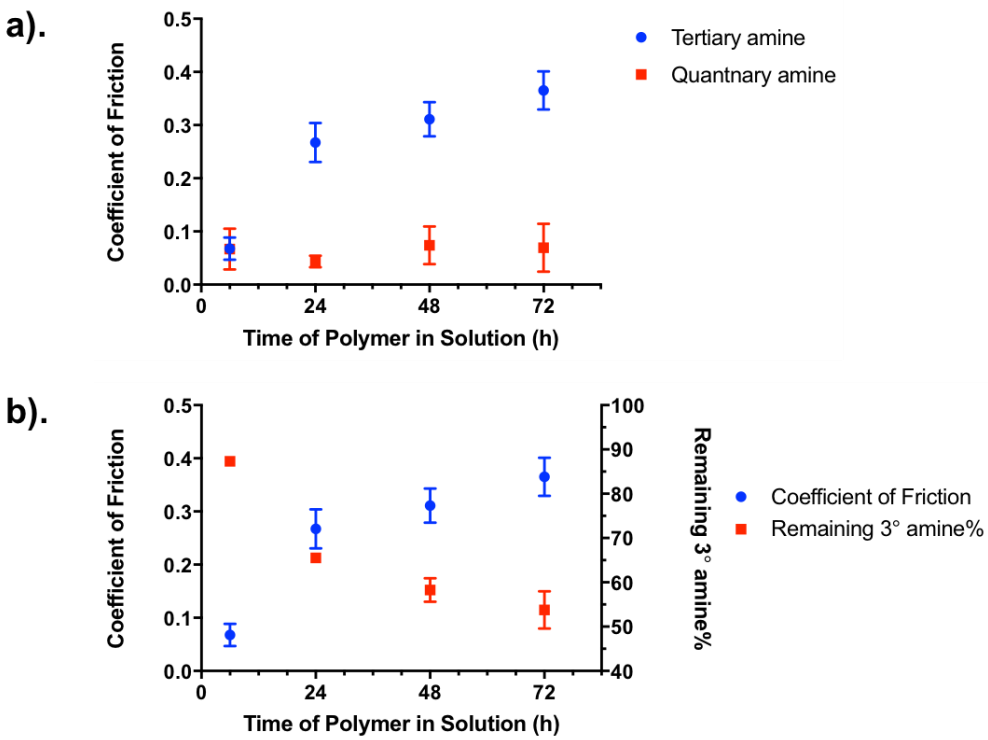

Figure 3.1. a). Stability of diblock copolymers based on two types of amine measured by cartilage lubrication data over time in PBS. The polymer containing tertiary amine binding block gradually loss its lubrication ability over time (data represented in blue, n = 4) whereas the polymer containing quaternary amine binding block steadily lubricates the cartilage surface (data represented in red, n = 4) b). Correlation between the COF of diblock copolymer (data represented in blue, n = 4) and remaining tertiary amine in the binding block (data represented in red, n = 3). Polymer with more remaining tertiary amine produces lower COF. Error bars represent ± 1 standard deviation

diblock copolymer, suggesting a relationship between the number of amino groups and the lubricating ability. The best lubrication was achieved when the number of amino group was greater than 20, further hydrolysis gradually led to an elevated COF, and the lubricating ability was completely lost when the number dropped to about 12. It is worth noting that excellent lubrication was achieved for both types of amine, indicating their similar binding affinity to articular cartilage. However, the degradation caused by the tertiary amine under physiological conditions eliminated its further application as a binding block component.

3.3.2 Polymer Library Synthesis

A library of eight lubricin-mimetic diblock copolymers with the quaternary amine based binding block was created with a range of binding block length (DP = 12, 24, 54, 90) and lubrication block length (DP = 200, 400) (Fig. 3.2a). The modular design of the diblock copolymers was aimed at creating a lubricin mimic with tunable length of both lubrication and binding blocks and investigating their influence on the tribological properties. As expected, the hydrodynamic size of the copolymer increases from 17.2 nm to 29.9 nm along with the length of either binding or lubrication block (Fig.3.2b) of the diblock.

3.3.3 Binding Kinetics and Lubrication

Time-dependent lubrication behaviors of diblock copolymers were evaluated by the custom-built tribometer as a function of incubation time: 2, 5, 15, 30, 60, 120 min. Six out of eight polymers successfully reduced the COF over the incubation time and the friction data fit well to a first order decay model (R^2 = 0.77 - 0.96). The two exceptions are polymers with the smallest binding block (DP = 12), showing no lubrication of cartilage surface across all incubation periods (Fig 3.3). The lack of lubricating ability for these two polymers matched with the results

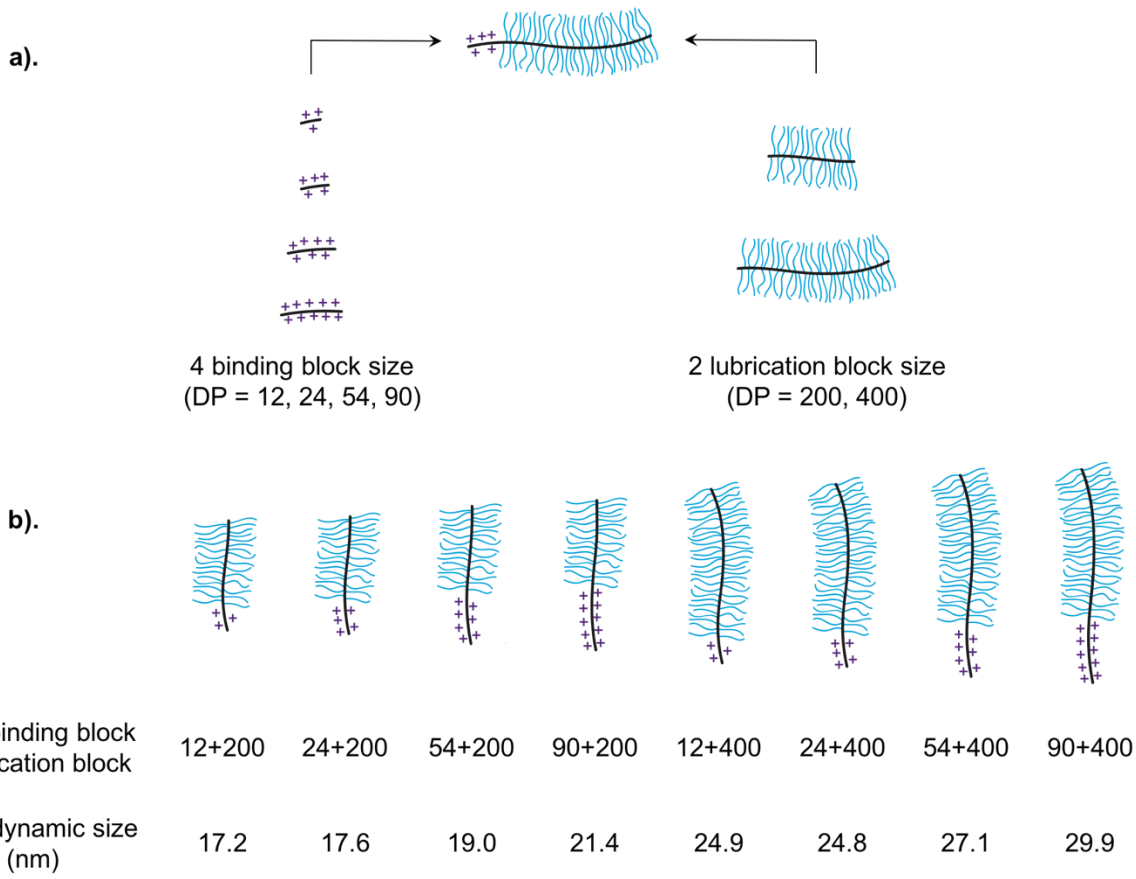

DP of binding block + lubrication block	12+200	24+200	54+200	90+200	12+400	24+400	54+400	90+400
Hydrodynamic size (nm)	17.2	17.6	19.0	21.4	24.9	24.8	27.1	29.9

Figure 3.2. a). Schematic representation of design criteria of quaternary based polymer library featured with tunable binding and lubrication block length. Two different lubrication block lengths and four different binding block length were adopted to give eight polymers in total. b). Schematic representation of polymer structures and their hydrodynamic sizes. The size of polymer increases with the length of either block.

obtained from studies on the polymer containing tertiary amine binding block, confirming that a minimal binding block length is required to lubricate the cartilage surface by anchoring the lubricant on the cartilage surface under compression.

An interesting trend of the COF_{min} tagging along with the increase of binding block length (Fig 3.4a) was observed in both polymer series (lubrication block DP = 200 or 400). The six lubricating polymers bound rapidly to cartilage surfaces (Fig 3.4b). The binding time constants were affected by the length of both binding and lubrication blocks. Increasing the binding block length from DP = 24 to 54 or 90 significantly reduced the binding time constants for polymers with lubrication block DP = 400. Reducing the lubrication block length from DP = 400 to 200 also decreased the binding time constants for polymers with binding block DP = 24. However, no significant difference in binding time constants was observed among the diblock copolymers with larger binding blocks (DP = 54 or 90), indicating that the binding rates were maximized at this increased binding block length. Overall, five out of six diblock copolymers produced very similar binding time constants, and the only exception (binding block DP = 24, lubrication block DP = 400) was attributed to its small binding block length and big lubrication block length. The binding time constants for the two polymers with binding block DP =12 were unable to be derived due to their poor fit (R^2 = 0.23 - 0.26) to the one phase decay model.

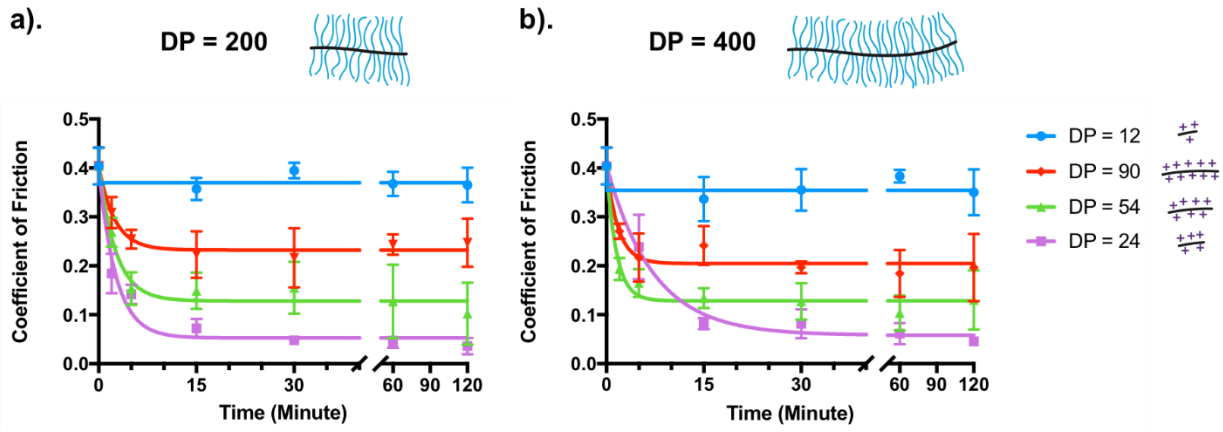

Figure 3.3. Time dependent lubrication behaviors of polymers with two different lubrication block length: a). DP = 200 b). DP = 400. The lubrication ability of diblock copolymer is solely dependent on the length of binding block length within the range of lubrication length studied. No lubrication is observed for the polymers containing a binding block with DP = 12. Most effective lubrication is observed at a binding block with DP =24. Further increased binding block length resulted in a reduction of lubrication ability. (n = 4-7, error bars represent ± 1 standard deviation)

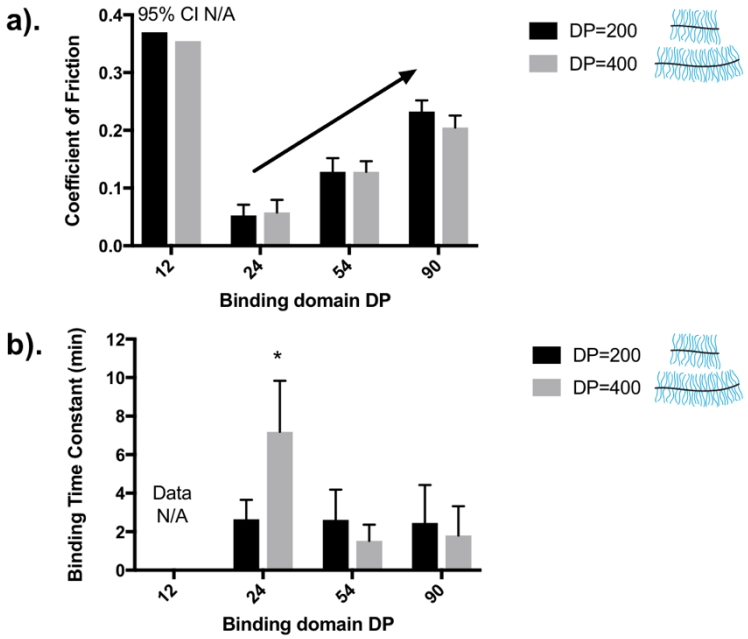

Figure 3.4. Tribological characteristics derived from the binding kinetic curve of the polymer library: a). minimal coefficient of friction b). binding time constant. Error bars represent 95% confidence interval.

3.4 Discussion

Tribological properties of bottle brush polymers have attracted considerable attention recently based on their bio-inspired structures[31,34,35]. Much effort on their structure-property relationships has illustrated the dependence of lubricating ability on the conformation of the bottlebrush-like architecture. Samaroo *et al* reported an analogue of bottle-brush polymers with a mucin-like structure whose lubrication and binding depended on structural parameters including backbone length, side chain length, and side chain grafting density[30]. Perry *et al* published a series of work summarizing the influence of polylysine-*g*-poly(ethylene glycol) architecture on tribological properties by AFM, and concluded that the properties were determined by the spatial density of PEG side chains to adopt either fully extended or mushroom-like conformation[31]. The relationship between the binding structure of polymers to their tribological properties, however, has been neglected. Many strategies such as electrostatic interactions[35], covalent bonding[36], and specific peptide targeting[37] have successfully adhered boundary lubricants on the articulating surface, yet very few have been systematically investigated for their structure-property relationships.

In our previous study, we reported the design and synthesis of a diblock copolymer inspired by the architecture of the natural glycoprotein lubricin. The integrity of the binding block was proven to be essential for cartilage lubrication. To further explore the relationship between the molecular structure and the lubricating properties, a family of lubricant analogues with tunable length of the binding and lubrication blocks were designed and synthesized. Surprisingly, lubrication is found to be solely dependent on the length of the binding block, at least for the size of the lubrication blocks studied. The optimal result was obtained with a quaternary amine functionalized binding block at DP = 24, and a minimal length of binding block (DP > 12) was

required for the polymer to reduce COF. Results indicated a binary relationship (Fig. 3.5) between the lubrication ability and the number of amino group in the binding block. Both proportionality in the range between the minimal length and the optimal length (DP = 12 to 24) and disproportionality with increasing length (DP = 24 to 90) were observed.

The binding strategy adopted in this study is a non-specific electrostatic interaction leveraged from the highly negatively charged nature of articular cartilage. The high concentration of negatively charged aggrecan inside cartilage offers a distinctive advantage for using electrostatic interactions to bind cationic nanoparticles[38]. Amino groups are selected as the cartilage binding composition for two reasons: 1. they bind to negatively charged surfaces such as mica[27] due to their positively charged nature at physiological conditions (pH = 7.4); 2. both tertiary and quaternary amines are able to form a confined nano-layer of water films between them and the binding surface, and therefore are highly efficient in the hydration lubrication context[39,40]. In this study, both types of amines were evaluated and show similar ability to reduce the COF of the cartilage surface. Tertiary amine-based polymer was less effective likely due to degradation via an intramolecular catalyzed ester hydrolysis mechanism[33]. Further investigation into the hydrolysis revealed a correlation between the lubricating ability and the number of amino groups, suggesting a strong dependence of lubrication on the ability of the boundary lubricant to adhere to the cartilage surface under compression. These results are consistent with previous studies that show stronger binding leads to the formation of a more resistant lubricating film to shear under high compression[40,41].

The lubricating abilities of the diblock copolymers were time dependent, suggesting that lubrication is also dependent on the amount of polymer adhered to the surface[30]. The short time constants and excellent lubrication properties underscore the therapeutic potential of this class of

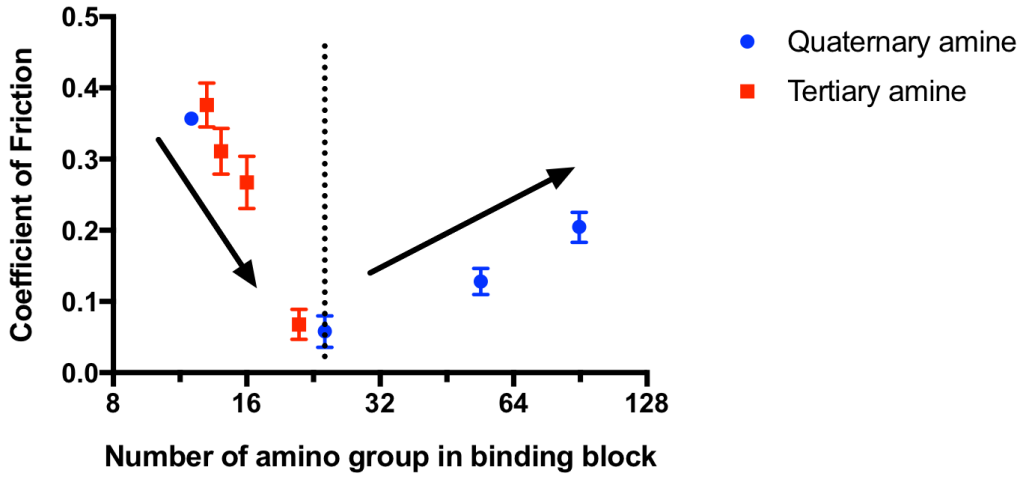

Figure 3.5. The binary relationship between the lubricating ability and the number of amino groups. With less amino groups in the binding block, as shown on the left side of the dotted line, the lubrication ability increases with the number of amino groups. This trend switches as shown on the right side of the dotted line, increased lubrication block reduces the lubrication ability. Red squares represent data from the polymer containing tertiary amine based binding block, n = 4, error bars represent ± 1 standard deviation. Blue dots represent data derived from the binding kinetic curves of polymers containing the quaternary amine based binding block, error bars represent 95% confidence interval.

lubricating polymer, as they would bind to the cartilage surfaces long before they would be cleared from the synovial fluid[42]. The phenomenon that increased binding block length (DP = 24 to 90) reduces the lubricating ability is counter-intuitive. One possible explanation is that the increased length of binding block can occupy more binding sites on the cartilage surface and prevent other polymers from binding nearby due to charge-charge repulsion. This may result in a decreased coating density upon surface saturation and thus affect the ability of the lubricating polymer film to bear the load and dissipate the energy upon shearing[30,42].

In this study, a library of lubricin mimetic polymers were synthesized with different binding functional groups, binding block lengths, and lubrication block lengths. Six copolymers bound to cartilage surfaces with binding time constants ranging from 1.7 to 7.4 min, and effectively lubricated cartilage surfaces *in vitro*. The most significant reduction in friction occurred with the polymer containing a binding block with DP = 24. Two factors were suggested as the possible primary reasons for the lubricating ability: the binding affinity of polymer to the cartilage surface and the polymer coating density on the cartilage surface. Binding affinity seems to dominate the overall effect within the range of smaller DP of binding blocks, as increasing the binding block length likely increased electrostatic interaction and resulted in an increased lubricating ability. With longer binding blocks, the coating density possibly outweighs the binding affinity as increasing binding block length resulted in a decreased coating density and lubricating ability. The observed trends in frictional properties for binding properties are highly relevant to the design of future applications entailing boundary layer lubricants or biomimetic lubricants. Specifically, the results highlight the need for proper binding to maintain the lubrication film and high adsorption density at interfaces.

3.5 References

(1) Dowson, D. Bio-Tribology. *Faraday Discuss.* **2012**, *156*, 9–30.

(2) Jahn, S.; Seror, J.; Klein, J. Lubrication of Articular Cartilage. *Annu. Rev. Biomed. Eng* **2016**, *18*, 235–258.

(3) Gleghorn, J. P.; Jones, A. R. C.; Flannery, C. R.; Bonassar, L. J. Boundary Mode Lubrication of Articular Cartilage by Recombinant Human Lubricin. *J. Orthop. Res.* **2009**, *27* (6), 771–777.

(4) Jay, G. D.; Waller, K. A. The Biology of Lubricin: Near Frictionless Joint Motion. *Matrix Biol.* **2014**, *39*, 17–24.

(5) Schmidt, T. A.; Gastelum, N. S.; Nguyen, Q. T.; Schumacher, B. L.; Sah, R. L. Boundary Lubrication of Articular Cartilage: Role of Synovial Fluid Constituents. *Arthritis Rheum.* **2007**, *56* (3), 882–891.

(6) Jay, G. D. Characterization of a Bovine Synovial Fluid Lubricating Factor. I. Chemical, Surface Activity and Lubricating Properties. *Connect. Tissue Res.* **1992**, *28* (1–2), 71–88.

(7) Balazs, E. a; Watson, D.; Duff, I. F.; Roseman, S. Hyaluronic Acid in Synovial Fluid. I. Molecular Parameters of Hyaluronic Acid in Normal and Arthritis Human Fluids. *Arthritis Rheum.* **1967**, *10* (4), 357–376.

(8) Swann, D. A.; Radin, E. L.; Nazimiec, M.; Weisser, P. A.; Curran, N.; Lewinnekt, G. Role of Hyaluronic Acid in Joint Lubrication. *Ann. Rheum. Dis.* **1974**, No. 33, 318–326.

(9) Waller, K. A.; Zhang, L. X.; Fleming, B. C.; Jay, G. D. Preventing Friction-Induced Chondrocyte Apoptosis: Comparison of Human Synovial Fluid and Hylan G-F 20. *J. Rheumatol.* **2012**, *39* (7), 1473 LP-1480.

(10) Benz, M.; Chen, N.; Israelachvili, J. Lubrication and Wear Properties of Grafted

Polyelectrolytes, Hyaluronan and Hylan, Measured in the Surface Forces Apparatus. *J. Biomed. Mater. Res. - Part A* **2004**, *71* (1), 6–15.

(11) Swann, D. A.; Silver, F. H.; Slayter, H. S.; Stafford, W.; Shore, E. The Molecular Structure and Lubricating Activity of Lubricin Isolated from Bovine and Human Synovial Fluids. *Biochem. J.* **1985**, *225* (1), 195–201.

(12) Musumeci, G. The Role of Lubricin in Normal and Pathological Joint Tissue: A Contemporary Review. *OA Anat.* **2013**, *1* (1), 1–6.

(13) Wieland, H. A.; Michaelis, M.; Kirschbaum, B. J.; Rudolphi, K. A. Osteoarthritis - An Untreatable Disease? *Nat. Rev. Drug Discov.* **2005**, *4* (4), 331–344.

(14) Holyoak, D. T.; Tian, Y. F.; van der Meulen, M. C. H.; Singh, A. Osteoarthritis: Pathology, Mouse Models, and Nanoparticle Injectable Systems for Targeted Treatment. *Ann. Biomed. Eng.* **2016**, *44* (6), 2062–2075.

(15) Jay, G. D.; Fleming, B. C.; Watkins, B. A.; McHugh, K. A.; Anderson, S. C.; Zhang, L. X.; Teeple, E.; Waller, K. A.; Elsaid, K. A. Prevention of Cartilage Degeneration and Restoration of Chondroprotection by Lubricin Tribosupplementation in the Rat Following Anterior Cruciate Ligament Transection. *Arthritis Rheum.* **2010**, *62* (8), 2382–2391.

(16) Teeple, E.; Elsaid, K.; Fleming, B.; Jay, G. Coefficients of Friction, Lubricin, and Cartilage Damage in the Anterior Cruciate Ligament-Deficient Guinea Pig Knee. *J. Orthop. Res.* **2008**, *26* (2), 231–237.

(17) Young, A. A.; McLennan, S.; Smith, M. M.; Smith, S. M.; Cake, M. A.; Read, R. A.; Melrose, J.; Sonnabend, D. H.; Flannery, C. R.; Little, C. B. Proteoglycan 4 Downregulation in a Sheep Meniscectomy Model of Early Osteoarthritis. *Arthritis Res. Ther.* **2006**, *8* (2), R41.

(18) Elsaid, K. A. A.; Fleming, B. C. C.; Oksendahl, H. L. L.; Machan, J. T. T.; Fadale, P. D. D.; Hulstyn, M. J. J.; Shalvoy, R. M.; Jay, G. D. D. Decreased Lubricin Concentrations and Markers of Joint Inflammation in the Synovial Fluid of Patients with Anterior Cruciate Ligament Injury. *Arthritis Rheum.* **2008**, *58* (6), 1707–1715.

(19) Jay, G. D.; Jahn R. Torres; Rhee, D. K.; Helminen, H. J.; Hytinnen, M. M.; Cha, C.-J.; Elsaid, K.; Kim, K.-S.; Cui, Y.; And; et al. Association Betwwen Friction and Wear in Diarthrodial Joints Lacking Lubricin. *Arthritis Rheum.* **2007**, *56* (11), 3662–3669.

(20) Flannery, C. R.; Zollner, R.; Corcoran, C.; Jones, A. R.; Root, A.; Rivera-Bermúdez, M. A.; Blanchet, T.; Gleghorn, J. P.; Bonassar, L. J.; Bendele, A. M.; et al. Prevention of Cartilage Degeneration in a Rat Model of Osteoarthritis by Intraarticular Treatment with Recombinant Lubricin. *Arthritis Rheum.* **2009**, *60* (3), 840–847.

(21) Cui, Z.; Xu, C.; Li, X.; Song, J.; Yu, B. Treatment with Recombinant Lubricin Attenuates Osteoarthritis by Positive Feedback Loop between Articular Cartilage and Subchondral Bone in Ovariectomized Rats. *Bone* **2015**, *74*, 37–47.

(22) Jay, G. D.; Harris, D. A.; Cha, C. J. Boundary Lubrication by Lubricin Is Mediated by O-Linked β(1-3)Gal-GalNAc Oligosaccharides. *Glycoconj. J.* **2001**, *18* (10), 807–815.

(23) Al-Sharif, A.; Jamal, M.; Zhang, L. X.; Larson, K.; Schmidt, T. A.; Jay, G. D.; Elsaid, K. A. Lubricin/Proteoglycan 4 Binding to CD44 Receptor: A Mechanism of the Suppression of Proinflammatory Cytokine-Induced Synoviocyte Proliferation by Lubricin. *Arthritis Rheumatol.* **2015**, *67* (6), 1503–1513.

(24) Schmidt, T. A.; Sullivan, D. A.; Knop, E.; Richards, S. M.; Knop, N.; Liu, S.; Sahin, A.; Darabad, R. R.; Morrison, S.; Kam, W. R.; et al. Transcription, Translation, and Function of Lubricin, a Boundary Lubricant, at the Ocular Surface. *JAMA Ophthalmol.* **2013**, *131*

(6), 766–776.

(25) Samsom, M. L.; Morrison, S.; Masala, N.; Sullivan, B. D.; Sullivan, D. A.; Sheardown, H.; Schmidt, T. A. Characterization of Full-Length Recombinant Human Proteoglycan 4 as an Ocular Surface Boundary Lubricant. *Exp. Eye Res.* **2014**, *127*.

(26) Samaroo, K. J.; Tan, M.; Andresen Eguiluz, R. C.; Gourdon, D.; Putnam, D.; Bonassar, L. J. Tunable Lubricin-Mimetics for Boundary Lubrication of Cartilage. *Biotribology* **2017**, *9*, 18–23.

(27) Banquy, X.; Burdynska, J.; Lee, D. W.; Matyjaszewski, K.; Israelachvili, J. Bioinspired Bottle-Brush Polymer Exhibits Low Friction and Amontons-like Behavior. *J. Am. Chem. Soc.* **2014**, *136* (17), 6199–6202.

(28) Coles, J. M.; Chang, D. P.; Zauscher, S. Molecular Mechanisms of Aqueous Boundary Lubrication by Mucinous Glycoproteins. *Curr. Opin. Colloid Interface Sci.* **2010**, *15* (6), 406–416.

(29) Zappone, B.; Greene, G. W.; Oroudjev, E.; Jay, G. D.; Israelachvili, J. N. Molecular Aspects of Boundary Lubrication by Human Lubricin: Effect of Disulfide Bonds and Enzymatic Digestion. *Langmuir* **2008**, *24* (4), 1495–1508.

(30) Samaroo, K. J.; Mingchee Tan; Putnam, D.; Bonassar, L. J. Binding and Lubrication of Biomimetic Boundary Lubricants on Articular Cartilage. *J. Orthop. Res.* **2017**, *35*, 548–557.

(31) Perry, S. S.; Yan, X.; Limpoco, F. T.; Lee, S.; Müller, M.; Spencer, N. D. Tribological Properties of Poly(L-Lysine)-Graft-Poly(Ethylene Glycol) Films: Influence of Polymer Architecture and Adsorbed Conformation. *ACS Appl. Mater. Interfaces* **2009**, *1* (6), 1224–1230.

(32) Gleghorn, J. P.; Jones, A. R. C.; Flannery, C. R.; Bonassar, L. J. Boundary Mode Frictional Properties of Engineered Cartilaginous Tissues. *Eur. Cells Mater.* **2007**, *14*, 20–28.

(33) Fife, T. H.; Singh, R.; Bembi, R. Intramolecular General Base Catalyzed Ester Hydrolysis. The Hydrolysis of 2-Aminobenzoate Esters. *J. Org. Chem.* **2002**, *67* (10), 3179–3183.

(34) Pettersson, T.; Naderi, A.; Makuška, R.; Claesson, P. M. Lubrication Properties of Bottle-Brush Polyelectrolytes: An AFM Study on the Effect of Side Chain and Charge Density. *Langmuir* **2008**, *24* (7), 3336–3347.

(35) Mu, M.; Lee, S.; Spikes, H. A.; Spencer, N. D. The Influence of Molecular Architecture on the Macroscopic Lubrication Properties of the Brush-like Co-Polyelectrolyte Poly (L-Lysine)-g-Poly (Ethylene Glycol) (PLL-g-PEG) Adsorbed on Oxide Surfaces. *Tribol. Lett.* **2003**, *15* (4), 395–405.

(36) Morgese, G.; Cavalli, E.; Rosenboom, J. G.; Zenobi-Wong, M.; Benetti, E. M. Cyclic Polymer Grafts That Lubricate and Protect Damaged Cartilage. *Angew. Chemie - Int. Ed.* **2018**, *57* (6), 1621–1626.

(37) Singh, A.; Corvelli, M.; Unterman, S. A.; Wepasnick, K. A.; Mcdonnell, P.; Elisseeff, J. H. Enhanced Lubrication on Tissue and Biomaterial Surfaces through Peptide-Mediated Binding of Hyaluronic Acid. *Nat. Mater.* **2014**, *13* (October), 988–995.

(38) Bajpayee, A. G.; Grodzinsky, A. J. Cartilage-Targeting Drug Delivery: Can Electrostatic Interactions Help? *Nat. Rev. Rheumatol.* **2017**, *13*, 183–193.

(39) Klein, J. Hydration Lubrication. *Friction* **2013**, *1* (1), 1–23.

(40) Chen, M.; Briscoe, W. H.; Armes, S. P.; Klein, J. Lubrication at Physiological Pressures by Polyzwitterionic Brushes. *Science.* **2009**, *323* (5922), 1698–1701.

(41) Klein, J. Polymers in Living Systems: From Biological Lubrication to Tissue Engineering and Biomedical Devices. *Polym. Adv. Technol.* **2012**, *23* (4), 729–735.

(42) Brown, T.; Laurent, U.; Fraser. Turnover of Hyaluronan in Synovial Joints: Elimination of Labelled Hyaluronan from the Knee Joint of the Rabbit. *Exp. Physiol.* **1991**, *76* (1), 125–134.

CHAPTER 4

BONE LUBRICATION BY LUBRICIN MIMETICS FOR LATE-STAGE OSTEOARTHRITIS TREATMENT

4.1 Introduction

Affecting about 27 million Americans[1], osteoarthritis (OA) is a disease of whole joint organ[2,3] characterized by irreversible cartilage damage[4–7], subchondral bone sclerosis[4,8], osteophyte formation[9,10], and inflammation of synovial tissue[11–14]. Therapeutic interventions of OA may relieve the symptoms in the short term[15–18], but progression of the disease into late-stage is almost inevitable[19]. In late-stage OA of the knees and hips, the subchondral bone surface is often exposed due to wear of articular cartilage, causing joint stiffness, pain, and disability. Very few options are available to improve the quality of patient life beyond joint arthroplasty[20], which is only suitable to otherwise healthy patients aged 55 or older.

These symptoms, mostly caused by direct contact of bone-on-bone and bone on other tissues, could potentially be relieved by lubricating the exposed bone surface. The strategy of lubricating the articulating surfaces in the joint has proved its efficacy for early to moderate stage OA treatment[21,22]. Intraarticular injection of hyaluronic acid (HA) is a popular way to treat moderate OA through restoration of synovial fluid viscosity[21–23]. However, HA injection is only indicated in less severe OA but not late-stage OA[24], since it does not interact with the bone surface. To the best of our knowledge, no such material that can effectively lubricate bone surfaces has been previously reported.

In Chapter 2 we reported the design criteria and synthesis of a diblock copolymer with substantial lubrication capacity, which effectively reduces the coefficient of friction (COF) of articular cartilage. Herein, we report that this diblock copolymer, using similar design criteria, can bind to both subchondral and trabecular bone surfaces and significantly reduce their COFs. The lubrication ability comes from the structure of the polymer which consists of a large bottlebrush-like lubrication block (Mn ~ 200 kDa) and a small positively charged binding block (Mn ~3 kDa). The lubrication block can attract and retain water to resist compression. The binding block is designed to interact with the negatively charged bone composition (e.g. phosphate groups in hydroxyapatite) to anchor the polymer at the bone surface. To our knowledge, this is the first study that shows a synthetic lubricant with effective bone lubricating ability, which could serve as a potential treatment for late-staged OA when bone surfaces are exposed.

4.2 Materials and Methods

4.2.1 Materials and Equipment

All chemicals were purchased from Sigma-Aldrich, or Fisher at the highest purity grade. All monomers were purified by a column filled with aluminum oxide (basic or neutral) prior to use. Phosphate buffered saline (PBS) was purchased from Sigma-Aldrich. Dextran was purchased from Sigma-Aldrich with the average molecular weight of 1.5 – 2.8 MDa. The ^{1}H NMR spectra were performed on an Inova 400 MHz spectrometer with deuterated chloroform or deuterium oxide as the solvent. Broad or overlapping peaks, noted in spectra of polymers, are denoted “br”. Degree of polymerization (DP) was determined by initial monomer to CTA ratio and monomer conversion ratio. Gel permeation chromatography (GPC) was performed with PBS (pH 7.4) at a flow rate of 0.8 ml/min. Using a Waters gel permeation chromatography system equipped with

three Waters Ultrahydrogel™ columns in series (2000 Å, 500 Å, and, 250 Å) at 30 °C, the molecular weights were measured against poly (methacrylic acid), sodium salt standards (1,670 to 110,000 g/mol). Bone polishing was performed on a M-PREP 5™ polisher at 50 RPM for 30 s, using MetLab Corp Abrasive Grinding P.S.A Premium Discs (800 grit) as the polishing counterface.

4.2.2 Polymer Synthesis

The diblock copolymer was synthesized in three steps, as shown in Scheme 2.1. Starting with RAFT[25] polymerization of 2-(dimethylamino) ethyl acrylate, a precursor "pre-binding" block was produced. Subsequent RAFT polymerization of poly(ethylene glycol) methyl ether acrylate (Mn 480), using the "pre-binding" domain as the macro-initiator, added the lubrication block to the copolymer. Finally, the tertiary amines in the "pre-binding" cartilage binding block precursor were converted to quaternary amines by treatment with an excess of ethyl bromide to give the final product.

A typical reaction scheme to produce the diblock copolymer ($qPDMAEA_{24}$-$PEGMEA_{400}$) is as follows: A mixed solution of DMAEA (4.30 g, 30 mmol), ACPA (14.0 mg, 0.05 mmol), and CPADB (139.5 mg, 0.5 mmol) in 5 mL of anisole was deoxygenated by 5 freeze-vacuum-thaw cycles. The reaction was sealed and stirred at 70 °C for 48 h before it was quenched in a liquid nitrogen bath. The residue polymer was diluted with/dissolved in dichloromethane (DCM) first and then purified by precipitation in hexane (repeated 5 times). In the following step, PEGMEA (3.46 g, 7.2 mmol) was added to a solution containing $PDMAEA_{24}$ **(**30.9 mg, 0.009 mmol), and ACPA (0.5 mg, 0.0018 mmol) in 6 ml of anisole. The mixture was deoxygenated by 5 freeze-vacuum-thaw cycles and then was sealed and stirred for 8 h at 65 °C. After quenching in a liquid nitrogen bath, the residual polymer was diluted with/dissolved in DCM and then purified by

precipitation in hexane (repeated 5 times). The obtained product from the second step was then converted into the final product by dropwise addition of ethyl bromide (0.3 ml, 4,0 mmol) into a solution containing $PDMAEA_{24}$-$PEGMEA_{400}$ (865.9 mg) in 3 ml of acetone at 0 °C. The mixture was stirred for 48 h at room temperature and was then concentrated by evaporating the solvent with a dry nitrogen flow. The residue was dissolved in 3 ml of methanol and purified by precipitation in hexane (repeated 5 times). The product was then dissolved in DI water and further purified by dialysis using Spectra/Por regenerated cellulose dialysis tubing (2 kDa MWCO) against DI water for additional 48 hours before lyophilization. All the intermediates and final product were characterized by ^1H NMR and GPC. Characterization results of intermediates and final product are listed in the Appendix.

4.2.3. Sample Preparation

Bone samples (Fig. 4.1) were extracted from the femoral condyle of neonatal (1-3 day old) bovine stifles. The bone plugs were obtained by drilling through the cartilage layer to the growth plate with a 6 mm diameter hollow drill bit. Each plug was then trimmed to small samples with 2 mm height by a razor blade. The subchondral surface was exposed by removing the cartilage layer and the trabecular bone surfaces were obtained by cutting the medial part of the drilled bone plugs. After polishing, bone samples were incubated in PBS and then in a solution containing the polymer for further testing.

Cartilage plates were obtained from the lateral tibial plateau or patellofemoral groove (PFG) of neonatal (1-3 day old) bovine stifles. The cartilage samples (with bone underneath in the case of the tibial plateau) were gently cut from the flat areas with cartilage surface untouched, shaped into 5 mm×10 mm×2 mm plates by scalpel, and subsequently frozen at -20 °C. At the time of testing, the tissue was thawed in a water bath at 37 °C and then mounted onto the glass surface of

a custom-built tribometer. The articulate cartilage surfaces in this experiment possessed their natural curvature.

4.2.4. Tribological Testing

COFs were measured using our custom-built tribometer[26]. For bone-on-glass friction tests, the bone samples were incubated in PBS for half an hour before they were treated with polymer solutions (1 h incubation in 1mg/ml solution in PBS or 2 h incubation in 10 mg/ml solution in PBS). After loading onto the tribometer, samples were compressed against a polished glass flat counterface in a PBS bath at a normal load of 400 g and then depressurized to average normal load of 240 g within 15 min. The glass counterface was then reciprocated at linear oscillation speeds of 0.3, 1, and 3 mm/s. Both the normal load and friction force were measured by a biaxial load cell. COFs were calculated as average ratios of friction force to normal load during the sliding and averaged for both the forward and reverse sliding directions.

In bone-on-cartilage tests, subchondral bone was used and further cut into 3 mm diameter plugs by biopsy punches. To evaluate the lubrication ability of the polymer (Fig.4.2 1a to 1c), bone plugs and cartilage plates were first tested in a PBS bath, and then both were incubated in the polymer solution (10 mg/ml in PBS) for 1 h followed by subsequent testing in the polymer bath and PBS bath. For each test, the cartilage counterface was reciprocated after the contact (within 5s) with bone plugs (normal load less than 10 g) at linear oscillation speeds of 0.3 mm/s (both PFG and tibial plateau) and 1 mm/s (PFG only). To evaluate the effects of viscosity and sliding speed (Fig. 4.2. 2a to 2c), subchondral bone plugs sliding on PFG plates were tested in a PBS bath, 7% dextran (w/v) bath, and 23% dextran (w/v) bath subsequently at siding speeds of 0.1, 0.3, and 1 mm/s. The lubrication wells were gently rinsed with PBS after each test. Both the

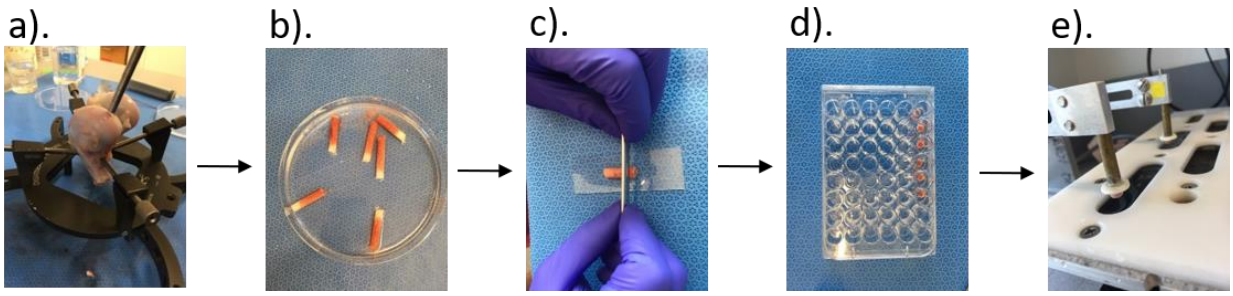

Figure 4.1. Preparation of bone samples: a). Bone plugs (6 mm in diameter) are extracted from the bovine distal femur b). Extracted bone plugs in PBS c). Bone plugs are cut into 2 mm height samples d). Bone samples are incubated with polymer solution e). Lubrication analysis using a custom built tribometer.

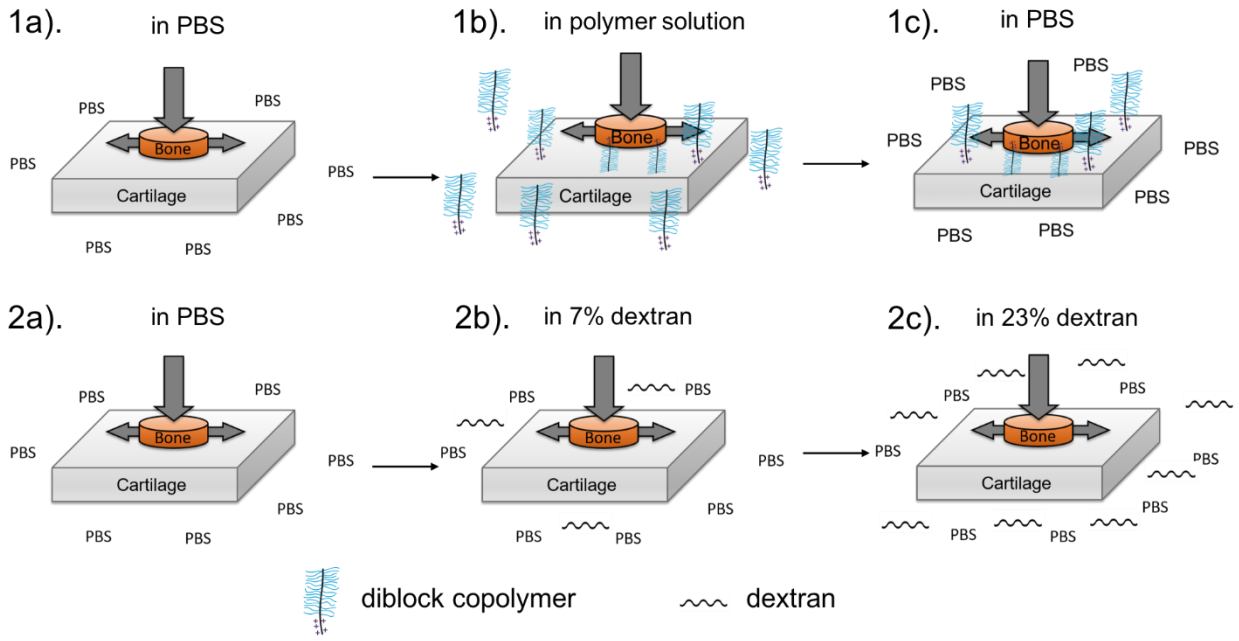

Figure 4.2. Schematic representation of two series of bone-on-cartilage tests: 1a). Bone plugs (3 mm in diameter) slide in PBS bath against flat cartilage surfaces, which were extracted from patellofemoral grooves or tibial plateaus 1b). The same bone plug and cartilage samples were incubated in polymer solution (10mg/ml) for 1 h and tested in the same polymer bath 1c). The same samples are gently rinsed with PBS, then tested in PBS bath 2a). Same as 1a) 2b). The same samples from 2a were tested in 7% dextran 2c). The same samples were tested in 23% dextran after gently rinsing with PBS.

normal load and friction forces were measured using a biaxial load cell. Increases in normal loads and friction forces were observed before sliding happened due to static friction. COFs were calculated as average ratios of friction force to normal load during the sliding and averaged for both sliding directions.

4.2.5. Statistics

The effects of polymer treatment in both bone-on-glass and bone-on-cartilage studies were assessed by a two factor repeated measures analysis of variance (ANOVA) except the bone-on-tibial plateau test which was analyzed by a one-way repeated measures ANOVA. All data are presented as mean ± SD and all analyses were carried out using Prism GraphPad 7 with calculated p values being considered significant for $p < 0.05$.

4.3 Results

4.3.1 Bone-on-glass tribology

The experiments were performed under similar conditions for cartilage friction measurement under boundary mode conditions (Chapter 2 and 3). Both polished trabecular and subchondral bones produced higher COFs by more than 30% than cartilage (Fig. 4.3). The treatment that was effective for cartilage lubrication (1 mg/ml, 1 h incubation) failed to reduce the COF of trabecular bone in comparison to the PBS controls. However, incubation with an increased concentration (10 mg/ml) of polymer and prolonged incubation time (2 h) resulted in decreased COFs by more than 40% across all the sliding speeds ($\Delta COF \sim -0.20$, $p < 0.001$). This trend of reduction was also observed for subchondral bone ($\Delta COF \sim -0.15$, $p < 0.001$), indicating the lubricating efficacy of the diblock copolymer for both types of bones.

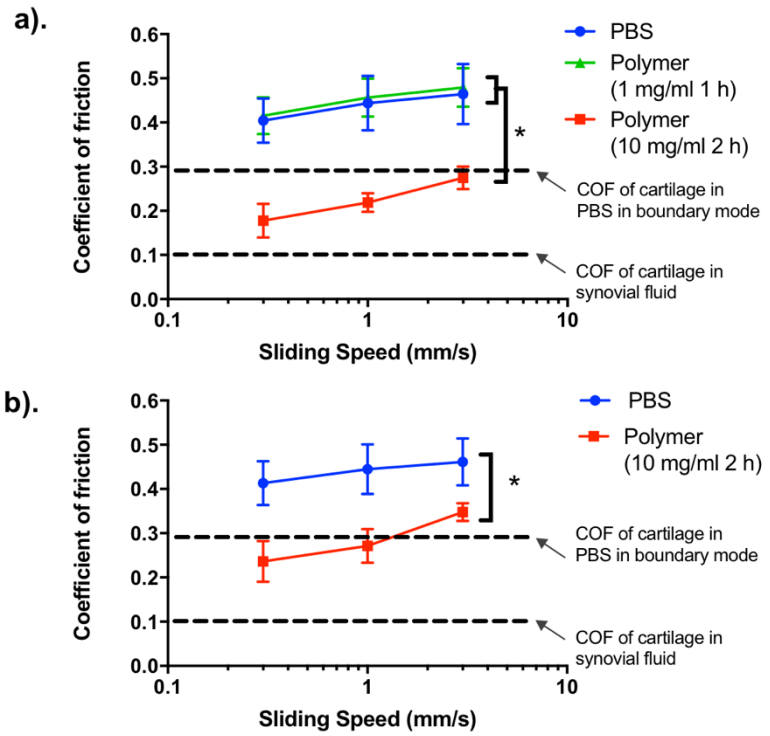

Figure 4.3. Incubation with the polymer reduces the COFs of a). trabecular bone-on-glass interface b). subchondral bone-on-glass interface. In the case of trabecular bone-on-glass, the samples are not lubricated when evaluated under conditions previously used for cartilage lubrication (data represented in green line, incubated with the polymer solution at concentration of 1 mg/ml for 2h.). Effective lubrication is observed with increased polymer concentration (10 mg/ml) and prolonged incubation time (2 h) as shown by the data represented as the red line. A similar trend is observed in the subchondral bone-on-glass configuration. n = 4 – 6, error bars represent ± 1 standard deviation, *: $p<0.0001$.

4.3.2 Bone-on-cartilage tribology

The tribological properties of bone surfaces were further assessed by a subchondral bone-on-cartilage configuration. Incubation with the polymer solution reduced the average COFs by 30% (ΔCOF ~ -0.25, $p < 0.001$) of the surface between subchondral bone and PFG cartilage at both sliding speeds (Fig. 4.4a). Removing the polymer from the bath slightly increased the COF by 11% (ΔCOF ~ -0.05, $p = 0.025$) at sliding speed of 0.3 mm/s, but this elevation was not observed ($p = 0.746$) at 1mm/s. Similar trends were observed in the case of the subchondral bone-on-tibial plateau cartilage test (Fig. 4.4b). Treatment with the polymer solution reduced the COF by 40% (ΔCOF ~ -0.30, $p = 0.004$) and removing the polymer from the lubrication bath had no significant effect ($p = 0.979$).

To further analyze the tribological behavior in the bone-on-cartilage mode, COFs of this interface were collected over speeds ranging 1 order of magnitude (0.1-1 mm/s) while bathed in lubricants with viscosity varying across 3 orders of magnitude (1-884 mPas dynamic viscosity). The lubricants used were PBS (1 mPas dynamic viscosity), 7% dextran solution (w/v) in PBS (108 mPas dynamic viscosity), and 23% dextran solution (w/v) in PBS (884 mPas dynamic viscosity)[27]. The lubricants with elevated viscosities provided lower COFs of the interface (Fig. 4.5). Notably, 23 % dextran (w/v) reduced the COFs at 2 out of 3 sliding speeds (0.1 and 1 mm/s) while the increase in sliding speed had no significant impact.

4.4 Discussion

In this study, we show that a novel polymer with a di-block structure is able to effectively lubricate bone at both glass and cartilage interfaces. Effective lubrication of bone surfaces was achieved at higher concentration (10 mg/ml) and prolonged incubation time (2 h) in comparison

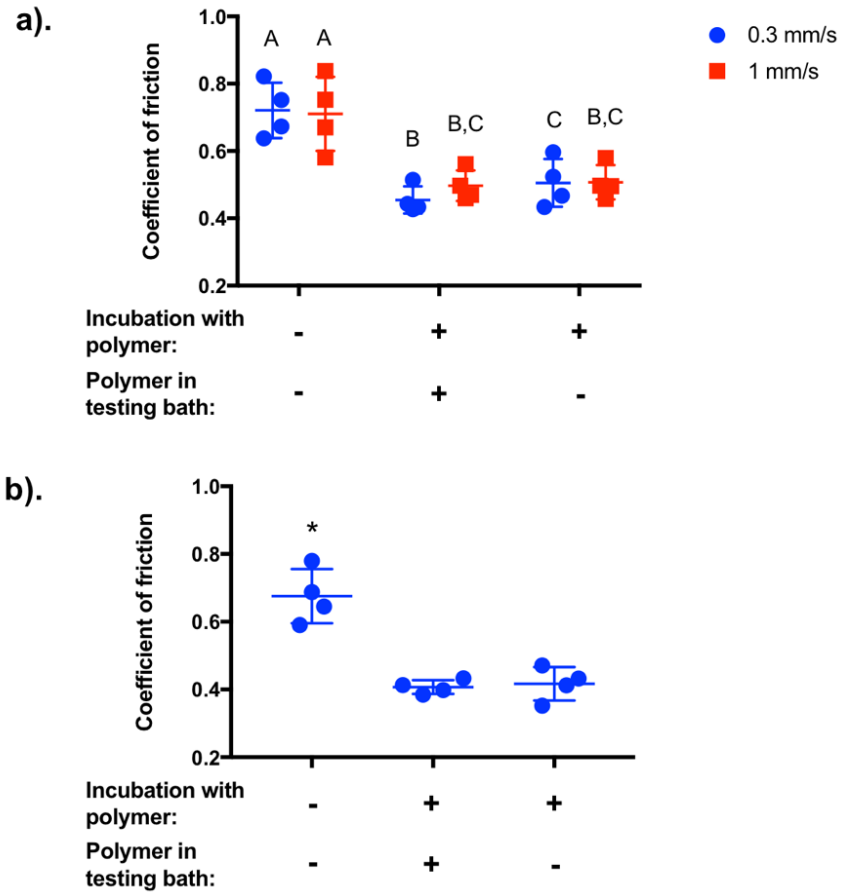

Figure 4.4. Incubation with polymer reduces the COFs of a). subchondral bone-on-patellofemoral groove cartilage b). subchondral bone-on-tibial plateau cartilage. With or without polymer in the lubrication bath, incubation with polymer solutions at concentration of 10 mg/ml for 1 h significantly reduces the COFs for both interfaces. n = 4 – 6, error bars represent ± 1 standard deviation, *: $p<0.05$, letters: $p< 0.05$.

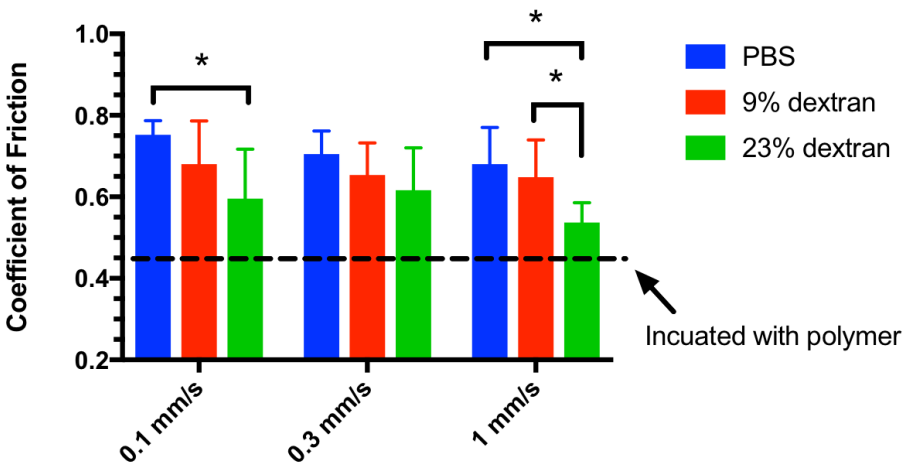

Figure 4.5. Tribological effects of sliding speed and viscosity to subchondral bone-on-patellofemoral groove cartilage configuration. Incubation with polymer achieves better lubrication than increasing viscosity using 23% dextran (w/v). Sliding speed has no significant effect. n = 3, error bars represent ± 1 standard deviation, *: $p<0.05$.

to cartilage lubrication which only required incubation for 30 min at concentration of 1 mg/ml. Those increases in the incubation conditions suggested a decreased binding efficiency of the polymer onto the bone surfaces due to a lack of highly negatively charged material in bone. The major components of bone (collagen I and hydroxyapatite) could potentially attract the positively charged binding block of the polymer via electrostatic interactions through negatively charged domains or phosphate groups respectively. Such charge-charge interaction is less efficient in comparison to the binding to the aggrecan in cartilage, requiring a higher incubation concentration and longer binding time to reduce the COF, which implies a higher dose might be required for future clinical applications.

One of the major characteristics of late-stage OA is the exposure of subchondral bone surfaces due to complete wear of the articular cartilage layer[28]. Thus, the ability to reduce the friction between subchondral bone and other tissues is critical to restore the flexibility of the damaged joint. Using a bone-on-cartilage configuration, we evaluated the lubrication ability of this novel polymer at the interface between the subchondral bone and cartilage from PFG and from tibial plateau. With or without the presence of polymer in the lubrication bath, the COFs after incubation with the polymer were significantly reduced in comparison to the PBS control for cartilage from both regions, indicating the presence of polymer on the tissue surface leading to lubrication. The similar level of lubrication achieved after rinsing with PBS also implied the sufficient binding affinity of polymer to the bone and cartilage surfaces, underscoring the therapeutic potential of this type of polymer. Additionally, high binding affinity to the tissue surface may also decrease the rate at which it is cleared from the joint. Measured COFs of subchondral bone against tibial plateau were lower than that against PFG (Fig. 4.4) with or without polymer incubation (ΔCOF ~ -0.05), which was consistent with their COFs previously

identified[29]. These results were in agreement with the function of tibial plateau as the major weight bearing area of joint. In summary, the polymer with a diblock architecture effectively lubricated the bone surfaces and therefore demonstrated its potential to help relieve the late-stage OA symptoms.

The bone plug-on-cartilage plate configuration was selected over the cartilage plug-on-bone plate due to the challenge to obtain flat subchondral bone surfaces from a naturally curved layer with thickness of only a few hundred micrometers. This type of testing configuration, analogous to the migrating contact area discussed by Ateshian *et al*[30], reasonably mimics the physiological conditions in diarthrodial joints by allowing the various cartilage regions to be compressed by the load. Lower frictions are usually obtained since the bath fluid is able to diffuse back into the cartilage to restore the interstitial fluid pressure before the load is applied again on the same contact area[31].

To further characterize the bone-on-cartilage tribology, we investigated how changes in viscosity and sliding speed affected the measured COF. The reduction of COF in 23% dextran (w/v) bath is consistent with the results reported by Bonnevie *et al*[27] in which increased viscosity can lubricate porous surfaces by promoting the formation of liquid films between the articulating surfaces. Dextran solution at 23% (w/v) concentration has an equivalent lubrication capacity to hyaluronic acid (HA)[27], yet its lubrication didn't reach our polymer lubricant in this study. The lubricating ability of 7% dextran is less pronounced. Sliding speed has no significant effect on tribology behavior within the range of test conditions.

The elevated COFs from bone-on-cartilage configuration in comparison to the bone-on-glass configuration suggested the friction of bone can be influenced by the articulating surfaces. During compression, the high porosity of subchondral bone surfaces inhibited the formation of

sufficient liquid film to support the normal load and resulted in a boundary friction mode which is primarily governed by the entanglement of the asperities between the two opposing surfaces. Porous and soft cartilage surfaces are more likely to generate entanglement in comparison to smooth non-porous glass surface and therefore produce higher friction.

Our previous studies indicated that successful lubrication requires sufficient polymer binding to surfaces and the capacity to resist compression. The diblock structure inspired by these design criteria enables the polymer to interact with negatively charged bone components and to resist normal compression via a bottlebrush-like architecture. To the best of our knowledge, this is the first report on the lubrication of bone surfaces using synthetic polymers consisting of a bone-binding and a surface lubrication block. Results of this study highlight the potential of the polymer as a new approach for the treatment of late-stage OA.

4.5 References

(1) Lawrence, R. C.; Felson, D. T.; Helmick, C. G.; Arnold, L. M.; Choi, H. Estimates of the Prevalence of Arthritis and Other Rheumatic Conditions in the United States, Part II. *Arthritis Rheum* **2008**, *58* (1), 26–35.

(2) Loeser, R. F.; Goldring, S. R.; Scanzello, C. R.; Goldring, M. B. Osteoarthritis: A Disease of the Joint as an Organ. *Arthritis Rheum.* **2012**, *64* (6), 1697–1707.

(3) Lories, R. J.; Luyten, F. P. The Bone–cartilage Unit in Osteoarthritis. *Nat. Rev. Rheumatol.* **2010**, *7*, 43.

(4) Goldring, M. B.; Goldring, S. R. Articular Cartilage and Subchondral Bone in the Pathogenesis of Osteoarthritis. *Ann. N. Y. Acad. Sci.* **2010**, *1192*, 230–237.

(5) Pearle, A. D.; Warren, R. F.; Rodeo, S. A. Basic Science of Articular Cartilage and Osteoarthritis. *Clin. Sports Med.* **2005**, *24* (1), 1–12.

(6) Stolz, M.; Gottardi, R.; Raiteri, R.; Miot, S.; Martin, I.; Imer, R.; Staufer, U.; Raducanu, A.; Düggelin, M.; Baschong, W.; et al. Early Detection of Aging Cartilage and Osteoarthritis in Mice and Patient Samples Using Atomic Force Microscopy. *Nat. Nanotechnol.* **2009**, *4*, 186.

(7) Ding, C.; Garnero, P.; Cicuttini, F.; Scott, F.; Cooley, H.; Jones, G. Knee Cartilage Defects: Association with Early Radiographic Osteoarthritis, Decreased Cartilage Volume, Increased Joint Surface Area and Type II Collagen Breakdown. *Osteoarthr. Cartil.* **2005**, *13* (3), 198–205.

(8) Hayami, T.; Pickarski, M.; Wesolowski, G. A.; McLane, J.; Bone, A.; Destefano, J.; Rodan, G. A.; Duong, L. T. The Role of Subchondral Bone Remodeling in Osteoarthritis: Reduction of Cartilage Degeneration and Prevention of Osteophyte Formation by

Alendronate in the Rat Anterior Cruciate Ligament Transection Model. *Arthritis Rheum.* **2004**, *50* (4), 1193–1206.

(9) Hernborg, J.; Nilsson, B. E. The Relationship Between Osteophytes in the Knee Joint, Osteoarthritis and Aging. *Acta Orthop.* **1973**, *44* (1), 69–74.

(10) Suri, S.; Gill, S. E.; De Camin, S. M.; Wilson, D.; McWilliams, D. F.; Walsh, D. A. Neurovascular Invasion at the Osteochondral Junction and in Osteophytes in Osteoarthritis. *Ann. Rheum. Dis.* **2007**, *66* (11), 1423–1428.

(11) Berenbaum, F.; Eymard, F.; Houard, X. Osteoarthritis, Inflammation and Obesity. *Curr. Opin. Rheumatol.* **2013**, *25* (1), 114–118.

(12) Benito, M. J.; Veale, D. J.; FitzGerald, O.; Van Den Berg, W. B.; Bresnihan, B. Synovial Tissue Inflammation in Early and Late Osteoarthritis. *Ann. Rheum. Dis.* **2005**, *64* (9), 1263–1267.

(13) Bonnet, C. S.; Walsh, D. A. Osteoarthritis, Angiogenesis and Inflammation. *Rheumatology* **2005**, *44* (1), 7–16.

(14) Dieppe, P. Inflammation in Osteoarthritis. *Rheumatol. (United Kingdom)* **1978**, *17* (5), 59–63.

(15) Gallagher, B.; Tjoumakaris, F. P.; Harwood, M. I.; Good, R. P.; Ciccotti, M. G.; Freedman, K. B. Chondroprotection and the Prevention of Osteoarthritis Progression of the Knee: A Systematic Review of Treatment Agents. *Am. J. Sports Med.* **2015**, *43* (3), 734–744.

(16) Sharma, L. Osteoarthritis Year in Review 2015: Clinical. *Osteoarthr. Cartil.* **2016**, *24* (1), 36–48.

(17) Zhang, W.; Moskowitz, R. W.; Nuki, G.; Abramson, S.; Altman, R. D.; Arden, N.;

Bierma-Zeinstra, S.; Brandt, K. D.; Croft, P.; Doherty, M.; et al. OARSI Recommendations for the Management of Hip and Knee Osteoarthritis, Part I: Critical Appraisal of Existing Treatment Guidelines and Systematic Review of Current Research Evidence. *Osteoarthr. Cartil.* **2007**, *15* (9), 981–1000.

(18) Zhang, W.; Ouyang, H.; Dass, C. R.; Xu, J. Current Research on Pharmacologic and Regenerative Therapies for Osteoarthritis. *Bone Res.* **2016**, *4*, 15040.

(19) Wieland, H. A.; Michaelis, M.; Kirschbaum, B. J.; Rudolphi, K. A. Osteoarthritis - An Untreatable Disease? *Nat. Rev. Drug Discov.* **2005**, *4* (4), 331–344.

(20) Gillam, M. H.; Lie, S. A.; Salter, A.; Furnes, O.; Graves, S. E.; Havelin, L. I.; Ryan, P. The Progression of End-Stage Osteoarthritis: Analysis of Data from the Australian and Norwegian Joint Replacement Registries Using a Multi-State Model. *Osteoarthr. Cartil.* **2013**, *21* (3), 405–412.

(21) Gossec, L.; Dougados, M. Intra-Articular Treatments in Osteoarthritis: From the Symptomatic to the Structure Modifying. *Ann. Rheum. Dis.* **2004**, *63* (5), 478–482.

(22) Waller, K. A.; Zhang, L. X.; Fleming, B. C.; Jay, G. D. Preventing Friction-Induced Chondrocyte Apoptosis: Comparison of Human Synovial Fluid and Hylan G-F 20. *J. Rheumatol.* **2012**, *39* (7), 1473 LP-1480.

(23) Bowman, S.; Awad, M. E.; Hamrick, M. W.; Hunter, M.; Fulzele, S. Recent Advances in Hyaluronic Acid Based Therapy for Osteoarthritis. *Clin. Transl. Med.* **2018**, *7* (1), 6.

(24) Maheu, E.; Rannou, F.; Reginster, J. Y. Efficacy and Safety of Hyaluronic Acid in the Management of Osteoarthritis: Evidence from Real-Life Setting Trials and Surveys. *Semin. Arthritis Rheum.* **2016**, *45* (4), S28–S33.

(25) Pelet, J. M.; Putnam, D. High Molecular Weight Poly (Methacrylic Acid) with Narrow

Polydispersity by RAFT Polymerization. *Macromolecules* **2009**, *42* (5), 1494–1499.

(26) Gleghorn, J. P.; Bonassar, L. J. Lubrication Mode Analysis of Articular Cartilage Using Stribeck Surfaces. *J. Biomech.* **2008**, *41* (9), 1910–1918.

(27) Bonnevie, E. D.; Galesso, D.; Secchieri, C.; Cohen, I.; Bonassar, L. J. Elastoviscous Transitions of Articular Cartilage Reveal a Mechanism of Synergy between Lubricin and Hyaluronic Acid. *PLoS One* **2015**, *10* (11), 1–15.

(28) TRUETA, J. Osteoarthritis of the Hip. *Ann. R. Coll. Surg. Engl.* **1954**, *15* (3), 174–192.

(29) Peng, G.; McNary, S. M.; Athanasiou, K. A.; Reddi, A. H. The Distribution of Superficial Zone Protein (SZP)/Lubricin/PRG4 and Boundary Mode Frictional Properties of the Bovine Diarthrodial Joint. *J. Biomech.* **2015**, *48* (12), 3406–3412.

(30) Caligaris, M.; Ateshian, G. A. Effects of Sustained Interstitial Fludi Pressurization Under Migrating Contact Area, and Boundary Lubrication by Synovial Fluid, on Cartialge Friction. *Osteoarthr. Cartil.* **2008**, *16* (10), 1220–1227.

(31) Shi, L.; Sikavitsas, V. I.; Striolo, A. Experimental Friction Coefficients for Bovine Cartilage Measured with a Pin-on-Disk Tribometer : Testing Configuration and Lubricant Effects. *Ann. Biomed. Engienering* **2011**, *39* (1), 132–146.

CHAPTER 5

CONCLUSION AND FUTURE DIRECTIONS

5.1 Conclusion

Biomimicry of natural materials is an expanding field in biomedical engineering and the life sciences. The incredible science behind how nature solves a problem has inspired scientists and engineers to design artificial materials that mimic their natural mode's extraordinary functions generation after generation[1–4]. One biological wonder is how weight bearing joints can provide incredibly low friction under tremendous loads for decades[5,6]. Even the best engineered structures cannot rival its tribological properties. Naturally, the body creates biomacromolecules as lubricants to protect and maintain the integrity of joint cartilage[7]. One of the biolubricants, lubricin, which is an O-glycosylated protein, plays pivotal roles for boundary mode lubrication[8,9] where the greatest friction and wear occurs. Its preclinical application has demonstrated promising effects for the treatment[10–13] of osteoarthritis (OA) which, to date, has been considered as an incurable disease unless treated by arthroplasty[14]. Likely to be an effective treatment in humans, the scale-up of lubricin production or purification is hindered by the degree of protein glycosylation[15], preventing its production recombinantly in prokaryotic cells such as *E. coli*. Further, the high affinity of lubricin to other molecules in synovial fluid, such as fibronectin[16], pose a challenge in cost-efficient purification methods for clinical use. With these aspects in mind, production of a synthetic version of lubricin mimetics may prove effective.

This dissertation presented the design and synthesis of a class of biomimetic polymers with analogous structure and function to the glycoprotein lubricin, and their evaluation as an artificial

lubricant to treat OA. Chapter 2 demonstrated the ability of one lubricin mimetic to lubricate lubricin-deficient articular cartilage surfaces as effectively and efficiently as natural lubricin. Chapter 3 characterized the effects of how changing the structural parameters affected the lubrication on cartilage surfaces. Chapter 4 explored the ability of a biomimetic polymer to bind to and lubricate bone surfaces, which is absent in natural lubricin, thus extending its potential application as a therapeutic for late-stage OA treatment.

In Chapter 2, we evaluated the tribological properties of one lubricin mimetic and demonstrated its lubrication ability which arose from its diblock architecture. Synthesized via three-step RAFT polymerization, the polymer consisted of a large lubrication block (Mn ~ 200 kDa) to mimic the mucin-like domain of lubricin and a small cartilage-binding block (Mn ~3 kDa) to mimic the C-terminus domain. This architecture enables the molecule to quickly bind (binding time constant = 7.4 min) onto the cartilage surface via electrostatic interactions and efficiently (EC_{50} = 0.404 mg/ml) lubricate the cartilage surface at a level that is comparable to natural lubricin. Further investigation of the architecture using the Surface Force Apparatus (SFA) revealed the importance of the diblock architecture to maintain the binding of polymers on the articulating surface under high compression load.

The study in Chapter 3 characterized how the structure of lubricin mimetics affected their binding to cartilage surfaces and how these changes affected their lubrication ability. The most significant outcome of the work in Chapter 3 was that the lubrication ability of the lubricin mimetic diblock copolymer solely depended on the length of the binding block. A binary relationship between the lubrication ability and the number of amino group in the binding block was unveiled as they are proportional in the range between the minimal length and the optimal length and disproportional with increased length. Two factors that were theoretically affected

oppositely by the binding block length, the binding affinity and the polymer coating density, were speculated as possible factors to account for these phenomena together. With short binding blocks, binding affinity dominated the overall effect possibly due to the increased number of amino groups enabling the polymer to form a more shear-resistant layer. With longer binding blocks, the coating density seemed to outweigh the binding affinity, thus the lubrication ability decreased with the increased binding block length, likely because of a decreased coating density that resulted from increased charge-charge repulsion. These results suggested the importance of the proper design of binding features for the synthetic lubricants to maintain the lubrication film and high adsorption density at the interface.

Chapter 4 demonstrated that this type of lubricant can bind to and lubricate the bone surfaces by following similar design criteria reported in the previous chapters. Using a bone-on-glass configuration, the diblock copolymer is able to effectively reduce the coefficient of friction (COF) of bone surfaces at both glass and cartilage interfaces. A further investigation using bone-on-cartilage configuration show that the presence of polymer on the surface rather than in the lubrication bath is essential for effective lubrication, suggesting a boundary mode mechanism at this interface. This to our knowledge is the first report of bone lubrication and results of this chapter highlighted the potential of a lubricating polymer as a new approach to treat late-stage OA when the bone surfaces are exposed.

The major contributions of this work are twofold: 1) the development of supplemental boundary lubricants that have the potential to treat cartilage injury and joint disease at various stages, and 2) a mechanistic understanding of how cartilage boundary lubrication and the structure of synthetic lubricants are linked. Chapter 2 and 4 examined the ability of the lubricin mimetics to lubricate different types of tissue surfaces and thus demonstrated their therapeutic

potential for the treatment of OA at different stages. Chapter 3 explained that this ability was mainly affected by the binding block length whereas the lubrication block had no major influence within the range in our study.

5.2 Study Limitations and Future Directions on Cartilage Lubrication

The promising *in vitro* results were not successfully translated into animal studies. In collaboration with the Rodeo lab at Weill Cornell Medicine, the effects of lubricin mimetics to delay or stop the progression of post-traumatic OA were evaluated using an anterior cruciate ligament transection (ACLT) rat model. Four types of lubricin-mimetics were used, and they varied in architecture type (diblock vs random) and amine type (tertiary vs quaternary) in the binding block. Those four types of lubricin mimetics were intra-articularly (IA) injected twice a week from week one through week four post-surgery. The cartilage integrity was evaluated by Safranin-O and H&E staining and the mechanical properties of the explanted cartilage were evaluated *ex vivo* using the custom-built tribometer. Contrary to the *in vitro* results, neither histology nor mechanical evaluation of any polymer treated groups show significant improvement in comparison to the PBS controls. One possible explanation for the lack of chondroprotective effect by the lubricin-mimetics *in vivo* is the deficiency of the polymer to bind to the cartilage surface in a complex biological environment. Only one group showed weak polymer binding signal on the cartilage surfaces by the end of study using PEG immunohistochemistry (IHC) analysis. Further investigations showed that the non-specific binding strategy resulted in polymer binding to synovium, meniscus, tendon, and potentially hyaluronic acid as well, which possibly suppressed its ability to bind to the cartilage and lubricate the surface.

To overcome this drawback, successful delivery of the polymers onto the cartilage surfaces

after IA injection must be guaranteed. One straightforward method to achieve this is to increase the dose and achieve a concentration gradient high enough in the synovial fluid for the polymer to diffuse onto the cartilage. Two injections at concentration of 100 mg/ml (in comparison to 3 mg/ml in the rat study) performed by Dr. Krotscheck and Dr. Hayashi at Cornell Veterinary School alleviated the symptoms of two late-stage OA dogs by improving their gait, demonstrating the therapeutic potential of polymers for OA treatment. However, an increased concentration might raise safety concerns due to the possible toxicity of the quaternary amine and other compositions. An alternative approach to improve the targeting affinity is by modifying the binding block with cartilage binding peptides. For example, the peptide sequences TKKTLRT, SQNPVQP, and WYRGRL bind to collagen with IC_{50} values within the range of 100-300 nM[17,18], and they have been used to bind nanoparticles to type II collagen of cartilage tissue[17] and serve as a tether for the attachment of other cartilage lubricants[19]. Similarly, the drawback of introducing peptide sequences will raise safety concerns such as immunogenicity which might prevent the further clinical application of this type of polymer.

Recently, Bajpayee and Grodzinsky *et al* reported a novel cartilage-targeting drug delivery approach utilizing charge-charge interactions to enhance drug penetration and transport into cartilage[20–22]. By coupling drugs to positively charged nanoparticles such as avidin with optimal size and charge, cartilage can be converted from a drug barrier into a drug reservoir for sustained intra-tissue delivery. Tissue sGAG content correlates positively with avidin uptake and half-life, with the highest concentration and longest retention time found in cartilage[20]. These promising results encourage the further application of our binding strategies. Although the optimal size and charge for our system remains unknown, tuning the molecular factors such as binding block length, charge distribution, or molecular size could potentially optimize the targeting of polymers

to cartilage surfaces.

5.3 Study Limitations and Future Directions on Structure-Property Relationship

The binary relationship between the binding block and the lubrication ability remains elusive due to the challenge to characterize the surface layer of articular cartilage without disrupting its integrity. Many techniques such as light, electron, and force microscopy techniques have been applied in this field[23], yet the mechanism of how the biomacromolecules bind to and interact with the surface is still unclear, and the amount of lubricants binding to the surface are undetermined. Methods such as immunofluorescence or enzyme-linked immunosorbent assay can semi-quantify the amount of polymer uptake by the cartilage and reveal their spatial distribution. However, little information is known regarding the outermost layer of articular cartilage, which prevents the further understanding of its boundary mode lubrication. A direct way to analyze the cartilage surface is therefore needed to better understand how the lubricants modify the articulating surface.

An alternative approach that could potentially help to interpret the polymer structure and binding property relationship is to utilize techniques such as SFA and atomic force microscopy (AFM) to characterize the polymer conformations on ideal surfaces such as mica. The contour length of the polymer is measured to be around 55 nm by a bridging experiment performed on SFA by The Gourdon lab. This result, in combination with the measured uncompressed film thickness (25 nm), indicates the polymer adopted a coiled “mushroom-like” conformation before compression. At maximum compression, the film thickness is reduced to about 5 nm, which is equal to two-fold of the contour length of the PEG side chains, suggesting the polymer adapted a flat configuration with side chains pointing vertically on the surface. Aside from the above information, little is known about other characteristics such as the binding force, surface

distribution, and the fluidity of the film, and how they are influenced by the polymer architecture. Such questions, which could potentially be answered by the application of surface characterization technologies, will guide the understanding of lubrication mechanism on cartilage surface.

5.4 Study Limitations and Future Directions on Bone Lubrication

As the pioneering study on bone lubrication, many questions are left open and are worth further investigation. Firstly, a systematic evaluation of the lubrication abilities to pathological bones is necessary to fully explore the clinical potential of this type of polymer. As the major weight bearing materials in the biological system, bone possesses unique structures and compositions that are dynamically evolved with the progression of joint diseases[24,25]. The subchondral layer in late-stage OA has histopathological features that are not found in healthy tissues. The ability to lubricate diseased bones is thus critical for further application of the polymer in clinical studies.

In addition, comprehensive analysis of the key lubrication parameters of polymers such as EC_{50} values and binding time constants will enable the definition of new design criteria for bone lubricants. As a porous and stiff material, bone has lubrication characteristic fundamentally different from those of cartilage. Understanding how the molecular structure affects the lubrication will inspire the design of the next generation of polymers that can lubricate bones more effectively and efficiently.

Studies that evaluated the effect of the viscosity and sliding speed to bone lubrication seem to give a Stribeck-like trend as increased viscosity reduces the COF. With deficient evidence to conclude this to be the transition from the boundary mode to the mixed mode as shown in the classic Stribeck curve, we need to carry out a full exploration of the tribological behaviors of

bones in the future. Using the bone-on-glass configuration, tribological factors such as normal load and surface roughness in addition to viscosity and sliding speed could be adjusted to broaden the range of Stribeck curve, allowing the full description of the bone tribology within the frame of a classic Stribeck analysis. Comparison of the tribological behaviors of bone to the classic Stribeck curve or that of cartilage will provide insights into the understanding of bone lubrication mechanisms.

Further interpretation of the results from the friction test using the bone-on-cartilage configuration is difficult due to the unconfined experimental conditions. Normal load varied by orders of magnitude during sliding and the interstitial fluid pressure fluctuated between compression and release. This drawback could potentially be solved by adapting a rotating rod-on-rod configuration to overcome the limitation of obtaining flat subchondral bone surfaces. In comparison to our tribometer characterized for sliding motion, this type of tribometer is able to measure smaller tissue samples at the cost of measurement consistency and physiologically relevance on displacement. An alternative approach is to measure the tribological behaviors of the surface between the cartilage plugs and the trabecular plates. Both materials are accessible for the experiment although the physiological relevance of this type of set-up might be diminished in comparison to the interface between the cartilage and subchondral bone.

Last but not least, friction between subchondral bone plugs and trabecular bone plates (bone-on-bone) were tested and the results were perplexing. Instead of smooth sliding, intermittent displacement or “stick-slip” phenomenon was observed during the test even in the polymer or 23% dextran bath. The huge static COF prevented the measurement of kinetic COF as was shown in the previous study, demonstrating the need for a new data analysis method to interpret the results. Parameters such as the maximum friction force and the frequency of stick-slip could

be derived for analysis. Similar to bone-on-cartilage tribology, displacement on subchondral bone surfaces is challenging to accomplish. A subchondral bone layer harvesting technique is needed in the future.

5.5 References

(1) Liu, K.; Jiang, L. Bio-Inspired Design of Multiscale Structures for Function Integration. *Nano Today* **2011**, *6* (2), 155–175.

(2) Liu, K.; Yao, X.; Jiang, L. Recent Developments in Bio-Inspired Special Wettability. *Chem. Soc. Rev.* **2010**, *39* (8), 3240.

(3) Bar-Cohen, Y. Biomimetics - Using Nature to Inspire Human Innovation. *Bioinspiration and Biomimetics* **2006**, *1* (1).

(4) Bar-Cohen, Y. Biomimetics: Mimicking and Inspired-by Biology. **2005**, No. May 2005, 1.

(5) Ateshian, G. A. The Role of Interstitial Fluid Pressurization in Articular Cartilage Lubrication. *J. Biomech.* **2009**, *42* (9), 1163–1176.

(6) McCutchen, C. W. The Frictional Properties of Animal Joints. *Wear* **1962**, *5* (1), 1–17.

(7) Schmidt, T. A.; Gastelum, N. S.; Nguyen, Q. T.; Schumacher, B. L.; Sah, R. L. Boundary Lubrication of Articular Cartilage: Role of Synovial Fluid Constituents. *Arthritis Rheum.* **2007**, *56* (3), 882–891.

(8) Musumeci, G. The Role of Lubricin in Normal and Pathological Joint Tissue: A Contemporary Review. *OA Anat.* **2013**, *1* (1), 1–6.

(9) Jay, G. D.; Waller, K. A. The Biology of Lubricin: Near Frictionless Joint Motion. *Matrix Biol.* **2014**, *39*, 17–24.

(10) Flannery, C. R.; Zollner, R.; Corcoran, C.; Jones, A. R.; Root, A.; Rivera-Bermúdez, M. A.; Blanchet, T.; Gleghorn, J. P.; Bonassar, L. J.; Bendele, A. M.; et al. Prevention of Cartilage Degeneration in a Rat Model of Osteoarthritis by Intraarticular Treatment with Recombinant Lubricin. *Arthritis Rheum.* **2009**, *60* (3), 840–847.

(11) Jay, G. D.; Fleming, B. C.; Watkins, B. A.; McHugh, K. A.; Anderson, S. C.; Zhang, L.

X.; Teeple, E.; Waller, K. A.; Elsaid, K. A. Prevention of Cartilage Degeneration and Restoration of Chondroprotection by Lubricin Tribosupplementation in the Rat Following Anterior Cruciate Ligament Transection. *Arthritis Rheum.* **2010**, *62* (8), 2382–2391.

(12) Waller, K. a; Zhang, L. X.; Elsaid, K. a; Fleming, B. C.; Warman, M. L.; Jay, G. D. Role of Lubricin and Boundary Lubrication in the Prevention of Chondrocyte Apoptosis. *Proc. Natl. Acad. Sci. U. S. A.* **2013**, *110* (15), 5852–5857.

(13) Bao, J. P.; Chen, W. P.; Wu, L. D. Lubricin: A Novel Potential Biotherapeutic Approaches for the Treatment of Osteoarthritis. *Mol. Biol. Rep.* **2011**, *38* (5), 2879–2885.

(14) Wieland, H. A.; Michaelis, M.; Kirschbaum, B. J.; Rudolphi, K. A. Osteoarthritis - An Untreatable Disease? *Nat. Rev. Drug Discov.* **2005**, *4* (4), 331–344.

(15) Jay, G. D.; Harris, D. A.; Cha, C. J. Boundary Lubrication by Lubricin Is Mediated by O-Linked β(1-3)Gal-GalNAc Oligosaccharides. *Glycoconj. J.* **2001**, *18* (10), 807–815.

(16) Flowers, S. A.; Zieba, A.; Örnros, J.; Jin, C.; Rolfson, O.; Björkman, L. I.; Eisler, T.; Kalamajski, S.; Kamali-Moghaddam, M.; Karlsson, N. G. Lubricin Binds Cartilage Proteins, Cartilage Oligomeric Matrix Protein, Fibronectin and Collagen II at the Cartilage Surface. *Sci. Rep.* **2017**, *7* (1), 1–11.

(17) Rothenfluh, D. A.; Bermudez, H.; O'Neil, C. P.; Hubbell, J. A. Biofunctional Polymer Nanoparticles for Intra-Articular Targeting and Retention in Cartilage. *Nat. Mater.* **2008**, *7* (3), 248–254.

(18) De Souza, S. J.; Brentani, R. Collagen Binding Site in Collagenase Can Be Determined Using the Concept of Sense-Antisense Peptide Interactions. *J. Biol. Chem.* **1992**, *267* (19), 13763–13767.

(19) Singh, A.; Corvelli, M.; Unterman, S. A.; Wepasnick, K. A.; McDonnell, P.; Elisseeff, J.

H. Enhanced Lubrication on Tissue and Biomaterial Surfaces through Peptide-Mediated Binding of Hyaluronic Acid. *Nat. Mater.* **2014**, *13* (10), 988–995.

(20) Bajpayee, A. G.; Scheu, M.; Grodzinsky, A. J.; Porter, R. M. Electrostatic Interactions Enable Rapid Penetration, Enhanced Uptake and Retention of Intra-Articular Injected Avidin in Rat Knee Joints. *J. Orthop. Res.* **2014**, *32* (8), 1044–1051.

(21) Bajpayee, A. G.; Quadir, M. A.; Hammond, P. T.; Grodzinsky, A. J. Charge Based Intra-Cartialge Delivery of Single Dose Dexamethasone Using Avidin Nano-Carriers Suppresses Cytokine-Induced Catabolism Long Term. *Osteoarthr. Cartil.* **2016**, *24* (1), 71–81.

(22) Bajpayee, A. G.; Grodzinsky, A. J. Cartilage-Targeting Drug Delivery: Can Electrostatic Interactions Help? *Nat. Rev. Rheumatol.* **2017**, *13*, 183–193.

(23) Rexwinkle, J. T.; Hunt, H. K.; Pfeiffer, F. M. Characterization of the Surface and Interfacial Properties of the Lamina Splendens. *Front. Mech. Eng.* **2017**, *12* (2), 234–252.

(24) Li, G.; Yin, J.; Gao, J.; Cheng, T. S.; Pavlos, N. J.; Zhang, C.; Zheng, M. H. Subchondral Bone in Osteoarthritis: Insight into Risk Factors and Microstructural Changes. *Arthritis Res. Ther.* **2013**, *15* (6).

(25) Hayami, T.; Pickarski, M.; Wesolowski, G. A.; McLane, J.; Bone, A.; Destefano, J.; Rodan, G. A.; Duong, L. T. The Role of Subchondral Bone Remodeling in Osteoarthritis: Reduction of Cartilage Degeneration and Prevention of Osteophyte Formation by Alendronate in the Rat Anterior Cruciate Ligament Transection Model. *Arthritis Rheum.* **2004**, *50* (4), 1193–1206.

APPENDIX

CHARACTERIZATION OF LUBRICIN MIMETIC DIBLOCK COPOLYMERS

Methods

The ^{1}H NMR spectra were performed on an Inova 400 MHz spectrometer with deuterated chloroform or deuterium oxide as the solvent. Broad or overlapping peaks, noted in spectra of polymers, are denoted “br”. Degree of polymerization (DP) was determined by initial monomer to chain transfer agent (CTA) ratio and monomer conversion ratio. Gel permeation chromatography (GPC) was performed with PBS (pH 7.4) at a flow rate of 0.8 ml/min. The eluent flowed through a Waters gel permeation chromatography system equipped with three Waters UltrahydrogelTM columns in series (2000 Å, 500 Å, and, 250 Å) at 30 °C. The molecular weights were measured against poly (methacrylic acid), sodium salt standards (1,670 to 110,000 g/mol).

PDMAEA$_{24}$:

^{1}H NMR(400 MHz, $CDCl_3$): δ 4.13 (br, 2H, -(C=O)O-**CH_2**-CH_2-), 2.55 (br, 2H, -O-CH_2-**CH_2**-N$(CH_3)_2$), 2.31 (br, 7H, -N(**CH_3**)$_2$, -CH_2C**H**(C=O)-), 2.02 – 1.36 (m, 2H, -**CH_2**CH(C=O)-), 5.30 (s, residue dichloromethane).

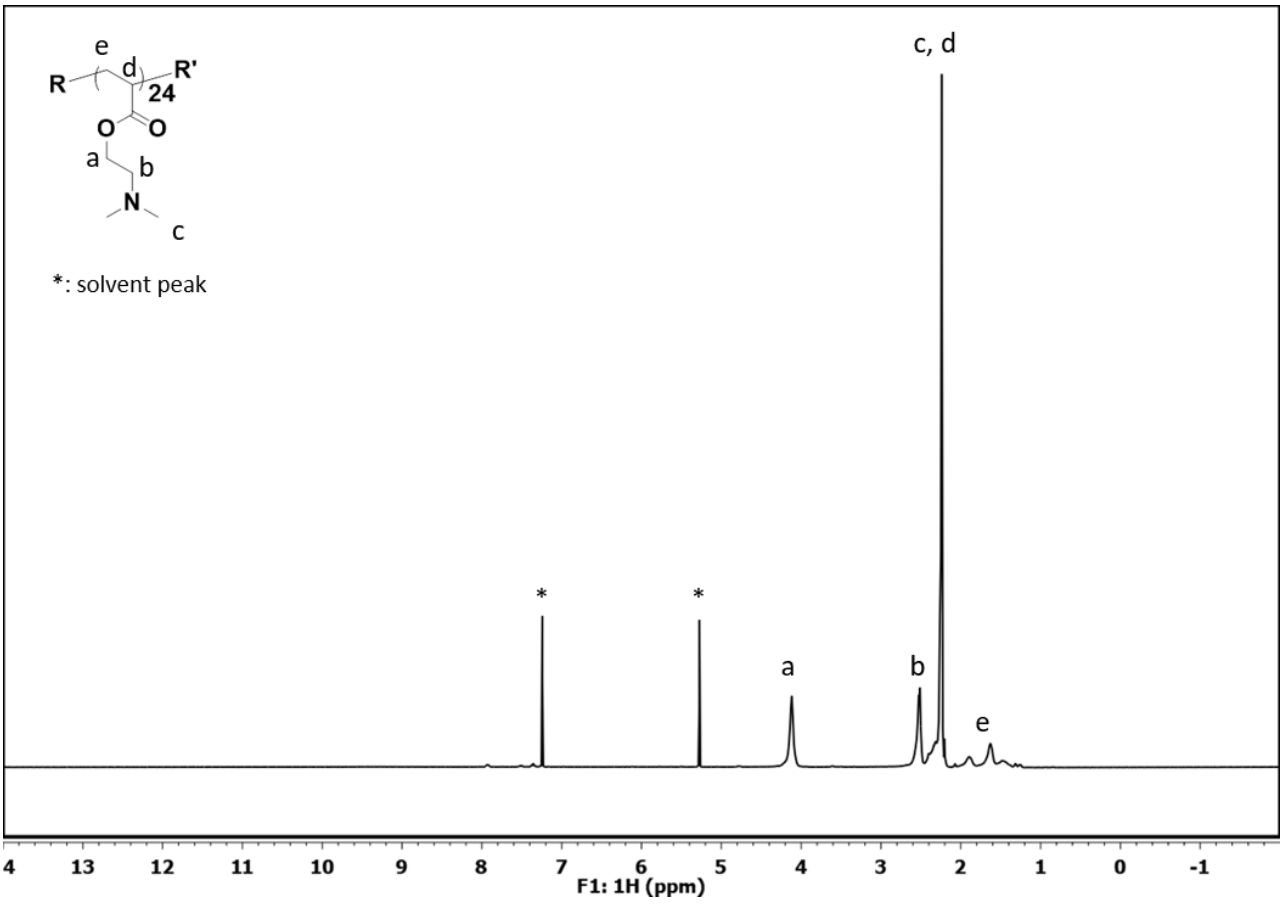

PDMAEA$_{24}$-PEGMEA$_{400}$ (diblock copolymer):

^{1}H NMR (400 MHz, $CDCl_3$): δ 4.13 (br, 2H, -(C=O)O-**CH$_2$**-CH$_2$-), 3.75 – 3.44 (m, 34H, -O-**CH$_2$-CH$_2$**-O-), 3.35 (s, 3H, -O-**CH$_3$**), 2.24 (br, ~1H, -CH$_2$C**H**(C=O)-, -N(**CH$_3$**)$_2$), 1.93 – 1.26 (m, 2H, -**CH$_2$**CH(C=O)-), 5.30 (s, residue dichloromethane).

SEC: Mn = 44,900; PDI = 1.58.

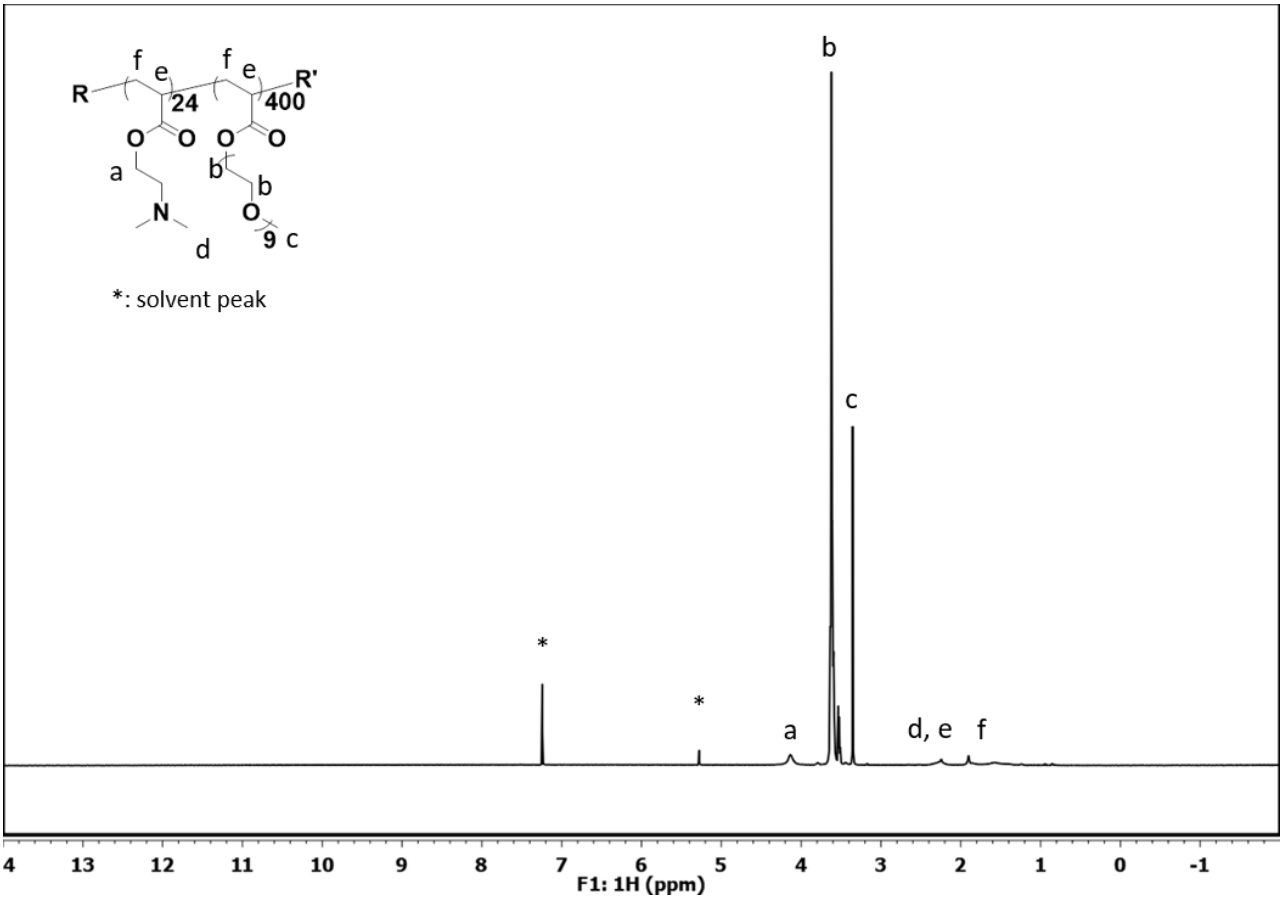

qPDMAEA$_{24}$-PEGMEA$_{400}$ (diblock copolymer):

^{1}H NMR (400 MHz, D_2O): δ 4.08 (br, 2H, -(C=O)O-**CH$_2$**-CH$_2$-), 3.75 – 3.46 (m, 34H, -O-**CH$_2$**-**CH$_2$**-O-), 3.21 (s, 3H, -O-**CH$_3$**), 3.02 (s, ~0.4H, -N$^+$(**CH$_3$**)$_2$CH$_2$CH$_3$), 2.21 (br, 1H, -CH$_2$C**H**(C=O)-), 2.01 – 1.36 (m, 2H, -**CH$_2$**CH(C=O)-), 1.25 (br, ~ 0.2 H, -N$^+$(CH$_3$)$_2$CH$_2$**CH$_3$**).

SEC: Mn = 46,100; PDI = 1.58.

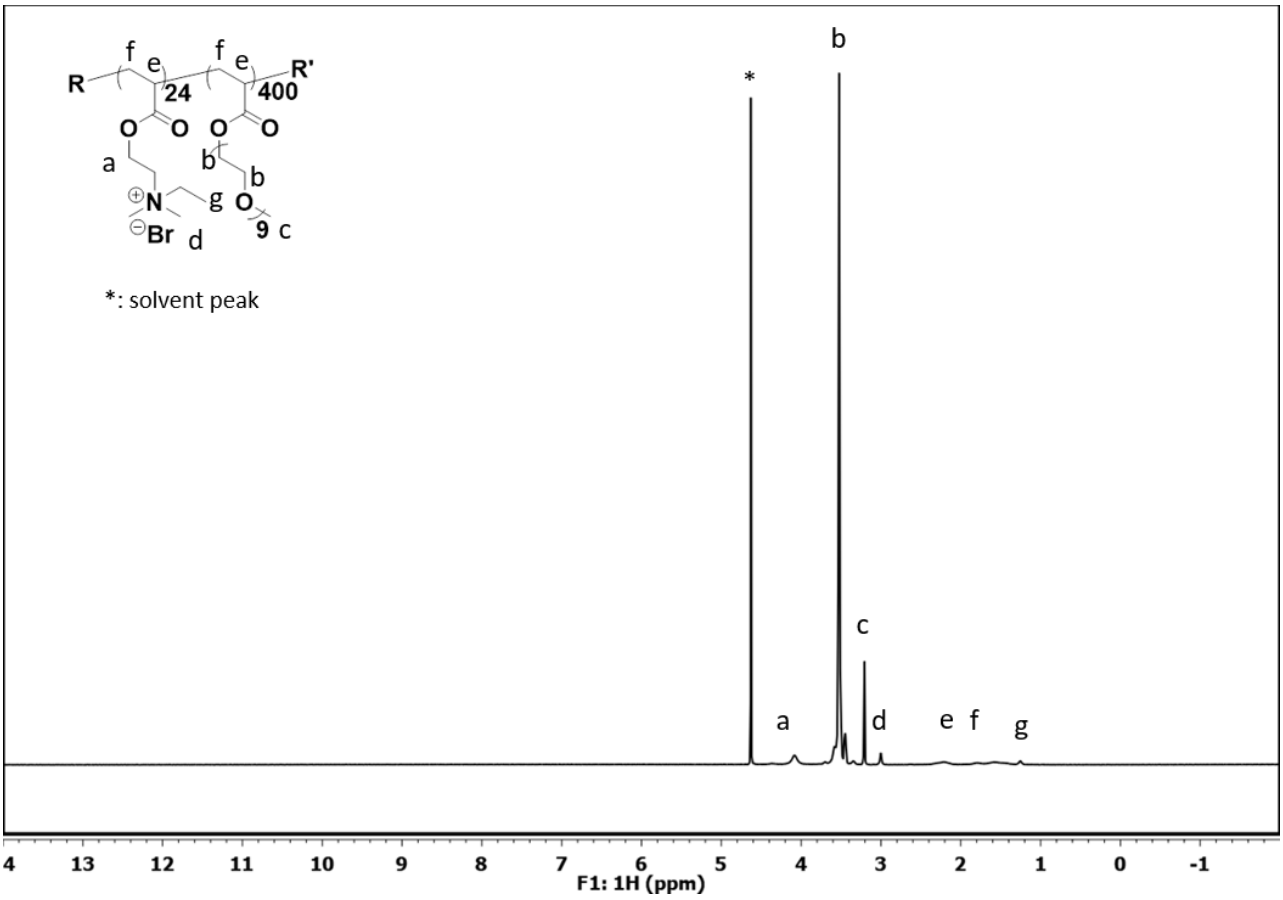

qPDMAEA$_{24}$ (binding block):

^{1}H NMR (400 MHz, D_2O): δ 4.40 (br, 2H, -(C=O)O-**CH$_2$**-CH_2-), 3.61 (br, 2H, -O-CH_2-**CH$_2$**-$N^+(CH_3)_2CH_2CH_3$), 3.38 (br, 2H, -$N^+(CH_3)_2$**CH$_2$**CH_3), 3.02 (s, 6H, -N^+(**CH$_3$**)$_2CH_2CH_3$), 2.41 (br, 1H, -CH_2C**H**(C=O)-), 2.02 – 1.45 (m, 2H, -**CH$_2$**CH(C=O)-), 1.26 (s, 3H, -$N^+(CH_3)_2CH_2$**CH$_3$**).

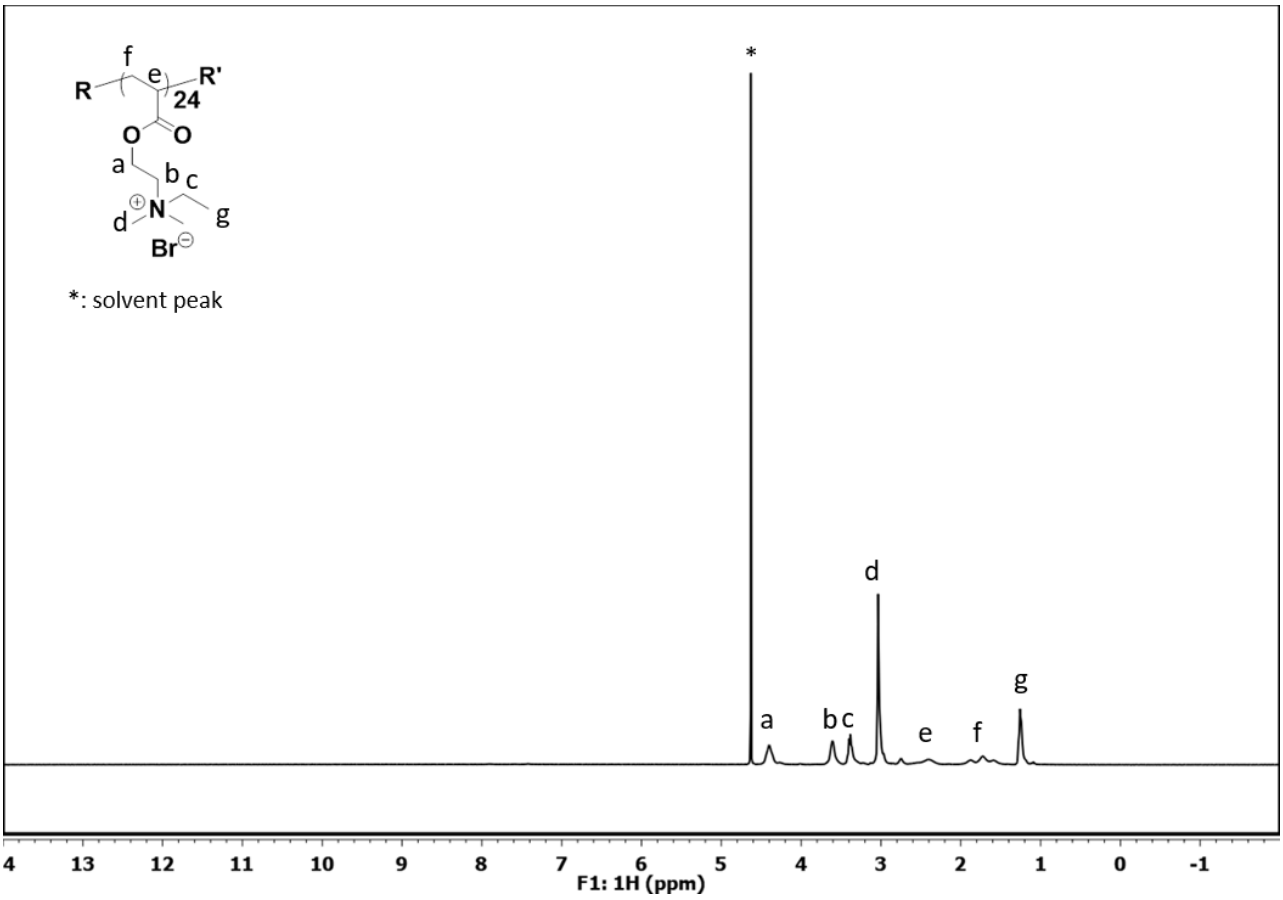

PEGMEA$_{400}$ (lubrication block):

^{1}H NMR (400 MHz, CDCl3): δ 4.12 (br, 2H, -(C=O)O-**CH$_2$**-CH$_2$-), 3.81 – 3.39 (m, 34H, -O-**CH$_2$-CH$_2$**-O-), 3.34 (s, 3H, -O-**CH$_3$**), 2.10 (br, 1H, -CH$_2$C**H**(C=O)-) 2.02 – 1.36 (m, 2H, -**CH$_2$**CH(C=O)-).

SEC: Mn = 33,800; PDI = 1.52.

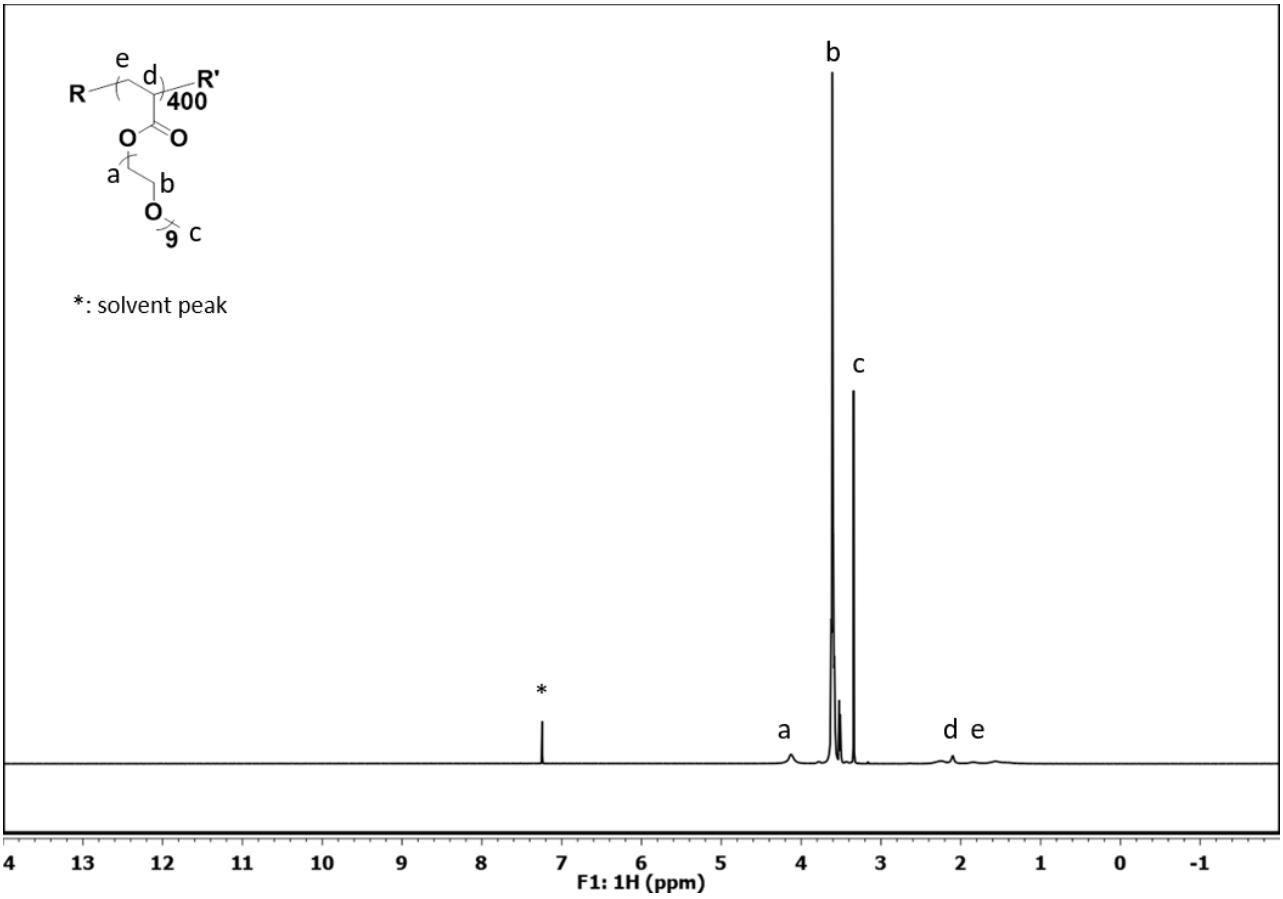

PDMAEA$_{24}$-PEGMEA$_{400}$ (random copolymer):

^{1}H NMR (400 MHz, $CDCl_3$): δ 4.12 (br, 2H, -(C=O)O-**CH$_2$**-CH$_2$-), 3.75 – 3.44 (m, 34H, -O-**CH$_2$-CH$_2$**-O-), 3.35 (s, 3H, -O-**CH$_3$**), 2.26 (br, ~1H, -CH$_2$C**H**(C=O)-, -N(**CH$_3$**)$_2$), 1.93 – 1.36 (m, 2H, -**CH$_2$**CH(C=O)-), 5.30 (s, residue dichloromethane).

SEC: Mn = 32,700; PDI = 1.94.

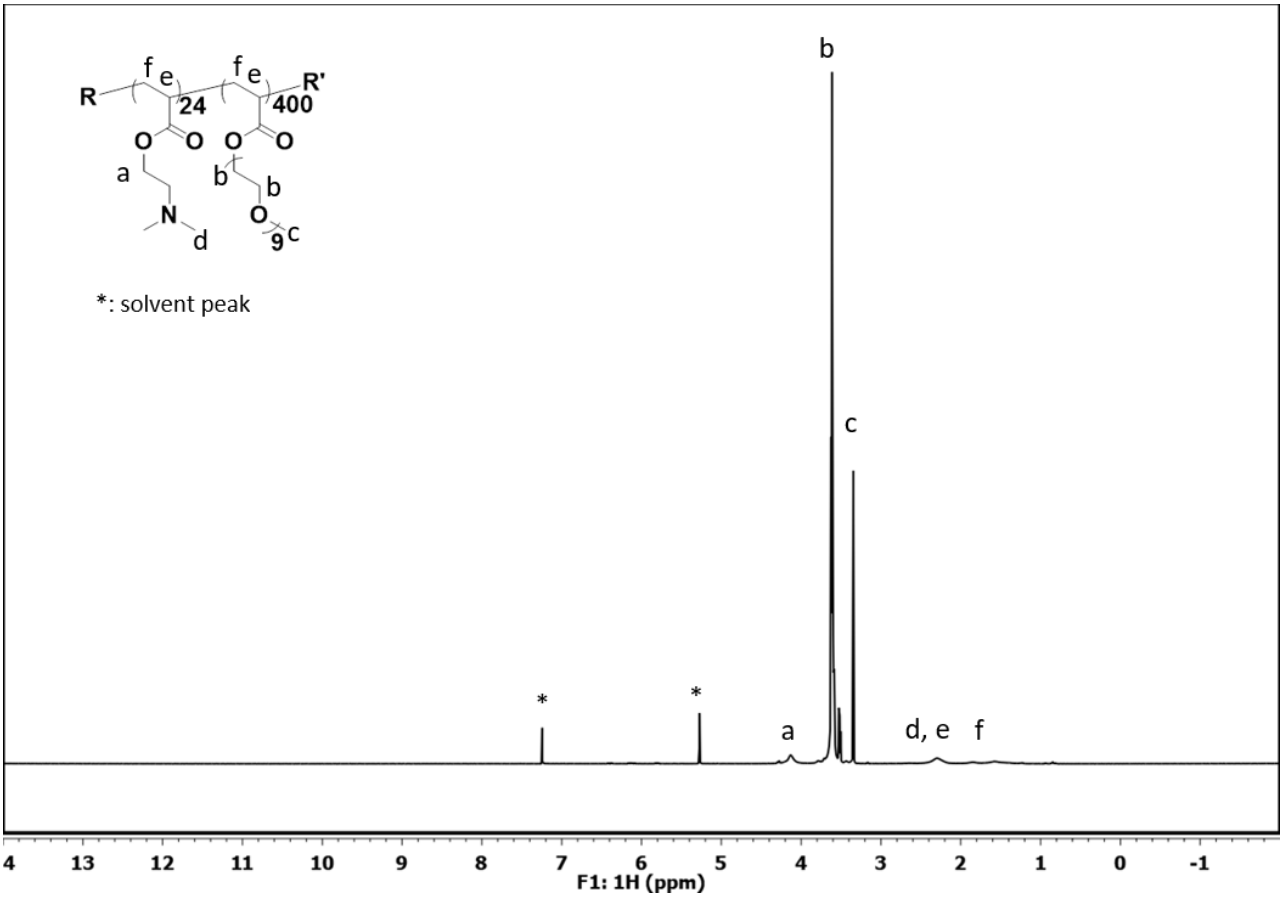

qPDMAEA$_{24}$-PEGMEA$_{400}$ (random copolymer):

^{1}H NMR (400 MHz, D_2O) δ 4.08 (br, ~2H, -(C=O)O-**CH$_2$**-CH$_2$-), 3.75 – 3.44 (m, 34H, -O-**CH$_2$**-**CH$_2$**-O-), 3.21 (s, 3H, -O-**CH$_3$**), 3.02 (s, ~0.3H, -N$^+$(**CH$_3$**)$_2$CH$_2$CH$_3$), 2.21 (br, 1H, -CH$_2$C**H**(C=O)-), 2.02 – 1.44 (m, 2H, -**CH$_2$**CH(C=O)-), 1.25 (br, ~ 0.1H, -N$^+$(CH$_3$)$_2$CH$_2$**CH$_3$**).

SEC: Mn = 33,400; PDI = 1.71.

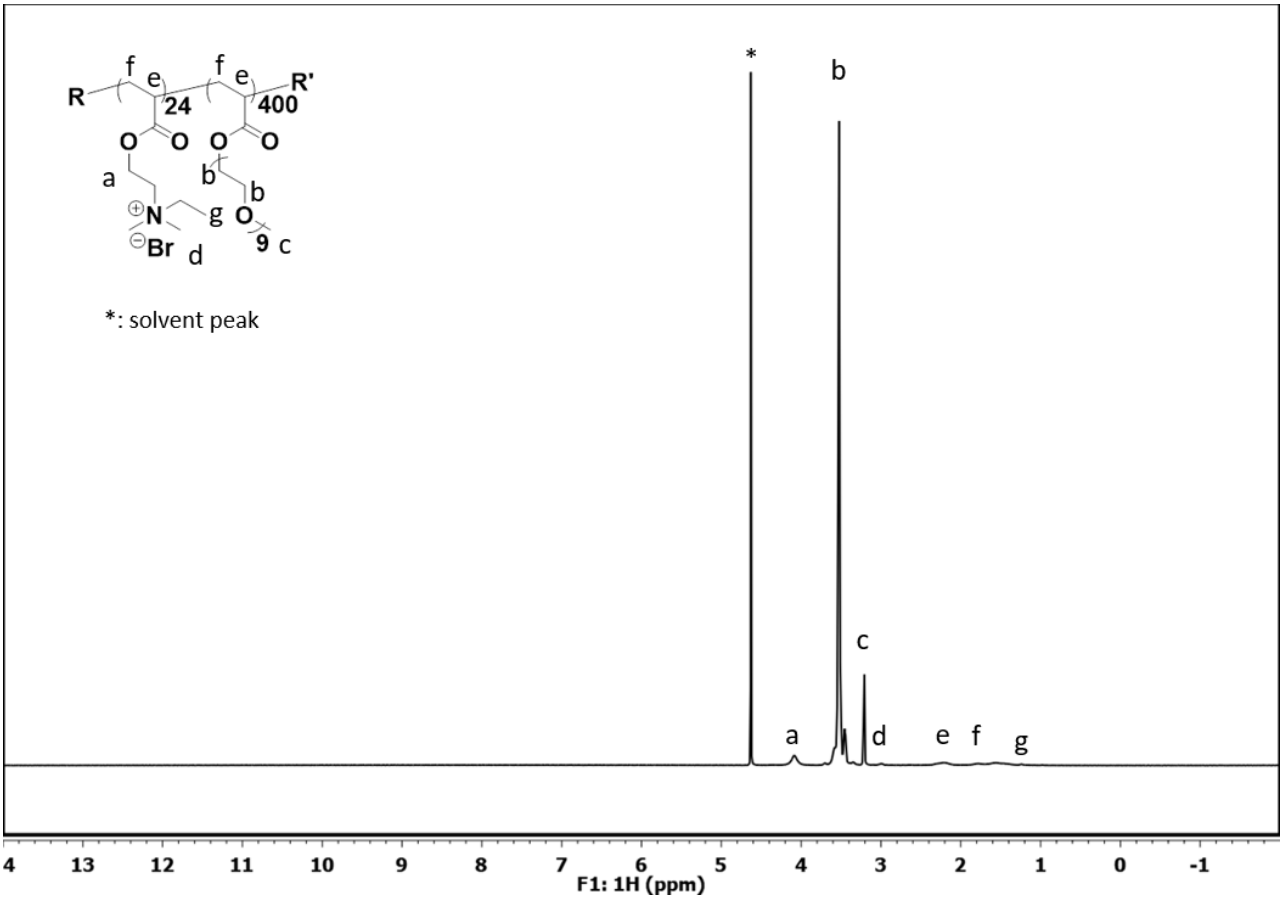

qPDMAEA$_{12}$-PEGMEA$_{200}$ (diblock copolymer):

^{1}H NMR (400 MHz, D_2O): δ 4.08 (br, 2H, -(C=O)O-**CH$_2$**-CH$_2$-), 3.75 – 3.46 (m, 34H, -O-**CH$_2$**-**CH$_2$**-O-), 3.21 (s, 3H, -O-**CH$_3$**), 3.02 (s, ~0.2H, -N$^+$(**CH$_3$**)$_2$CH$_2$CH$_3$), 2.21 (br, 1H, -CH$_2$C**H**(C=O)-), 2.01 – 1.36 (m, 2H, -**CH$_2$**CH(C=O)-), 1.25 (br, ~ 0.1 H, -N$^+$(CH$_3$)$_2$CH$_2$**CH$_3$**).

SEC: Mn = 26,800; PDI = 1.79.

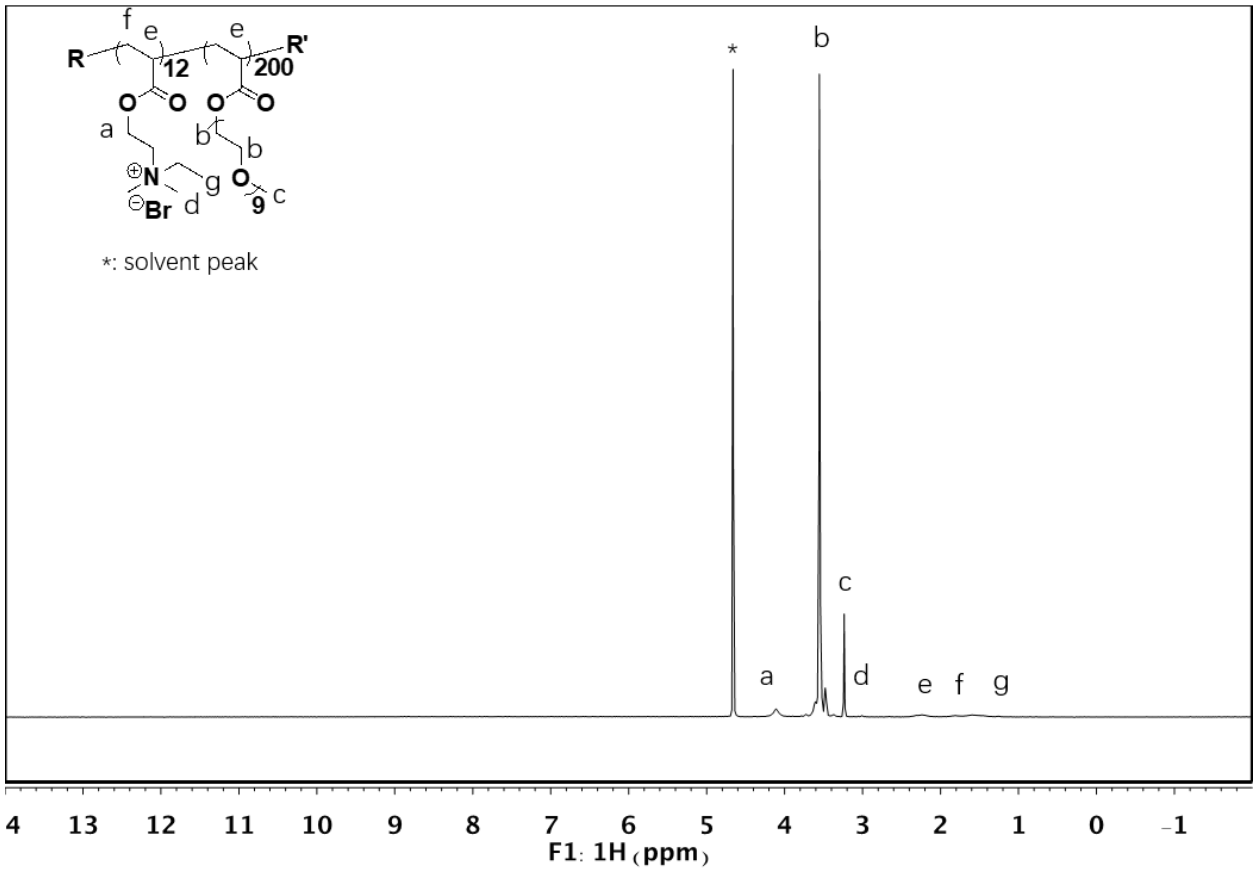

qPDMAEA$_{12}$-PEGMEA$_{400}$ (diblock copolymer):

^{1}H NMR (400 MHz, D_2O): δ 4.08 (br, 2H, -(C=O)O-**CH$_2$**-CH$_2$-), 3.75 – 3.46 (m, 34H, -O-**CH$_2$**-**CH$_2$**-O-), 3.21 (s, 3H, -O-**CH$_3$**), 3.02 (s, ~0.2H, -N$^+$(**CH$_3$**)$_2$CH$_2$CH$_3$), 2.21 (br, 1H, -CH$_2$C**H**(C=O)-), 2.01 – 1.36 (m, 2H, -**CH$_2$**CH(C=O)-), 1.25 (br, ~0.1H, -N$^+$(CH$_3$)$_2$CH$_2$**CH$_3$**).

SEC: Mn = 44,700; PDI = 1.89.

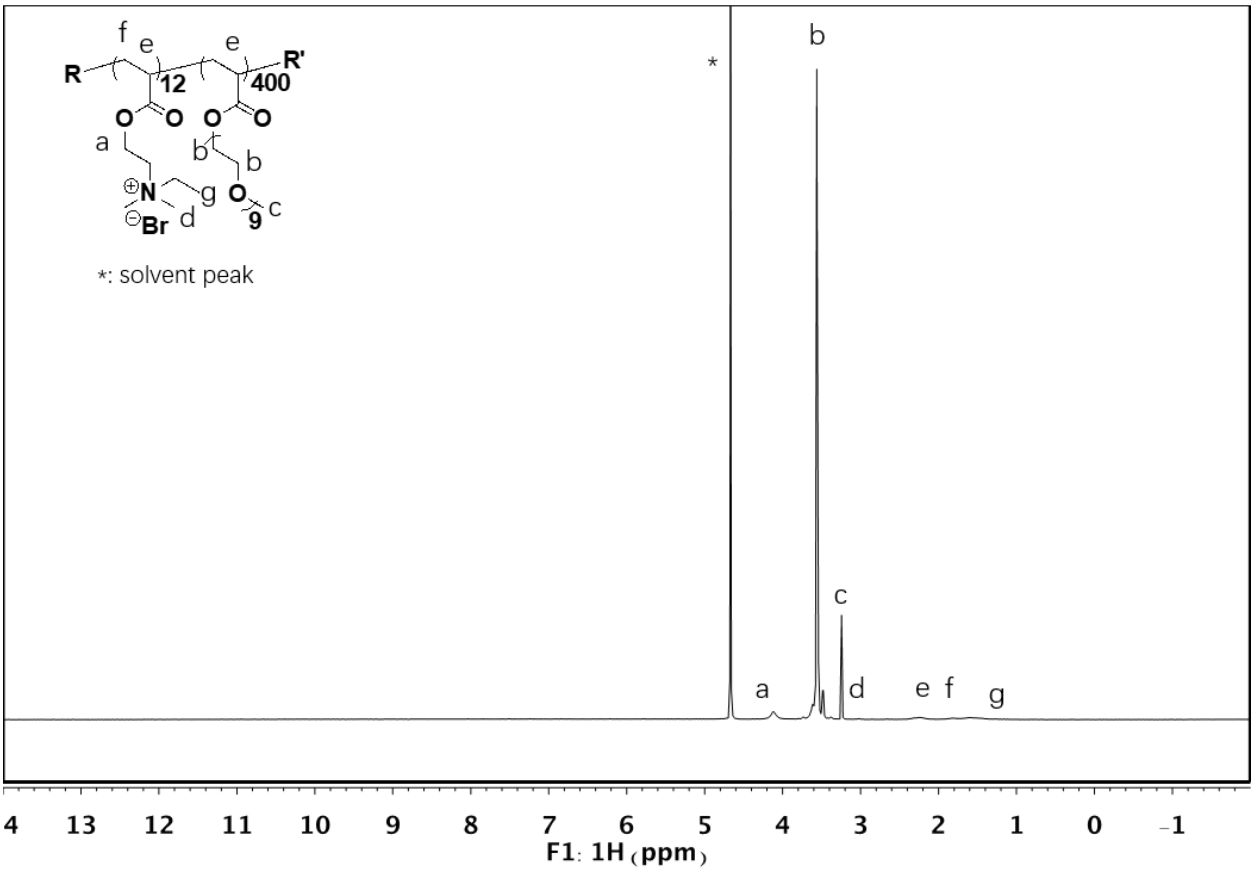

qPDMAEA$_{24}$-PEGMEA$_{200}$ (diblock copolymer):

^{1}H NMR (400 MHz, D_2O): δ 4.08 (br, 2H, -(C=O)O-**CH$_2$**-CH$_2$-), 3.75 – 3.46 (m, 34H, -O-**CH$_2$-CH$_2$**-O-), 3.21 (s, 3H, -O-**CH$_3$**), 3.02 (s, ~0.4H, -N$^+$(**CH$_3$**)$_2$CH$_2$CH$_3$), 2.21 (br, 1H, -CH$_2$C**H**(C=O)-), 2.01 – 1.36 (m, 2H, -**CH$_2$**CH(C=O)-), 1.25 (br, ~0.2H, -N$^+$(CH$_3$)$_2$CH$_2$**CH$_3$**).

SEC: Mn = 24,100; PDI = 1.76.

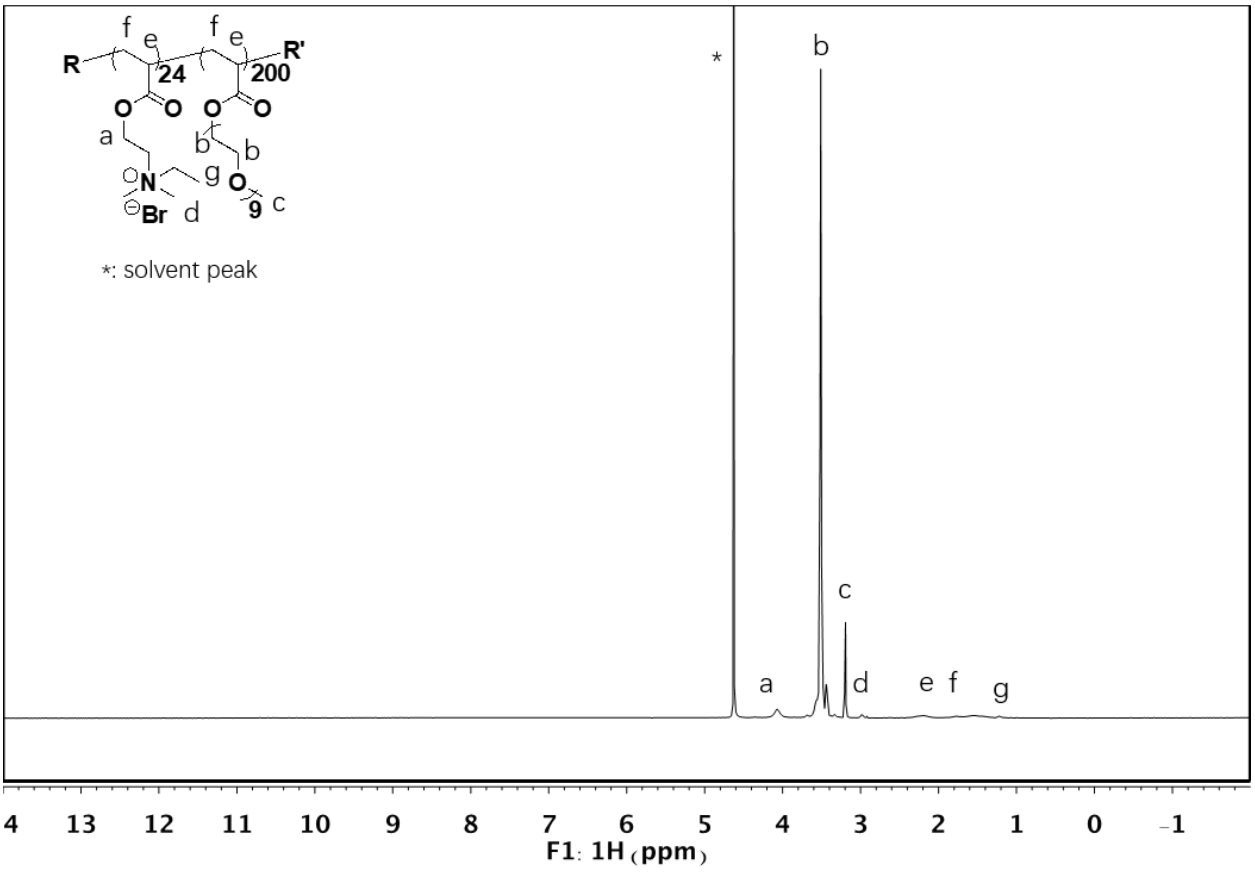

qPDMAEA$_{54}$-PEGMEA$_{200}$ (diblock copolymer):

^{1}H NMR (400 MHz, D_2O): δ 4.08 (br, 2H, -(C=O)O-**CH_2**-CH_2-), 3.75 – 3.46 (m, 34H, -O-**CH_2-CH_2**-O-), 3.21 (s, 3H, -O-**CH_3**), 3.02 (s, ~1.2H, -N^+(**CH_3**)$_2$CH_2CH_3), 2.21 (br, 1H, -CH_2C**H**(C=O)-), 2.01 – 1.36 (m, 2H, -**CH_2**CH(C=O)-), 1.25 (br, ~ 0.6 H, -N^+(CH_3)$_2$CH_2**CH_3**).

SEC: Mn = 28,700; PDI = 1.86.

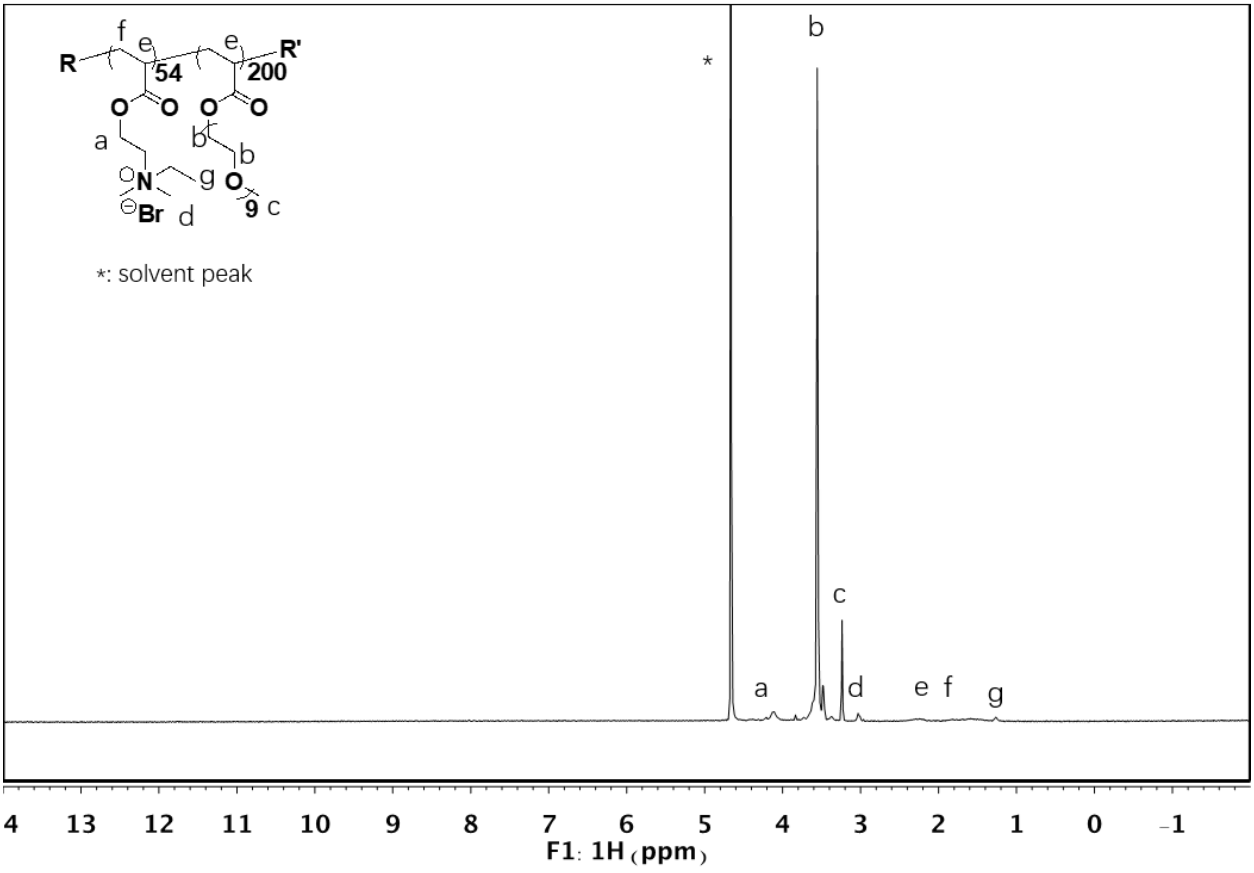

qPDMAEA$_{54}$-PEGMEA$_{400}$ (diblock copolymer):

^{1}H NMR (400 MHz, D_2O): δ 4.08 (br, 2H, -(C=O)O-**CH_2**-CH_2-), 3.75 – 3.46 (m, 34H, -O-**CH_2**-**CH_2**-O-), 3.21 (s, 3H, -O-**CH_3**), 3.02 (s, ~0.5H, -N^+(**CH_3**)$_2$$CH_2CH_3$), 2.21 (br, 1H, -$CH_2$C**H**(C=O)-), 2.01 – 1.36 (m, 2H, -**CH_2**CH(C=O)-), 1.25 (br, ~ 0.3 H, -N^+(CH_3)$_2$$CH_2$**$CH_3$**).

SEC: Mn = 48,400; PDI = 1.84.

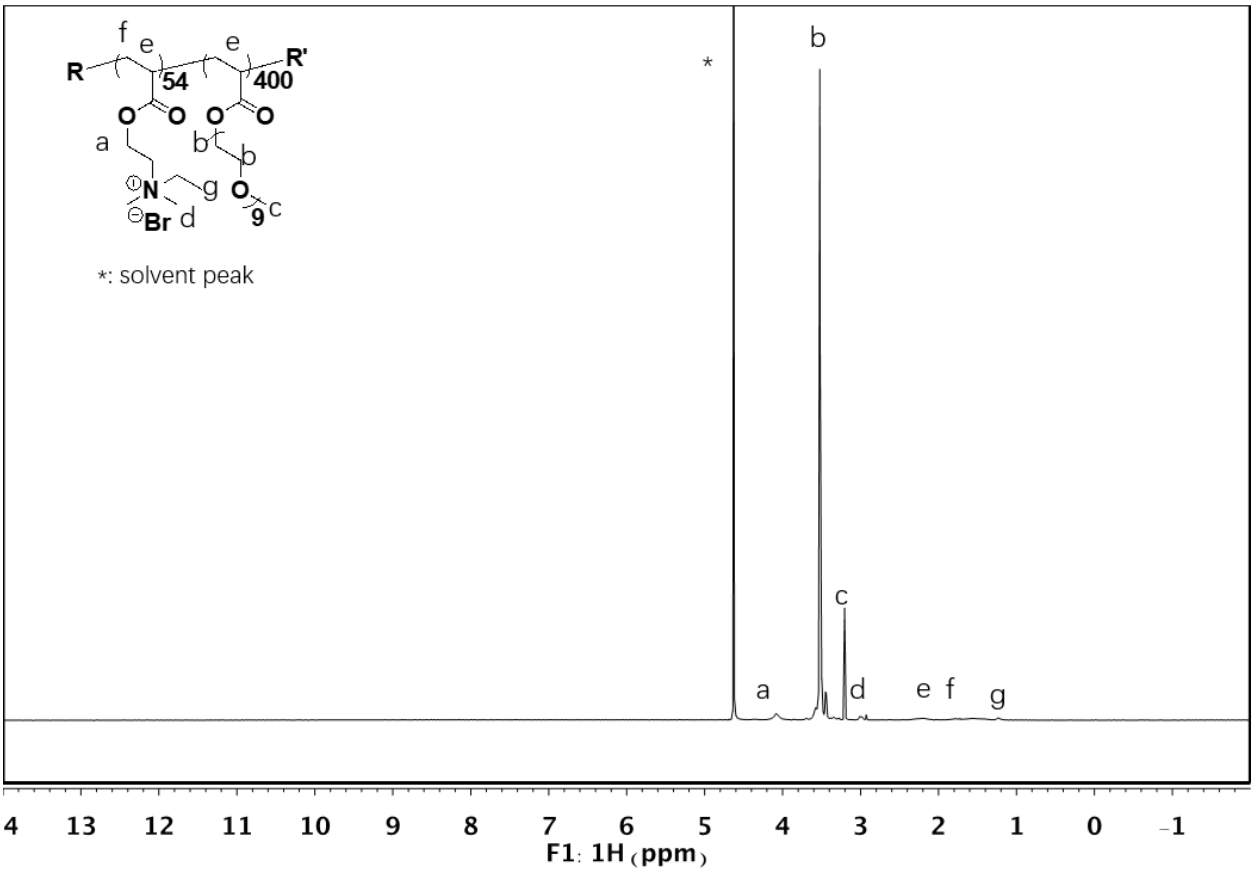

qPDMAEA$_{90}$-PEGMEA$_{200}$ (diblock copolymer):

^{1}H NMR (400 MHz, D_2O): δ 4.08 (br, 2H, -(C=O)O-**CH$_2$**-CH$_2$-), 3.75 – 3.46 (m, 34H, -O-**CH$_2$**-**CH$_2$**-O-), 3.21 (s, 3H, -O-**CH$_3$**), 3.02 (s, ~2.7H, -N$^+$(**CH$_3$**)$_2$CH$_2$CH$_3$), 2.21 (br, 1H, -CH$_2$C**H**(C=O)-), 2.01 – 1.36 (m, 2H, -**CH$_2$**CH(C=O)-), 1.25 (br, ~ 1.3H, -N$^+$(CH$_3$)$_2$CH$_2$**CH$_3$**).

SEC: Mn = 33,100; PDI = 1.63.

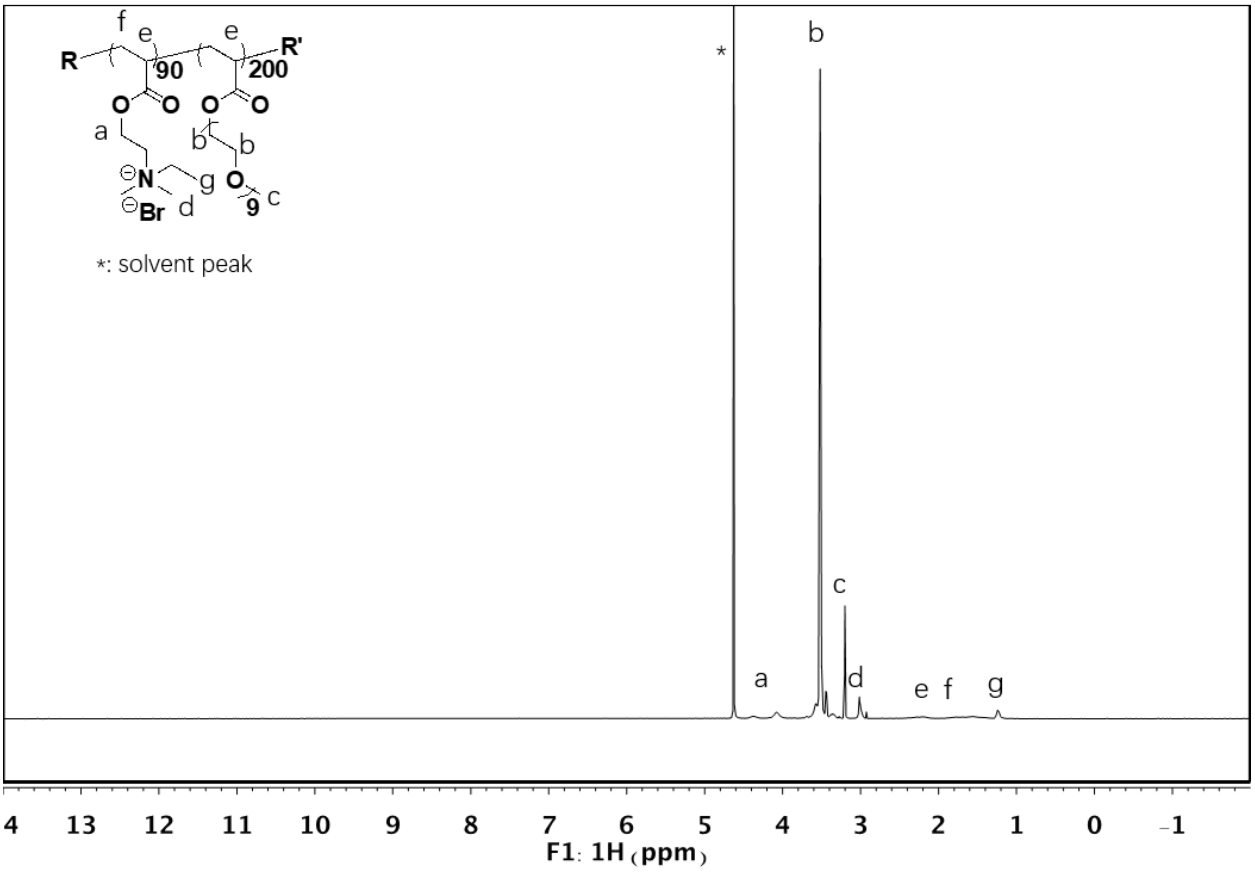

qPDMAEA$_{90}$-PEGMEA$_{400}$ (diblock copolymer):

^{1}H NMR (400 MHz, D_2O): δ 4.08 (br, 2H, -(C=O)O-**CH$_2$**-CH$_2$-), 3.75 – 3.46 (m, 34H, -O-**CH$_2$-CH$_2$**-O-), 3.21 (s, 3H, -O-**CH$_3$**), 3.02 (s, ~1.2H, -N$^+$(**CH$_3$**)$_2$CH$_2$CH$_3$), 2.21 (br, 1H, -CH$_2$C**H**(C=O)-), 2.01 – 1.36 (m, 2H, -**CH$_2$**CH(C=O)-), 1.25 (br, ~0.5H, -N$^+$(CH$_3$)$_2$CH$_2$**CH$_3$**).

SEC: Mn = 49,800; PDI = 1.95.